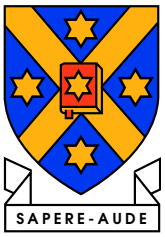

The Combined Modelling of the Regional Quasigeoid of New Zealand Using Gravity and GPS-levelling Data

Ahmed Abdalla

a thesis submitted for the degree of

Doctor of Philosophy

at the University of Otago, Dunedin,

New Zealand.

20 December 2012

Abstract

The NZGeoid2009 is currently the official quasigeoid model of New Zealand. It was computed to unify 13 separate local vertical datums (LVDs) in New Zealand. This study intends primarily to compute an improved gravimetric quasigeoid model in New Zealand. The computation of a gravimetric quasigeoid model depends on four input data sets namely the gravity data, DTM, GGM and GPS/levelling data. The accuracy of the input data sets plays an important role in the quality of the final gravimetric solution.

Therefore, the second objective has been devoted to analysing the levelling networks and investigating recent global geopotential models (GGMs). The joint adjustment approach is used to refine and readjust the levelling networks as well as for the unification of 13 separate local vertical datums (LVDs) in the North and South islands. The unification of LVDs has been done in two steps. The levelling networks in the North and South islands are jointly adjusted at first by fixing two tide gauges in Dunedin and Wellington. The gravity anomalies along levelling lines are generated from EGM2008. The cumulative normal to normal-orthometric height correction is computed from levelling and gravity anomaly data. The average offsets of these fixed points are then estimated relative to the World Height System (WHS). The average offset at Wellington and Dunedin are found to be 10.6 and 27.5 cm, respectively. These offsets are added to the newly derived orthometric and normal heights at the levelling networks for each island. The investigation of the recently released GGMs is conducted for a number of 11 GGMs (9 satellite-only and 2 combined models) by testing them using the newly adjusted levelling heights combined to GPS points. Among all tested satellite-only models, the GRACE/GOCE model GOCO-02S has the best RMS fit with GPS/levelling data of 56 cm when using the maximum degree/order 250 of spherical harmonic coefficients.

Three methods are reviewed for the gravimetric geoid/quasigeoid modelling and therefore three regional corresponding models have been computed, namely NZGM2010, NZQM2010 and OTG12.

NZGM2010 geoid model is compiled using the method of least-squares modification

of Stokes formula with additive corrections (widely known as the KTH method). The least-squares modified Stokes formula combines the terrestrial gravity and GGM in the context of the KTH method to provide an approximate estimator of the gravimetric solution. Hence, four additive corrections that account for the effects of topography, atmosphere, ellipsoidal approximation and downward continuation of the gravity data are applied to the approximate gravimetric solution. NZQM2010 quasigeoid model is computed using the boundary element method (BEM) based on the collocation and linear basis functions. The Earth's surface is discretised and considered as a constant boundary. The gravity disturbances derived from gravity anomaly data represent the oblique derivation boundary.

OTG12 quasigeoid model is computed using a new methodology based on the discretized-integral-equation (DIE) approach. The new method is successfully analysed and tested. The computation of OTG12 has been implemented in two steps. Step 1 involves testing the performance of DIE approaches when the gravity data is corrected for the residual terrain model (RTM) and reference gravity field. Four DIE approaches, namely the Poisson integral, Green integral, Point mass, and Radial multipole are tested and discretised at the locations of the gravity data at a constant depth below the Bjerhammar sphere to estimate the optimal depth. The optimal depth is based on the minimum RMS of residual between the observed and predicted gravity data. The investigation of DIE approaches revealed a good performance of Green's integral approach.

Step 2 involves the computation of the quasigeoid model (OTG12) using the remove-compute-restore (RCR) computation procedure. The near-zone contribution is computed using Green integral approach based on results from Step 1. The far-zone contribution is computed using the Earth Gravitational Model 2008 (EGM2008) coefficients from degree 251 up to degree 2160 of spherical harmonics. The reference gravity field is obtained using GOCO-02S global gravitational model coefficients complete to degree 250 of spherical harmonics. The comparison of OTG12 with the newly adjusted GPS-levelling data revealed that three gravimetric solutions (OTG12, NZGM2010 and NZGeoid2009) have similar accuracy (12 cm), and NZQM2010 (15cm) after applying the 3-parameter correction model.

Finally, the relative offset between the datums at Dunedin and Wellington tide gauges is extensively investigated by comparing the newly adjusted GPS-levelling data with the regional gravimetric solutions, EGM08 and the mean dynamic topography (MDT) models. Analysis reveals an existence of systematic discrepancies that can be attributed to the systematic errors within the gravimetric solutions.

Acknowledgements

First and foremost, all praise be to almighty Allah (God) for His ongoing protection and guidance and for granting me enough momentum and patience to carry out this work. Without Him, exalted is He! This work would not have been completed.

"*My Lord, enable me to be grateful for Your favor which You have bestowed upon me and upon my parents and to do righteousness of which You approve. And admit me by Your mercy into the ranks of Your righteous servants*". **Holy Quran; Al-Naml, verse 19**.

I would like to express my deepest gratitude to my supervisor Professor Robert Tenzer for his professional guidance and genuine support since the early communications prior to my enrollment to the University of Otago and then throughout the PhD's duration. His constructive criticism and insightful comments have surely assisted me to achieve this dissertation. Robert! I cannot thank you enough for the invaluable supervision and for always being available to answer my questions as well as for the crucial consultations regarding my work. I will never forget your daily visits to my office, our endless conversations and your amazing companionship during our conference trips to Auckland and Melbourne, and during our wonderful trip to Tahiti. I am truly indebted and owe you immense thanks for everything.

I would like to thank Dr Róbert Čunderlík of the Slovak University of Technology for his invaluable contribution in the computation of NZQM2010 quasigeoid. I am also thankful to Dr Nadim Dayoub of the University of Tishreen in Syria, for his contribution in the inter-islands offset analysis including mean dynamic topography models.

I greatly acknowledge my past officemate Dr Vladislav Gladkikh for his valuable support and nice companionship for a year. I thank him for introducing me to Linux and Fortran language. Vlad! I will never forget your great efforts and help by installing a Linux network to help me to survive my computations. I am also grateful to my colleague Dr Ali Fadil for his tremendous help in Linux and for introducing me to GMT software and shell script programming. His expertise and proficiency

have inspired me to learn and know more about GMT and Linux tricks: without his help they would have remained ambiguous. Thanks for being my supportive friend.

I would like to thank the staff members at the School of Surveying for being supportive of my endeavours. I would like to convey my especial thanks to Mrs. Fiona Webster and Mrs. Marg Newall of the departmental office for their timely help and support to sort out my administrative issues. Professor Brent Hall, Professor John Hannah, Dr Paul Denys, Dr Pascal Sirguey, Dr Tony Moore, Mr Alastair Neaves and Mr Peter Benfell for their support. My PhD study was funded by the University Of Otago Postgraduate Scholarship.

I am grateful to my current and past PhD colleagues, Robert Wayumba, Benjamin Quay, Chris Joseph, Judy Rodda, Jo Wright, Kambiz Borna and Dr. Mariano R. Recio, for the nice times and the joyful conversations, wish you all the best. I am also indebted to Mr Donald Reid and Dr Mahma Tawat for checking and correcting the thesis language. I am also thankful to Muslim community in Dunedin.

As I am sure that adequate words do not yet exist, I cannot find enough words to thank uncle Ibrahim Hassan, his sons Mohammed and Hassan, and the entire family for offering me social and homelike atmosphere in Dunedin. Their authentic hospitality and genuine support have undoubtedly encouraged me to be one of them. Meeting with them down under was one of the greatest coincidences I have ever had the pleasure to come across!

I am very indebted to my family back home in Sudan for their unwavering support and love. My brothers and sisters and their lovely kids are also acknowledged for their considerable support. Thanks for being my stable pillars of support and strength. I cannot repay my beloved parents for their invaluable love and support since the day I was conceived on this Earth. They have always been my backbone supporting me in every step. I pray to almighty Allah (God) to bless them and keep them always happy.

''*My Lord, have mercy upon them as they brought me up when I was small***''**. **Holy Quran; Al-Israa, verse 24**.

Last but not least, thanks to all my friends for their authentic support. As I must restate that I would like to thank all of those who supported me in any respect during the completion of my study and to express my apology for not mentioning them by name.

Ahmed Abdalla

Dunedin, December 2012

Contents

List of Figures

List of Tables

Glossary

Acronyms

CARS2009	CSIRO Atlas of Regional Seas 2009
DC	dynamic correction
DIE	Discretised Intergral indexEquationEquation
DIR	DIRect solution
DNSC	Danish National Space Centre
DORIS	Doppler Orbitography and Radiopositioning Integrated by Satellite
DTM	Digital Terrain Model
DTU	Technical University of Denmark
ECEF	Earth-Centered, Earth-Fixed
EGM2008	Earth Gravitational Model 2008
EGM96	Earth Gravitational Model 1996
FEM	Finite Element Method
FVM	Finite Volume Method
GEM	Global Elevation model
GGM	Global Geopotential Model
GNS	New Zealand's GNS Science institute
GOCE	Gravity Field and steady-state Ocean Circulation Explorer
GOCO	Gravity Observation COmbination
GPS	Global Positioning System
GRACE	Gravity Recovery and Climate Experiment
GRS80	Geodetic Reference System 1980

IAG	Internatonal Association of Geodesy
IAU	International Astronomical Union
ITRF1996	International Terrestrial Reference Frame 1996
LINZ	Land Information New Zealand
LLR	Lunar Laser Ranging
LVD	Local Vertical Datum
MDT	Mean Dynamic Topography
MSL	Mean Sea Level
NAVAD 1988	North American Vertical Datum 1988
NGS	US National Geodetic Survey
NZG2000	New Zealand Geodetic Datum 2000
NZGeoid05	New Zealand quasigeoid 2005
NZGeoid2009	New Zealand quasigeoid 2009
NZVD2009	New Zealand Vertical Datum 2009
RCR	Remove Compute Restore
RMS	Root Mean Square
RTM	Residual Terrain Model
SLR	Satellite Laser Ranging
SPW	Space-wise solution
SRBF	Spherical Radial Basis Function
SST	Sea Surface Topography
STD	Standard Deviation
TIM	Time-wise solution
VLBI	Very Long Baseline Interferometry
WGS	World Geodetic System

Symbols

$\bar{g}^t$	mean topography generated gravitational attraction
δg^{TC}	surface topography correction
δg_o^T	terrain correction at the geoid
(r,φ,λ)	Spherical coordinates
σ_0	truncated spherical cap
$\vec{g_1}$	gravitatioanl vector
$\vec{g_2}$	centrifugal vector
$\vec{g}$	gravity vector
α	azimuth counted form north
α	spherical azimuth
$\bar{\delta g}^{TC}$	integral mean topography correction along the plumbline
$\bar{\gamma}$	mean normal normal gravity
$\bar{\Omega}$	centrifugal potential
$\bar{g}$	mean value of gravity along the plumb line
$\bar{g}^M$	Mader's mean gavity
$\bar{g}^M$	Mader's mean gavity
$\bar{g}^N$	Niethammer's mean gravity
χ_{Moon}	Moon inclination to the ecliptic
χ_{Sun}	Sun inclination to the ecliptic
$\delta_{0,1}$	Kronecker delta
$\Delta g^{r,t}$	RTM-corrected residual gravity anomaly
Δg^r	residual gravity anomaly
Δg^{SB}	simple planar Bouguer gravity anomaly
Δg_{fz}	far-zone contribution to the gravity anomaly
$\delta H^{N,NO}$	cumulative normal to normal-orthometric height correction
$\delta H^{O,N}$	geoid-to-quasigeoid correction
ΔH_{AO}^{dyn}	dynamic height difference

Δh_i	levelling height differences
δN^A	combined atmospheric correction
δN^{dwc}	downward continuation correction
δN^{ell}	ellipsoidal correction
δN^T	combined topographic correction
$\delta W_{0,LVD}$	geopotential difference
$\Delta W_{zero-tide}$	zero-frequency gravitational potential
$\delta \bar{g}$	mean gravity disturbance
$\delta \bar{g}^{NT}$	mean atmosphere-generated gravitational attraction
$\delta\phi$	latitude difference between the benchmarks
$\Delta \upsilon_{AO}$	total height difference
$\Delta \upsilon_{AO}$	total measured height difference
$\delta \upsilon_i$	changes in geometric height along levelling section
$\frac{\partial \gamma}{\partial h}$	vertical normal gravity gradient
γ_e	normal gravity on the equator
γ_0	normal gravity at the reference ellipsoid
γ_ϕ	normal gravity
$\hat{r}$	unit vector in the direction $\mathbf{r}$
$\hat{r}'$	unit vector in the direction $\mathbf{r}'$
(ϕ,λ,h)	Geodetic coordinates
(r',Ω')	location of the integration point
(r,Ω)	location of the computation point
(u,β)	Ellipsoidal coordinates
(x,y,z)	Cartesian coordinates
$\mathbf{J}$	Jacobi's matrix
$\mathbf{M}$	system matrix of the integral equations
$\mathbf{t}$	vector of unknown disturbing potential
Q_k	Molodensky's truncation coefficients
$\mathrm{r_{lim}}$	upper limit of the atmosphere

Ω	Earth's surface
ω	velocity of the Earth's rotation
Ω_o	total solid angle
$\overline{\mathrm{P}}_{n,m}$	fully normalized associated Legendre functions
$\overline{c}_{n,m}$	fully normalized spherical harmonic coefficients
$\overline{Y}_{n,m}$	fully normalized solid spherical harmonic functions
ψ	spherical distance
$\rho(r',\Omega')$	actual spatial mass density distribution function
ρ^T	average topographic density
σ_n^2	terrestrial gravity anomaly error degree variances
G	Green integral kernel
M	radial multipole kernel
N	Point-mass kernel
P	Poisson integral kernel
$\tilde{\varsigma}$	approximate value of the height anomaly
$\tilde{N}$	approximate geoid height
$\triangle g^t$	RTM-corrected gravity anomalies
ε_{H^o}	Helmert's orthometric to rigorous orthometric height correction
$\vec{g_r}$	radial component of the gravitational vector
$\vec{g}_\lambda$	prime-vertical component of the gravitational vector
ζ	height anomaly
a	semi-major axis
$a_{k,r}$	coefficients design matrix
b_n	least-squares modification parameters
C^n	normal-geopotential number
$c_{n,m}$	GGM coefficients of the disturbing potential
$C_{n,m}$,$S_{n,m}$	spherical harmonic coefficients
c_n^{GGM}	gravity anomaly degree variances of the geopotential model
$d\sigma$	surface integration element

dc_n^{GGM}	error anomaly degree variances of the geopotential coefficients
e_{Moon}	Moon orbit eccentricity
e_{Sun}	Sun orbit eccentricity
ell	Eculidean distance
f	flattening
G	Newton's gravitational constant
GM_{Moon}	selenocentric gravitational
GM_{Sun}	heliocentric gravitational
H	orthometric height
h	Ellipsoidal height
H^N	Niethammer's orthometric height
H^{NO}	normal-orthometric height
H^N	normal height
H_{av}	average height of thelevelling instrument
H_A	orthometric height
H_{dyn}	dynamic height
$H_{mean-tide}$	height in mean-tide system
$H_{n,m}$	numerical coefficients of the global elevation model
H_n	surface (topographic) height functions of degree n
$H_{tide-free}$	height in tide-free system
$H_{zero-tide}$	height in zero-tide system
k	curvature of the plumb line
K_m	Gaussian measure of curvature
k_w, h_w	tidal Love numbers
M_{mp}	meridional radius of curvature
N	geoid height
N_{pv}	radius of curvature in the prime vertical
$P_{n,m}$	Legendre associated functions of degree n and order m
Q_n^{barn}	modified Molodensky's truncation coefficients

R_m	radius of curvature of any point at the azimuth
$S(\psi)$	original Stokes kernel
$S^{\bar{n}}(\psi)$	modified Stokes kernel
U	normal potential
V	gravitational potential
W	Earth's potential
NOC	Normal-orthometric correction

List of Publications*

Paper 1: Related to Chapter 6

Abdalla, A., Tenzer, R. (2011) The evaluation of the New Zealand's geoid model using the KTH method. *Journal of Geodesy and Cartography*. 37:1, 5-14. DOI:10:3846/13921341-2011-558326

Paper 2: Related to Chapter 6

Abdalla, A., Tenzer, R. (2012a) Compilation of the regional quasigeoid model for New Zealand using the discretized integral-equation approach. *Journal of Geodetic Sciences*. 2(3), 206-215. DOI:10.2478/v10156-011-0041-8

Paper 3: Related to Chapter 5

Abdalla, A., Tenzer, R. (2012b) The global geopotential and regional gravimetric geoid/quasigeoid models testing using the newly adjusted levelling dataset for New Zealand. *Journal of Applied Geomatics*. 4:187-195. DOI:10.1007/s12518-012-0089-x

Paper 4: Related to Chapter 6

Abdalla, A., Tenzer, R. (2012c) The integral-equation-based approaches for modelling the local gravity field in the remove-restore scheme, International Association of Geodesy Symposia, 7pp. Springer. (**accepted**).

Paper 5: Related to Chapter 6

Čunderlík, R., Tenzer, R., **Abdalla, A.**, Mikula, K. (2010) The quasigeoid modelling in New Zealand using the boundary element method. *Contributions to Geophysics and Geodesy*. Vol. 40/4, 283–297. DOI: 10.2478/v10126-010-0011-7

Paper 6: Related to Chapter 4

Tenzer, R., Vatrt, V., **Abdalla, A.**, Dayoub, N. (2011) Assessment of the LVD offsets for the normal-orthometric heights and different permanent tide systems. *Journal of Applied Geomatics*. 3:1–8. DOI:10.1007/s12518-010-0038-5

Paper 7: Related to Chapter 4

Tenzer, R., Vatrt, V., Luzi G, **Abdalla, A.**, Dayoub, N. (2011) Combined approach for the unification of levelling networks in New Zealand. *Journal of Geodetic Sciences*. 1(4), 324-332. DOI: 10.2478/v10156-011-0012-0

Paper 8: Related to Chapter 7

Tenzer, R., Dayoub, N. and **Abdalla, A.** (2013) Analysis of a relative offset between vertical datums at the North and South Islands of New Zealand. *Journal of Applied Geomatics*. DOI:10.1007/s12518-013-0106-8

*Author's contribution to the papers of the thesis

Papers 1 to 4: The **first author** prepared all numerical results and the first draft of manuscript. The second author prepared the final version of manuscript.

Paper 5: The first author (under instructions of the last author) prepared numerical results. The **third author** prepared all input data sets, numerical analysis of results and comparison with existing models. The second author prepared the final version of manuscript.

Paper 6: The first author prepared the final version of manuscript. The second and last authors estimated independently the LVD offsets in New Zealand. The **third author** analysed the GPS-levelling data and prepared conversions between different permanent tidal systems as well as height conversion.

Paper 7: The first author prepared the final version of manuscript. The second and last authors estimated the LVD offsets for the North and South Islands of New Zealand using different approaches. The third author readjusted the levelling networks in New Zealand. The **fourth author** analysed the differences between the gravimetric and geometric quasigeoid/geoid models for New Zealand and prepared the conversion between different height systems. He also conducted the error analysis and summary of results with major conclusions.

Paper 8: The first author prepared the manuscript. The second author computed and analysed the mean dynamic topography models offshore New Zealand. The rests of numerical realization, analysis and comparison of results was done by the **third author**.

Chapter 1

Introduction

1.1 Geoid/quasigeoid determination

The geoid is considered as an important surface in geodesy and its classical definition is that it represents the equipotential surface that approximately coincides with the mean sea level (MSL) and extends beneath the continental masses. Thegeoid at the oceans is efficiently measured by altimetry, bearing in mind that the near-shore measurements always suffer from low accuracy and reliability degradation (see e.g. Andersen and Knudsen, 2000; Andersen *et al.*, 2005). The extension of the geoid below the continents is assumed to correspond to the suppositional ocean level by converting the terrestrial surface gravity measurements to gravity anomalies prior to the computation of the geoid. The variations of the mass density and topography of the Earth generate the irregularity in the geoid shape. Thus, the reference ellipsoid of revolution has been proposed as an approximation (with differences due to geoid irregularities) to the geoid. The differences between the geoid and reference ellipsoid are known by the geoid undulations.

In the determination of a regional geoid model, heterogeneous data sets are optimally assimilated through an auxiliary procedure in order to produce the final geoid heights. These heterogeneous data sets are digital terrain model (DTM), gravity anomaly data, global geopotential model (GGM) and GPS-levelling data. The altimetry data can be used for marine geoid determination, principles of the altimetry technique were broadly described in literature (e.g. Wahr, 1996). A prominent procedure that combines the data sets for geoid determination is called remove-compute-restore (RCR), where short and long wavelength contents of DEM and GGM are removed from the gravity data before the computation started. To compute the geoid height RCR should be included in one of gravimetric geoid determination

methods. The determination of the geoid is a conversion process that transforms the refined terrestrial anomalies to geoid/quasigeoid heights. There are different methods to use, for instance the integration of Stokes kernel (Stokes, 1849) is most used. There is an alternative choice to use the Stokes kernel or the modified ones.

The broad extension in the number of the GPS users is rapidly increasing because of the high accuracy obtained by the GPS, which is being used in a wide range of geodetic and surveying applications. Despite the differences between the height systems in the GPS and traditional levelling measurements, the GPS has become more attractive especially when high-resolution gravimetric geoid/quasigeoid models are available. The GPS technique has many advantages compared with traditional levelling methods. For instance, it is not affected by weather conditions as in levelling; it is an all-weather and rapid technique in addition to its easy operational devices and high accuracy for relative positioning. The orthometric heights can be derived from a combination of the GPS and the gravimetric height modelling. The ellipsoidal height is integrated with the gravimetric geoid heights in one formula to provide the orthometric or normal heights that are used in the most of geodetic works.

1.2 Reference ellipsoid

A biaxial ellipsoid is obtained when the meridian ellipse rotates around the its minor axis. This rotation makes the ellipsoid very similar to the global geoid and therefore it is recognised as the best approximations of the Earth's figure. However, despite the similarity between the ellipsoid and the geoid, it is found that the ellipsoid diverges from the geoid by about ± 100 metres. The divergence happens as a consequence of the geoid irregularities.

Such an ellipsoid is not only a good approximation to the geoid, but also has a primary role to serve as a physical reference surface on which coordinates are to be defined and computations are made (Heiskanen and Moritz, 1967). The mean Earth ellipsoid is obtained by applying the least-squares fitting over the globe. The precise definition of the ellipsoid is based on the semi-major axis and the normal gravity at the equator for the purposes of obtaining accurate computations such as map projections, satellite navigation, normal gravity on Earth's surface and in Space (Li and Götze, 2001). The World Geodetic System (WGS) is used to replace the local horizontal datums for the purposes of mapping and navigation.

1.3 Geoid applications

The Geoid plays a key role as a reference surface for a different disciplines of the Earth sciences, therefore the various geoid applications can be confined into two main types, applications on marine and continental areas. Starting with applications on marine areas, the geoid is a very important tool in connecting vertical datums. A vertical datum represents a reference surface of a measurement point or a set of points from which all elevations are referred to. The existence of a unified local vertical datum at any region is a matter of importance because it is supposed that all heights within a certain region should have been measured and referred to the same reference surface. Contrarily, a point could have different elevation values rather than a unique one due to the offsets between the reference surfaces and that is considered as a main effect of datum change as well as it would yield an incorrect difference in elevations. Furthermore, the vertical datum is defined by the effects of Sea Surface Topography (SST) on the tide gauges and therefore it can be preferably used to connect the geodetic levelling networks to the geoid, not to MSL as commonly prevalent.

In the context of ocean circulation studies, the geoid is one of three major components that is employed to compute the SST. The other two components are satellite altimetry and satellite ephemeris. The three components have to be precise in order to achieve an accurate SST determination. Over the short-term periods, SST is daily exposed to several effects by the Moon and the Sun tides on the Earth, and throughout the long-term periods the ocean circulation affecting SST as well as the heat content of the water and ocean surface currents (Wahr, 1996). The aforementioned effects evoke SST anomalies due to the uneven distribution of mass at the sea floor; the variation between the SST anomalies and the global anomalies stems from the Earth's gravitational field by virtue of the crustal rearrangements of the continents and seamounts mass and rock redistribution.

The geoid also has a major contribution in prediction of gravity anomaly data over the oceans, where the satellite radar altimetry is utilised to compute regular grids of high resolution gravity anomalies. These grids are yielded by converting the data of the geoid height across ocean areas. SST data are collected by the altimetry spacecraft in a continuous profile of raw data. In addition, the geoid raw data are collected with different accuracies, track pacing and density qualities. After converting the geoid data into the gravity data, the yielded satellite-derived data have to be evaluated against the ship-tracked marine data and can be merged thereafter to construct global marine gravity data grid. Both data sets (ship-tracked and satellite-derived) are subject to errors; on one hand, the ship-tracked data set is distributed

in a dispersed pattern and this could increase the possibility of systematic errors. On the other hand, the satellite-derived data set, as aforementioned, can be affected by the contamination of the tracking-data variations.

The gravimetric geoid is a representation of the Earth's mass-density distribution, which is very important in geodynamics studies and interpretations. The essential data for any geophysical interpretations are not devoid of the following sources: seismological, magnetic, electrical, heat flow and gravimetric data (Yang, 1999).

In addition, the geoid is very important for tectonic structural features in oceans (e.g. ocean trenches and mid-ocean ridges). The geodynamical interpretations are based on a general assumption that the geoid is time dependent because the surface gravity on the Earth is subject to change with time according to the attraction of the Sun, Moon, planets, atmosphere and other geophysical phenomena.

Giving a precise definition for the figure of the Earth is one of the core objectives of geodesy. The geoid represents the proper tool to define the figure of the Earth by virtue of the fact that the geoid itself is a mathematical representation of the figure of the Earth. In addition, the revolutionized satellite positioning and geodetic techniques persistently require an existence of a high resolution geoid model.

On the land, the geoid is also used for connecting different height systems through the unification of local vertical datums for geodetic purposes (e.g. Amos, 2007; Amos and Featherstone, 2009), as establishment of a new height control in remote areas where traditional levelling work is onerous. With the presence of an accurate geoid model a direct conversion between the ellipsoidal and orthometric heights can be obtained at any arbitrary point on the Earth's surface. The geoid is also used for global plate tectonic and seismic studies by Silver *et al.* (1988), as well as studies of frictional and deformation processes (see e.g. Rizos, 1982), and studies of deep/near-Earth mass densities (cf. Bowin, 1983; Andersen *et al.*, 2005).

1.4 Reference systems in New Zealand

The New Zealand Geodetic Datum 2000 (NZGD2000), the official horizontal datum was defined based on Geodetic Reference System 1980 (GRS80) ellipsoid and was realised by the International Terrestrial Reference Frame 1996 (ITRF96). NZGD2000 was introduced to handle the crustal deformation processes through a velocity model that was employed to transform observations between the epoch (2000.0) and the observation epochs (Blick, 2003).

The national vertical datum in New Zealand was obviously not available before the computation of the first official quasigeoid model NZGeoid2005 . The New Zealand reference system was realised by 13 separate local vertical datums (LVDs) relative to MSL observed at 12 different tide-gauges stations at uneven times (Amos and Featherstone, 2009). LVDs were connected to tide gauges that used to be the main datum for establishing levelling networks for engineering purposes. Some of the datums were relatively defined with respect to levelling, for example, Dunedin-Bluff 1960 benchmarks rather than tide gauge stations. For a more detailed overview of the local levelling networks in New Zealand we refer readers to Gilliland (1987).

The geodetic vertical reference system in the North and South islands NZDV2009 is currently the official vertical datum. NZDV2009 is a geoid-based height system related to the NZGeoid2009 quasigeoid model which was implemented to unify 13 separate LVDs connected to local MSL estimated at uneven times. The Normal-orthometric heights are used in NZVD2009 because of the absence of the gravity measurements from the levelling network. The height system in New Zealand is defined by the approximate normal-orthometric heights based on the GRS67 normal gravity formula and computed approximately using a truncated form of Rapp's equation (Rapp and Pavlis, 1991). The LVDs were defined in the system of the (approximate) normal-orthometric heights. The cumulative normal-orthometric correction to levelled height differences was defined based on the GRS67 normal gravity field parameters. The computation of this correction was done approximately using a truncated form of the GRS67 normal-orthometric correction formula (Rapp, 1961).

The iterative gravimetric approach was applied to unify the LVDs in New Zealand using a regional gravimetric quasigeoid model and GPS-levelling data on each LVD (Amos, 2007; Amos and Featherstone, 2009). The principle of this method is based on an iterative quasigeoid modelling where the LVD offsets computed from an earlier model are used to apply additional gravity reductions from each LVD to that model. The iterative gravimetric approach was used to compile the first official gravimetric quasigeoid model for New Zealand, NZGeoid05 (Amos, 2007). NZGeoid05 was computed jointly by the Land Information New Zealand (LINZ) and the Western Australian Centre for Geodesy at Curtin University of Technology (Amos and Featherstone, 2008). NZGeoid05 was calculated from different heterogeneous ground-, seaborne- and altimetry-derived gravity data using the deterministic modification of the Stokes kernel. NZGeoid05 was complied on a $2' \times 2'$ geographical grid over New Zealand and its continental shelf (area bounded by the parallels of 25° and 60° southern spherical latitude and the meridians of 160° and 190° western spherical longitude). The estimated LVD offsets relative to the regional quasigeoid model

NZGeoid05 are from 26 cm (One Tree Point 1964, Nelson 1955, and Dunedin-Bluff 1960 LVDs) up to 59 cm (Gisborne 1926 LVD), see Table 1.1.

Table 1.1: The average offsets of LVDs relative to NZGeoid05 and NZGeoid2009 (Amos, 2007; Amos and Featherstone, 2008). Unit: 1 cm.

LVDs relative to NZGeoid05			
North Island		South Island	
LVD	offset	LVD	offset
Auckland 1946	-49	Bluff 1955	-38
Gisborne 1926	-58	Dunedin-Bluff 1960	-26
Moturiki 1953	-31	Dunedin 1958	-48
Napier 1962	-30	Lyttelton 1937	-34
One Tree Point 1964	-24	Nelson 1955	-25
Taranaki 1970	-45		
Wellington 1953	-50		
LVDs relative to NZGeoid2009			
Auckland 1946	-34	Bluff 1955	-36
Gisborne 1926	-34	Dunedin-Bluff 1960	-38
Moturiki 1953	-24	Dunedin 1958	-49
Napier 1962	-20	Lyttelton 1937	-30
One Tree Point 1964	-6	Nelson 1955	-30
Taranaki 1970	-32		
Wellington 1953	-44		

The New Zealand quasigeoid model NZGeoid2009 is the currently adopted official height reference surface for New Zealand. NZGeoid2009 was computed using a similar approach as NZGeoid05 (Claessens *et al.*, 2009, 2011). The main difference in computing NZGeoid05 and NZGeoid2009 is the use of different global geopotential models (GGMs); NZGeoid05 was computed using EGM96 (Lemoine *et al.*, 1998), while EGM2008 (Pavlis *et al.*, 2008) was used for the computation of NZGeoid2009. NZGeoid2009 model is provided to users on a $1' \times 1'$ geographical grid over the same area as NZGeoid05. GPS-levelling data were again used to determine LVD offsets in New Zealand relative to NZGeoid2009. The estimated LVD offsets relative to NZGeoid09 are within 6 cm (One Tree Point 1964 LVD) and 49 cm (Dunedin 1958 LVD), as seen in Table 1.1.

1.5 Research objectives

The main objective of this study of this study is to compute a new gravimetric quasigeoid model in New Zealand. Three computational methodologies, namely the KTH method, BEM and DIEA, will be reviewed, investigated and analysed. The accuracy improvement of the gravimetric quasigeoid models depends on the quality of the input data sets, for example, the gravity data, DTM, GGM and GPS-levelling data.

The second objective is devoted to levelling network readjustment and unification. The current levelling networks were realised by 13 separate LVDs in the North and South islands. These networks suffer from several deficiencies, among them these levelling networks were observed at different tide gauges connected to local MSL of each datum. The tide gauges were defined in very short-term records. As well the levelling networks have poor spatial coverage especially in the South Island. In addition, the tectonics vertical and horizontal motions as well as sea level variability are also affecting the levelling networks.

The readjustment and unification of the levelling networks using the joint adjustment approach will overcome these deficiencies due to inconsistencies between LVDs. The readjustment will be applied by fixing two tide gauge points at Wellington and Dunedin in the North and South islands, respectively. The unification of the readjusted networks is achieved by applying the geopotential-value approach to compute the vertical offsets of the fixed tide gauges at Wellington and Dunedin relative to WHS.

Finally, the combination of the newly adjusted levelling data associated with the GPS data will be used to assess the regional gravimetric solutions derived from the three used methods as well as the official quasigeoid model (NZGeoid2009). In addition, the old GPS-levelling data based on 13 LVDs relative to NZGeoid as well as WHS are also applied in the assessment.

The existing four regional gravimetric solutions and newly adjusted GPS-levelling data are giving a great motivation to investigate and analyse the relative offset between Wellington and Dunedin tide gauges. In addition, MDT models will be employed to compute the differences between these tide gauges by analysing the spatial variations of MSL in each tide gauge.

1.6 Thesis outline

Chapter 2: Defines three types of coordinates systems namely the Cartesian coordinate system, spherical coordinate, and geodetic coordinate system, and their transformations are also demonstrated. It also introduces the Earth's gravity field and normal gravity field.

Chapter 3: Reviews the theory of height systems and gives short descriptions for each of these: geopotential number, dynamic height, orthometric height and its rigorous definition, normal height, levelling heights and as normal-orthometric height, which is used in New Zealand, as well as its correction (NOC).

Chapter 4: Shows the definition of the LVDs relative to WHS using the geopotential-value method. The combination between the joint adjustment of the GPS-levelling data and the geoptential-value method is adopted to unify LVDs in North and South islands. The new adjusted normal-orthometric heights are described and incorporated with the GPS data (newly adjusted GPS-levelling data).

Chapter 5: Shows the testing of the recent GRACE/GOCE geoptential models using the newly adjusted GPS-levelling data. The following models were investigated in this chapter: GOCE and GRACE models namely GOCO-01S, GOCO-02S as well as the GRACE models namely ITG-GRACE2010S; the GOCE models compiled from the direct approach DIR-R1 and DIR-R2, time-wise approach TIM-R1 and TIM-R2, space-wise the SPW-R1 and SPW-R2. In addition, the combined models EGM2008 and EIGEN-GL04C were also investigated.

Chapter 6: Addresses in detail the computation of the regional geoid/quasigeoid model using local gravity database. The chapter starts with a demonstration of two initial gravimetric solutions computed from two different methods. The first experimental gravimetric geoid model (NZGM2010) for New Zealand is computed using the method of least-squares modification of Stokes formula. The second gravimetric solution (NZQM2010) is computed using the boundary element method (BEM).

The rest of the chapter is devoted to demonstrating the discretised integral-equation (DIE) approaches to compute our main quasigeoid model in this study. DIE approaches are utilised to investigate the accuracy of local gravity data using discretised integral-equation. Four types of the DIE approaches namely the Poisson integral, Green integral, Point-mass, and Radial multipole are investigated and analysed over the extracted testing area, which is situated in rugged terrain of the Southern Alps and flat coastal regions at the South Island of New Zealand, including offshore

areas. The implementation of DIE approaches is based on the procedure of downward continuation (DWC) of gravity data. The DWC problem is addressed and the Jacobi's iteration method is used as a practical solution. The compilation of the final quasigeoid (OTG12) model is undertaken using Green's approach. The compilation, results and analysis of all regional models are also addressed and demonstrated.

Chapter 7: Shows the investigation and analysis of relative offset between Wellington and Dunedin tide-gauges in the North and South islands using GPS-levelling data and regional gravimetric models, EGM2008 global geopotential model and mean dynamic topography (MDT) models to analyse the variations of mean sea level (MSL) between the same datums.

Chapter 8: Concludes by giving a brief summary of the thesis work and itemising the results and outcomes, plus pointing out some recommendations for future works.

Chapter 2

Coordinate systems and Earth's gravity field

2.1 Coordinate systems

Position of any point in space can be specified by different types of coordinate systems, for example, the Cartesian coordinate system (x,y,z) and spherical coordinate (r,φ,λ) and geodetic coordinate system (ϕ,λ,h). The point is defined in a three-dimensional way using one of the three systems.

The relation between the Cartesian coordinates (x,y,z) and the spherical coordinates (r,φ,λ) is given by the following equations

$$\begin{aligned} x &= r\ \cos\varphi\ \cos\lambda \\ y &= r\ \cos\varphi\ \sin\lambda \\ z &= r\ \sin\varphi \end{aligned} \tag{2.1}$$

where r is the radial distance, φ is the geocentric latitude. The relation between the Cartesian coordinates (x,y,z) and the Geodetic coordinates (ϕ,λ,h) is given by the following equations:

The prime-vertical radius of curvature N_{pv} in the prime vertical perpendicular to the meridian is given by

$$N_{pv} = \frac{a}{\sqrt{1 - e^2\ \sin^2\phi}} \tag{2.2}$$

The meridional radius of curvature M_{mp} is given by

$$M_{mp} = \frac{a(1 - e^2)}{\left(1 - e^2 \sin^2\phi\right)^{3/2}} \tag{2.3}$$

The first numerical eccentricity e of the ellipsoid can be obtained by

$$e = \frac{\sqrt{a^2 + b^2}}{a} \tag{2.4}$$

The second eccentricity e' is given by flattening f is given by second flattening f' is rarely used

$$f' = \frac{a - b}{b} \tag{2.5}$$

Three methods are used in the transformation from Cartesian to Geodetic coordinates (the closed-form method, the iterative method and the approximation method). The direct or the closed-form method being based on the solutions of both cubic and quartic polynomials. It was introduced by Paul (1973b) and later was extensively addressed by several scientists (Penev, 1978; Pick and Šimon, 1985; Vaníček and Krakiwsky, 1986; Borkowski, 1987, 1989; Soler and Hothem, 1989; Grafarend and Lohse, 1991; Lapaine, 1990; Hofmann-Wellenhof *et al.*, 1997). The iterative method was first introduced by (Hirvonen and Moritz, 1963; Heiskanen and Moritz, 1967) and followed later by (Benning, 1987; Borkowski, 1989; Lin and Wang, 1995; Torge, 2001; Pollard, 2002, 2005; Jones, 2002; Wu *et al.*, 2003; Sjöberg, 2008; Turner, 2009; Shu and Li, 2010). The approximation method was addressed by(Bowring, 1976, 1985; Vincenty, 1980; Olson, 1996; You, 2000; Turner, 2009).

The transformations from (x,y,z) to (ϕ,λ,h) is straightforward, when ($h = 0$)

$$\tan\phi = \frac{1}{1 - e^2} \frac{z}{\sqrt{x^2 + y^2}} \tag{2.6}$$

$$\tan\lambda = \frac{y}{x} \tag{2.7}$$

The transformation of ϕ in Equation 2.6 becomes a problematic when the point has an elevation over the ellipsoid where $h \neq 0$. The closed approximate estimation for (ϕ,h) by Paul (1973b) can be used

$$\tan\phi = \frac{z + \dfrac{a.e^2}{\sqrt{1 - e^2}} \left[\dfrac{za}{\sqrt{p^2b^2 + z^2a^2}} \right]^3}{p - \left[\dfrac{ae^2pb}{\sqrt{p^2b^2 + z^2a^2}} \right]^3} \tag{2.8}$$

$$h = \frac{p}{\cos\phi} - N_{pv} \tag{2.9}$$

An iterative solution for Equations 2.2, 2.8 and 2.9 introduced by Hirvonen and Moritz (1963, pp4) is given by the following equations

$$\tan\phi_{i+1} = \frac{z}{p\left(1 - e^2 \dfrac{N_i}{N_i + h_i}\right)} \tag{2.10}$$

$$N_{i+1} = \frac{a}{\sqrt{1 - e^2 \sin^2 \phi_i}} \tag{2.11}$$

$$h_i = \frac{p}{\cos \phi_i} - N_{pv(i)} \tag{2.12}$$

where $p = \sqrt{x^2 + y^2}$ and i = 2,3,....

2.2 Earth gravity field

All objects on the Earth's surface are always under the dominion of the gravitational force $\vec{g_1}$ of the Earth's masses and the centrifugal force of the Earth's rotation $\vec{g_2}$. The gravity vector is the summation of the two forces:

$$\vec{g} = \vec{g_1} + \vec{g_2} \tag{2.13}$$

If the objects are outside the Earth's surface, the effect of the gravity will remain the same and the corresponding forces can be represented in the following context :

$$W = V + \bar{\Omega} \tag{2.14}$$

where W is the Earth's potential, V is gravitational potential and $\bar{\Omega}$ is the centrifugal potential

The magnitude of the gravity vector along the normal direction in a Cartesian coordinate system can be shown as:

$$g = |\vec{g}| = \sqrt{\left(\frac{\partial W}{\partial x}\right)^2 + \left(\frac{\partial W}{\partial y}\right)^2 + \left(\frac{\partial W}{\partial z}\right)^2} \tag{2.15}$$

For any chain of points in the dimensional coordinate system having the same values of the gravity potential, they can be defined as an equipotential surface.

$$W(x,y,z) = \text{const} \tag{2.16}$$

The summation of the derivative of Equation 2.16 with respect to the vertical direction along the surface, showing that the equipotential surface is always vertical to the gravity vector as follows:

$$\frac{\partial W}{\partial x} dx + \frac{\partial W}{\partial y} dy + \frac{\partial W}{\partial z} dz = 0 \tag{2.17}$$

2.3 Normal gravity field

The normal gravity field was put to have a similar character as the Earth gravity field such as the total mass, rotation at the same velocity of the Earth's rotation and potential. Similarly, the geopotential and gravity magnitude of the normal field are called the normal potential U and the normal gravity γ, respectively.

The normal potential can be expressed by the following linear approximation (Sneeuw, 2006,):

$$U = \frac{GM}{R}\left[\frac{R}{r} + \left(\frac{R}{r}\right)^2\left(\frac{1}{2}\,m - f\right)\left(\cos^2\theta - \frac{1}{3}\right) + m\,\frac{1}{2}\left(\frac{r}{R}\right)^2\sin^2\theta\right] \tag{2.18}$$

where GM is the geocentric gravitational constant, θ is the co-latitude and m is Clairaut's constant defined by (Heiskanen and Moritz, 1967, Eq. 2-70)

$$m = \frac{\omega^2\, a^2\, b}{GM} \tag{2.19}$$

The normal gravity can be analytically obtained from a so-called Somigliana-Pizzetti formula (Somigliana, 1929):

$$\gamma_0(\phi) = \frac{a y_e \cos^2\phi + b y_p \sin^2\phi}{\sqrt{a^2\cos^2\phi + b^2\sin^2\phi}} \tag{2.20}$$

where γ_e is the normal gravity on the equator.

putting $k = (b\gamma_b - a\gamma_e)/(a\gamma_e)$, Equation 2.20 can be written as

$$\gamma(\phi) = \gamma_e\,\frac{1 + k\sin^2\phi}{\sqrt{1 - e^2\sin^2\phi}} \tag{2.21}$$

Residual gravity field

The difference between the potential and the normal potential of the Earth at arbitrary point is called the disturbing potential T

$$T_P = W_P - U_P \tag{2.22}$$

The gravity anomaly Δg at arbitrary point is defined as

$$\Delta g_P = -\frac{\partial T_P}{\partial r} - \frac{2}{r}T_P \tag{2.23}$$

The gravity disturbances δg at arbitrary point is defined as

$$\delta g_P = -\frac{\partial T_P}{\partial r} \tag{2.24}$$

2.4 Earth's gravitational potential

To define the gravitational field of the solid Earth including the atmosphere in the sequel of this chapter, temporal variations of the Earth's gravity field, the luni-solar and planetary gravity as well as the response of the Earth (tide and ocean loading) are not considered. Moreover, it is assumed that the origin of the geocentric coordinate system is identical to the mass centre of the Earth.

The gravitational potential V is defined by the Newton volume integral. It reads (see MacMillan, 1930)

$$V(r,\Omega) = G \iint_{\Phi} \int_{r'=0}^{\mathrm{r_{lim}}} \boldsymbol{\rho}(r',\Omega')\ell^{-1}(r,\Omega;r',\Omega')r'^{2}dr'd\Omega', \tag{2.25}$$

where G is Newton's gravitational constant, $\rho(r',\Omega')$ is the actual spatial mass density distribution function, $\ell(r,\Omega;\, r',\Omega')$ is the Euclidean spatial distance between the computation and integration points (r,Ω) and (r',Ω), that is, $\ell(r,\Omega;r',\Omega') = \sqrt{r^2 + r'^2 - 2rr'^2\cos\psi}$, $\mathrm{r_{lim}}$ the upper limit of the atmosphere, Ω_o the total solid angle and ψ the spherical distance computed from $\cos\psi = \sin\phi'\sin\phi + \cos\phi'\cos\phi\cos(\lambda' - \lambda)$.

The reciprocal value of the spatial distance in Equation 2.25 is further expanded into a series of the Legendre polynomials for the argument of cosine of the spherical angle. For the external convergence domain of $r \geq r'$, it reads (Hobson, 1931; Pick *et al.*, 1973)

$$\ell^{-1}(r,\Omega;r',\Omega') = \frac{1}{r}\sum_{n=0}^{\infty}\left(\frac{r'}{r}\right)^{n} P_n(\cos\psi) \tag{2.26}$$

Applying the additional theorem, given by Hobson (1931) and Novotný (1983)

$$\begin{aligned} P_n(\cos\psi) &= P_{n,0}\left(\sin\phi'\right)P_{n,0}(\sin\phi) \\ &+ \sum_{m=1}^{n}\frac{(n-m)!}{(n+m)!}\mathrm{P}_{n,m}\left(\sin\phi'\right)\mathrm{P}_{n,m}(\sin\phi)\cos m\left(\lambda' - \lambda\right) \end{aligned} \tag{2.27}$$

the external gravitational potential V of the Earth is expressed in the following form

$(\forall r < r_{lim})$ (e.g. Burša and Kostelecký, 1999)

$$V(r,\Omega) = \frac{\mathrm{GM}}{a}\left[1 + \sum_{n=2}^{\infty}\left(\frac{a_o}{r}\right)^{n+1}\sum_{m=0}^{n}(C_{n,m}\mathrm{cos}m\lambda + S_{nm}\mathrm{sin}m\lambda)P_{nm}(\mathrm{sin}\phi)\right] \tag{2.28}$$

where $P_{n,m}$ are the Legendre associated functions of degree n and order m, $P_{n,0} = P$(n and m are the non-negative integer numbers), and $C_{n,m}$ and $S_{n,m}$ the spherical harmonic coefficients.

Given as the dimensionless quantities, the spherical harmonic coefficients $C_{n,m}$ and $S_{n,m}$ are defined by (*ibid.*)

$$\left.\begin{matrix} C_{n,m} \\ S_{n,m} \end{matrix}\right\} = \frac{2-\delta_{0,1}}{Ma_o^n}\frac{(n-m)!}{(n+m)!}\int_M r'^n \left\{\begin{matrix} \mathrm{cos}m\lambda' \\ \mathrm{sin}m\lambda' \end{matrix}\right\} P_{n,m}\left(\mathrm{sin}\phi'\right)dm \tag{2.29}$$

where M is the total mass of the Earth including its atmosphere, and the Kronecker delta $\delta_{0,1}$ in Equation 2.29 is specified as follows: $\delta_{0,1} = 1$ for $m = 0$, and $\delta_{0,1} = 0$ for $m \neq 0$.

As stated previously, it is assumed that the coordinate origin is identical to the mass centre of the Earth. Therefore, the spherical harmonic coefficients $C_{n,m}$ and $S_{n,m}$ in Equation 2.28 equal zero for $C_{n,m} = S_{n,m} = 0$ for $n = 1$ and $m = 0{,}1$. The spherical harmonic coefficients are further classified as zonal if $m = 0$; tesseral if $m \neq 0$ and $m \neq n$; and sectorial if $m \neq 0$ and $m = 0$. A more detailed clarification of the physical meaning of the spherical harmonic coefficients can be found for instance in Burša and Kostelecký (1999, Chap. 4.3).

Stipulated for the exterior above the upper limit of atmosphere r_{lim} (above which the located atmospheric mass densities generate the gravitational field, which is negligible; approximately 50 km above the Earth's surface), it is assumed that the Earth's gravitational potential in Equation 2.28 satisfies the Laplace equation, so that $\forall r < r_{lim} : \Delta V(r,\Omega) = 0$.

Alternatively to Equation 2.28, the external gravitational potential of the Earth can be described in terms of the fully normalized solid spherical harmonic functions $\overline{Y}_{n,m}(r,\Omega)$ for $(\forall\, r < r_{lim})$ as follows:

$$V(r,\Omega) = \frac{\mathrm{GM}}{a}\sum_{n=0}^{\infty}\sum_{m=-n}^{n}\overline{c}_{n,m}\,\overline{Y}_{n,m}(r,\Omega) \tag{2.30}$$

where $\overline{c}_{n,m}$ are the fully normalized spherical harmonic coefficients. The fully nor-

malized (Laplace's) solid spherical harmonic functions $\overline{Y}_{n,m}(r,\Omega)$ read

$$\begin{aligned} \overline{\mathrm{Y}}_{n,m}(r,\Omega) &= \left(\frac{a}{r}\right)^{n+1} \overline{P}_{n,m}\ \overline{Y}_{n,m}(\Omega) \\ &= \left(\frac{a}{r}\right)^{n+1} \overline{P}_{n,m} \begin{cases} \cos m\lambda, m \geq 0, \\ \sin|m|\lambda, m < 0, \end{cases} \end{aligned} \tag{2.31}$$

where $\overline{P}_{n,m}$ are the fully normalized associated Legendre functions, and $\overline{Y}_{n,m}(\Omega)$ the fully normalized surface spherical harmonic functions.

2.4.1 Earth's gravitational attraction

The vector of gravitational attraction is defined by (Heiskanen and Moritz, 1967)

$$\mathbf{g}(r,\Omega) = \mathbf{grad}\ V(r,\Omega) \tag{2.32}$$

The geocentric spherical coordinate components of the gravitational vector $\vec{g_1}$; namely the meridional $\vec{g}_\phi$, prime-vertical $\vec{g}_\lambda$ and radial $\vec{g}_r$ components; are given by

$$\tilde{\mathrm{g}}_\phi(r,\Omega) = \frac{1}{r}\frac{\partial V(r,\Omega)}{\partial \phi},\ \tilde{\mathrm{g}}_\lambda(r,\Omega) = \frac{1}{r\cos\phi}\frac{\partial V(r,\Omega)}{\partial \lambda},\ \tilde{\mathrm{g}}_r(r,\Omega) = \frac{\partial V(r,\Omega)}{\partial r} \tag{2.33}$$

Equivalently, the gravitational vector $\vec{g_1}$ can be expressed in terms of the Cartesian geocentric coordinate components $g_\mathrm{x} = \partial V/\partial \mathrm{x}$, $g_\mathrm{Y} = \partial V/\partial \mathrm{Y}$ and $g_\mathrm{Z} = \partial V/\partial \mathrm{Z}$. The relation between the vectors of the geocentric and Cartesian coordinate components of the gravitational attraction vector, i.e. $\vec{g_1}(r,\phi,\lambda) = (g_\phi, g_\lambda, g_r)^\mathrm{T}$ and $\vec{g_1}(X,Y,Z) = (g_X, g_Y, g_Z)^\mathrm{T}$ respectively; is defined by the differential coordinate elements of Jacobi's matrix $\mathbf{J}$. The following relation is written

$$\vec{g_1}\ (X,Y,Z) = \mathbf{J}\ \tilde{g}_1(\mathrm{r},\phi,\lambda) \tag{2.34}$$

where the Jacobi's matrix $\mathbf{J}$ reads (see e.g. Burša and Kostelecký, 1999)

$$\mathbf{J} = \begin{bmatrix} \frac{\partial X}{\partial \phi} & \frac{\partial X}{\partial \lambda} & \frac{\partial X}{\partial r} \\ \frac{\partial Y}{\partial \phi} & \frac{\partial Y}{\partial \lambda} & \frac{\partial Y}{\partial r} \\ \frac{\partial Z}{\partial \phi} & \frac{\partial Z}{\partial \lambda} & \frac{\partial Z}{\partial r} \end{bmatrix} = \begin{bmatrix} -\sin\phi\cos\lambda & -\cos\phi\sin\lambda & \cos\phi\cos\lambda \\ -\sin\phi\sin\lambda & \cos\phi\cos\lambda & \cos\phi\sin\lambda \\ \cos\phi & 0 & \sin\phi \end{bmatrix} \tag{2.35}$$

The Earth's gravitational attraction is defined as (ibid.)

$$\mathrm{g}(r,\Omega) = |\mathbf{g}(r,\Omega)| = \sqrt{\left(\frac{\partial V(r,\Omega)}{\partial r}\right)^2 + \frac{1}{r^2}\left(\frac{\partial V(r,\Omega)}{\partial \phi}\right)^2 + \frac{1}{r^2 \cos^2\phi}\left(\frac{\partial V(r,\Omega)}{\partial \lambda}\right)^2} \tag{2.36}$$

where the partial derivatives of the gravitational potential V with respect to the geocentric spherical coordinates ϕ, λ and r are given by Burša and Kostelecký (1999)

$$\frac{\partial V(r,\Omega)}{\partial r} = -\frac{\mathrm{GM}}{r^2} \times \left[1 + \sum_{n=2}^{\infty}(n+1)\left(\frac{a_o}{r}\right)^n \sum_{m=0}^{n}(C_{nm}\cos m\lambda + S_{nm}\sin m\lambda)\mathrm{P}_{\mathrm{nm}}(\sin\phi)\right] \tag{2.37}$$

$$\frac{\partial V(r,\Omega)}{\partial \phi} = \frac{\mathrm{GM}}{r}\sum_{n=2}^{\infty}\left(\frac{a_o}{r}\right)^n \sum_{m=0}^{n}(C_{nm}\cos m\lambda + S_{nm}\sin m\lambda)\frac{\partial P_{\mathrm{nm}}(\sin\phi)}{\partial \phi} \tag{2.38}$$

$$\frac{\partial V(r,\Omega)}{\partial \lambda} = \frac{\mathrm{GM}}{r}\sum_{n=2}^{\infty}\left(\frac{a_o}{r}\right)^n \sum_{m=1}^{n}(-C_{nm}\cos m\lambda + S_{nm}\sin m\lambda)P_{\mathrm{nm}}(\sin\phi) \tag{2.39}$$

The partial derivative of the Legendre associated functions with respect to the geocentric latitude ϕ in Equation 2.38 can be computed recurrently from (*ibid.*)

$$\frac{\partial P_{nm}(\sin\phi)}{\partial \phi} = -m\tan\phi P_{nm}(\sin\phi) + \delta_{0,1}^{(1)} P_{nm}(\sin\phi), \tag{2.40}$$

where $\delta_{0,1}^{(1)} = 1$ for $m \leq n-1$ and $\delta_{0,1}^{(1)} = 0$ for $m = n$

Chapter 3

Theory of heights

3.1 Introduction

The heights of points on the Earth's surface can be determined through connection with a well-defined surface or datum with zero height as well as the vertical distance of points from the surface that must be determined. For heights, different collections of surfaces can be used as reference. A height system is defined as a one-dimensional coordinate system that is used in describing the metric distance relation between a point on the Earth and a particular datum to be known as a height of that point. It is possible to define the height of a point in different ways and accordingly the point will have different height coordinates.

Basically, there are two different types of height systems, however, both have nearly the same order of accuracy Torge (2001). The first one is related to the Earth's gravity field linked to its equipotential surfaces and plumblines. In other words, this system is based on spirit levelling and gravity data along the levelling lines for the sake of obtaining geopotential heights (see Balasubramania, 1994; Featherstone and Kuhn, 2006). The second type ignores the Earth's gravity field represented in the ellipsoidal height system. This system is based on satellite techniques such as Global Positioning System (GPS), Satellite Laser Ranging (SLR), Doppler Orbitography and Radio-positioning Integrated by Satellite (DORIS) and Satellite Altimetry. The selection of proper geodetic height systems is a matter of importance in the augmentation of national geodetic references. Proper geodetic height systems can successfully offer reliable computations in different geodetic aspects, for example, the geopotential heights, geodetic space techniques, updating of the navigation, geodetic and cartographic works, solving some geodynamic tasks, and reinforcing the relations between the countries that having the same systems.

3.2 Geopotential number

Many geodesists prefer using the geopotential numbers in network adjustment rather than heights. The geopotential difference between two equipotential surfaces is a constant, in contrast the height difference between is not constant as long as the gravity change between benchmarks: this so-called non-parallelism of level surface. The non-parallelism phenomenon happens due to several effects, for example, the figure of the Earth, the Earth rotation and the inhomogeneous mass density distribution under the Earth's surface. The geopotential number is also considered as a natural measure of height (Heiskanen and Moritz, 1967; Sneeuw, 2006; Meyer *et al.*, 2007).

To analytically define the geopotential number, let W_O refer to the geopotential benchmark O on the geoid and the geopotential on benchmark to be connected to the geopotential number of benchmark is simply the potential difference between A and O: the geopotential definition can be indicated as

$$\int_O^A g dh = W_O - W_A = C \tag{3.1}$$

where g is the gravity measured along the plumbline, dh is the height difference (in differential meaning). The unit for geopotential numbers is $m^2 s^{-2}$ (Heiskanen and Moritz, 1967, p.162, Eq. 4-8).

3.3 Dynamic height

The dynamic height is given by (Helmert, 1884):

$$H_{dyn} = \frac{C}{\gamma_\phi} \tag{3.2}$$

The choice for γ_ϕ is conventionally taken to be 45 degrees. Hence, dynamic heights and geopotential numbers are single-valued. In other words, dynamic heights come with the same fundamental properties as the geopotential numbers because geopotential numbers are not affected by dividing by variable gravity. Furthermore, dynamic heights are not geometric like the orthometric height. Two different points on the equipotential surface can have the same dynamic height but do not have the same orthometric height. This indicates a clear idea that the dynamic heights have only physical meaning (Heiskanen and Moritz, 1967; Jekeli, 2000). Dynamic heights are not measurable but they can be determined by adding the dynamic correction

to height differences derived from spirit levelling

$$\Delta H_{AO}^{dyn} = \Delta \upsilon_{AO} + DC_{AO} \tag{3.3}$$

where $\Delta \upsilon_{AO}$ is the total measured geometric height difference derived by differential leveling and DC_{AO} is the dynamic correction from station A to O, and it is given by Heiskanen and Moritz (1967, P.163, Eq.4-11) as

$$DC_{AO} = \sum_{O}^{A} \frac{g_i - \gamma_0}{\gamma_\phi} \delta \upsilon_i \tag{3.4}$$

where g_i is the (variable) force of gravity at each levelling observation station, $\gamma_\phi = \gamma_{45^\circ}$, and $\delta \upsilon_i$ are the observed changes in geometric height along each section of the levelling line. As γ_ϕ is always taken on latitude of 45, this enlarges the value of the dynamic correction over inland points that are far from the considered latitude. This could be significant if compared with other corrections applied in first-order levelling (Meyer *et al.*, 2007).

3.4 Orthometric height

The definition of the orthometric heights by Heiskanen and Moritz (1967, p.172), is "the natural heights above the sea level, that is, heights above the geoid". Accordingly they have an unequalled geometrical and physical significance (see, Vaníček and Krakiwsky, 1986, chap16.4). The orthometric height of a point on the Earth surface is measured from the point along the actual plumbline. National Geodetic Survey (1986) defines orthometric height (ibid.) as, "The distance between the geoid and a point measured along the plumbline and taken positive upward from the geoid", with plumbline defined (ibid.) as "A line perpendicular to all equipotential surfaces of the Earth's gravity field that intersect with it", see Figure 3.1. However, in fact they are the length of the plumbline. The plumbline is not a straight line, it has a slight curvature and it relies on gravity in two ways. Firstly, the curve starts from the geoid, which has a direct relation with gravity. Secondly, the plumbline stays everywhere perpendicular to equipotential surface through its passage so the shape of the curve is determined by the orientation of the equipotential surfaces.

From the above definitions, orthometric heights seem apparently geometric, and represent the typical geometric heights (Vaníček *et al.*, 1980) with a clear geometrical meaning (Featherstone and Kuhn, 2005). The orthometric heights are almost related to gravity in addition to being a geometric quantity.

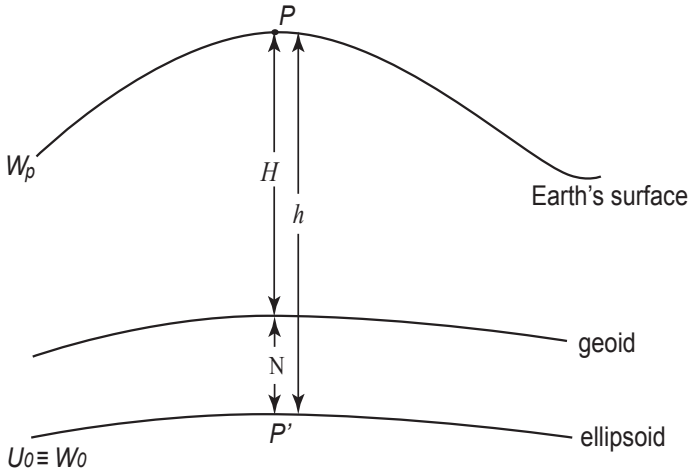

Figure 3.1: The relation between the orthometric, ellipsoidal and geoid heights.

To find the relation between the orthometric height, the gravity and the geopotential we take the equation

$$g = -\delta W/\delta H \tag{3.5}$$

replacing the finite differences by differentials and rearranging leads to the following equation (Heiskanen and Moritz, 1967):

$$C_A = \int_O^{H_A} g \, dh \tag{3.6}$$

where g is the gravity and it is not a constant, therefore, it is supposed to be known at all points along the plumbline between the point on the geoid and the point at the Earth surface. By solving the definite integral in Equation 3.6 the orthometric height at point A is given by dividing the geopotential number by the mean value of the gravity along the plumbline as follows:

$$H_A = \frac{C_A}{\bar{g}} \tag{3.7}$$

To obtain real values of gravity g in Equations 3.5 to 3.6 it requires having enough information about the precise path of the plumbline through the topography (Dentith and Featherstone, 2003; Featherstone and Kuhn, 2006) as well as the gravity variations (Strange, 1982) and actual density along the plumbline (see e.g. Martinec *et al.*, 1995; Hunegnaw, 2001a; Sjöberg, 2004a; Kiamehr and Sjöberg, 2006), which are not possible and hard to fulfill perfectly in practice. For that reason a constant value $\bar{g}$ is considered instead of the unknown values of g.

It is understandable from Equation 3.7 and the previous paragraph about the difficulty of measuring gravity along the plumbline, that it is consequently difficult to obtain the orthometric height in its real meaning. Therefore, the closest we have is

the approximation of the orthometric height. There are several approximations for the orthometric height: the differences between them is based on hypotheses and assumptions to determine the value of the gravity field $\bar{g}$ inside topography.

The following section addresses well-known approximation methods from attempts by several scientists to provide rigorous definitions of the orthometric heights.

3.5 Approximations for the orthometric height

3.5.1 Helmert orthometric height

The idea of computing the approximation of the gravity inside the Earth is based on Poincaré-Prey gravity gradient (Heiskanen and Moritz, 1967; Torge, 2001). The main assumption of using the gravity gradient is for evaluating the approximate value of mean gravity from gravity observed on the Earth's surface (Heiskanen and Moritz, 1967; Vaníček and Krakiwsky, 1986; Tenzer *et al.*, 2005).

The mean gravity $\bar{g}$ in Equation 3.7 is obtained by

$$\bar{g} = g - \left(\frac{1}{2}\frac{\partial\gamma}{\partial h} + 2\pi G\rho^T\right) H \tag{3.8}$$

where g is the surface gravity, the second term in Equation 3.8 is the Poisson equation, that is gravity gradient inside topography (see Tenzer *et al.*, 2005)

For simplicity, the second and third right-hand terms in Equation 3.8 can be numerically evaluated in terms of the orthometric height H as $-\frac{\partial\gamma}{\partial h} = 0.3086\ mGal\ m^{-1}$and by adopting a constant density $\left(\rho^T = 2670\ kg\ m^{-3}\right)$ all around we find the term $2\pi G\rho = 0.1119$

Substituting the terms values in Equation 3.8 we get

$$\bar{g} = g + 0.0424\ H \tag{3.9}$$

and inserting Equation 3.9 in 3.7 we finally get Helmert heights H in metres

$$H = \frac{C}{\bar{g}^H + 0.0424\ H} \tag{3.10}$$

where H denotes Helmert height in kilometres and g in gals.

According to Helmert's assumption, there is no need to account for density variations for quantities inside the Earth or terrain corrections (cf. Allister and Featherstone,

2001; Amos, 2007; Meyer *et al.*, 2007; Filmer, 2011). However, one of the two quantities must be added in the computation of Helmert heights in order to compensate the omission of the unmeasurable quantities (gravity and density variations). These are, firstly, by applying the geopotential number computed from levelling to the mean gravity value $\bar{g}$, or secondly, by adding the orthometric correction OC to the levelling heights differences $\Delta\nu_{AO}$ by the following equation:

$$\Delta H_{AO} = \Delta\nu_{AO} + OC_{AO} \tag{3.11}$$

The orthometric correction OC_{AO} is given by (Heiskanen and Moritz, 1967; Meyer *et al.*, 2007)

$$OC_{AO} = \sum_{A}^{O} \frac{g_i - \gamma_0}{\gamma_0}\,\delta\nu_i + \frac{\bar{g}_A - \gamma_0}{\gamma_0}\,H - \frac{\bar{g}_B - \gamma_0}{\gamma_0}\,H_O \tag{3.12}$$

where γ_0 is the value of normal gravity at 45° latitude, $\bar{g}_A$ and $\bar{g}_O$ are the average gravity values along the plumblines at A and O, and H_A, H_O are the orthometric heights of points A and OB.

It is realised from the above Equations 3.11 and 3.12 that the orthometric height is indirectly measured (Meyer *et al.*, 2007). However, it is practically computed by adding the levelling differences $\Delta\nu_{AO}$ to the orthometric correction OC_{AO}, which is involved with the availability of surface gravity and the average gravity along the plumbline (ibid)

3.5.2 Niethammer's orthometric height

Niethammer's orthometric height Niethammer (1932) represents a special case of Helmert orthometric heights that is taking topography into consideration, particularly in the mountainous areas. The Niethammer's orthometric height is computed based on Niethammer's mean gravity approximation derived by the following equation (cf. Niethammer, 1932; Rapp, 1961; Krakiwsky, 1965; Dentith and Featherstone, 2003).

$$g^N = g + \frac{1}{2}\frac{\partial\gamma}{\partial h}\,H - 2\pi G\rho H + \delta g^{TC} + \frac{1}{H}\int_0^H \bar{\delta g}^{TC}\,dH \tag{3.13}$$

where δg^{TC} is surface topography correction at the benchmark, and $\bar{\delta g}^{TC}$ represents the integral mean topography correction along the plumbline (between the benchmark at the Earth's surface and the geoid).

Considering the total terrain effect, Equation 3.13 is modified (Dentith and Feath-

erstone, 2003):

$$\bar{g}^N = g + \frac{1}{2}\frac{\partial \gamma}{\partial h} H - \delta g^{TC} + \bar{\delta g}^{TC} \tag{3.14}$$

The Niethammer's orthometric heights are considered as the closest approximation to the proper orthometric height by virtue of their superior consistency with topography-corrected gravimetric geoid/quasigeoid models (ibid), however, they need heavy computational efforts. Niethammer's orthometric heights are used in some countries where sufficient gravity and topography data are available.

3.5.3 Mader's orthometric height

Maders orthometric heights (Mader, 1954) are similar to Niethammer's heights with respect to consistency with geoid, but need less effort compared with Niethammer's heights. The error magnitude is positively correlated with mountainous topography (Dentith and Featherstone, 2003). The computation of Mader's orthometric heights is analogously based on adoption of the mean gravity along the plumbline using the following formula (ibid)

$$\bar{g}^M = g + \frac{1}{2}\frac{\partial \gamma}{\partial h} H - 2\pi G\rho H + \frac{1}{2}\left(\delta g^T - \delta g_o^T\right) \tag{3.15}$$

where δg_o^T is the terrain correction at the geoid.

3.6 Contributions in the definition of rigorous orthometric height

A number of contributions have been made by several scientists in order to introduce accurate orthometric height through precise procedures. The derived orthometric heights through these procedures are called the rigorous orthometric heights. This section addresses different outstanding methods for computing rigorous orthometric heights.

Review of recent attempts for computing rigorous orthometric heights

Hwang and Hsiao (2003) demonstrated a formula to compute orthometric correction grounding on mean gravity along the plumbline. The mean gravity along the plumbline was computed based on the modified Mader's method, a method done for

the purpose of considering the rock density variations to compute terrain correction and gravity anomaly gradient. Terrain correction was obtained with the help of an augmented method based on Gaussian quadrature. The impact of the density variations on the orthometric correction over the entire area of Taiwan was found to be very small ($\sim 3\,mm$) but not negligible due to the restricted accuracy of the first-order levelling, and the gravity anomaly gradient is small on flat areas while reaching a decimetre level at mountainous elevations.

Tenzer *et al.* (2005) presented a procedure for the determination of the rigorous orthometric height, which is the best over all attempts. It overcomes the major problem of gravity quantities inside the topography, a problem that prevents orthometric heights from being obtained precisely without approximations. In order to achieve that, the computation of the mean gravity $\bar{g}$ along the plumbline is separated into two parts: (i) The mean normal gravity: it stands for the mean values of gravity that are formed by the topographic and atmospheric masses. (ii) The mean value of the actual gravity disturbance $\delta\bar{g}$ that is generated by geoid-contained masses and the mean values of the topography gravitational attraction (Bouguer shell, terrain roughness and lateral density variations).

It was shown by (Tenzer *et al.*, 2005) that the effect of the mean gravity disturbance generated by masses within the geoid $\delta\bar{g}$ is significant on the obtained orthometric height. The effect magnitude ranges from 1 cm to 50 cm in the rugged part of the Rocky Mountains in Canada. The rigorous orthometric is based on mean gravity $\bar{g}^R$ given by the following equation:

$$\bar{g}^R = \bar{\gamma} + \delta\bar{g}^{NT} + \bar{g}^t + \bar{g}^a \tag{3.16}$$

where $\bar{\gamma}$ is the mean normal gravity inside the topography, $\delta\bar{g}^{NT}$ denotes the mean gravity disturbance generated by the masses inside the geoid, $\bar{g}^t$ denotes the mean topography generated gravitational attraction and $\bar{g}^a$ is the mean atmosphere-generated gravitational attraction.

Santos *et al.* (2006) continued the same way as Tenzer *et al.* (2005) and introduced another procedure to convert Helmert's approximation of the orthometric height into rigorous orthometric height by evaluating the effects of the mean value of the actual gravity disturbance $\delta\bar{g}$ in (Tenzer *et al.*, 2005). The Helmert's orthometric to rigorous orthometric height transformation is given by the total correction ε_{H^o} (cf. Santos *et al.*, 2006). It was found by Santos *et al.* (2006) that the geoid-generated gravity disturbance, the terrain-roughness-generated gravity and the topographic mass-density variations represent the most influential factor on the transformation procedure, while correction for normal gravity is proportionally increasing with re-

spect to the elevation.

Sjöberg (2006) presented a new method to compute the orthometric height as a result of the separation between the ellipsoidal height derived by GPS techniques and the geoid height obtained from downward-continuing the height anomaly derived from the geopotential numbers and local gravity data to the geoid level. As a result, the Helmert orthometric height is corrected in terms of the topographic roughness and lateral density variations of topography. The high correlation between the ellipsoidal and geoidal heights gives no chance for errors to propagate into the orthometric: this shows that the method is not sensitive to systematic errors related to different reference systems used for GPS, geoid model and orthometric height systems.

Manoussakis *et al.* (2008) introduced an analytical model to compute the orthometric height utilising the advantage of the information of the ellipsoidal height h and the surface gravity data while the gravity density variation is not essential. The employed methodology depends on the approximation of the circular-arc of the plumbline and it aims to compute the orthometric height through three elements: the geopotential number C, the magnitude of the gravity vector along the plumbline $\vec{g}$ and the curvature k of the plumbline, where C is derived from the Earth's gravity potential W using the GGM, $\vec{g}$ is computed using the first and second partial derivatives of the disturbing potential T and k derived from the normal potential U. The new orthometric heights were compared with the open source GPS-levelling benchmarks from the US National Geodetic Survey (NGS): 93% of the benchmark points showed an agreement with the NGS orthometric heights of a 3 cm level and 2 cm STD.

3.7 Normal height

The geodetic measurements are reduced to the geoid level, therefore, to fulfill this reduction the density of the Earth's interior masses must be known (Meyer *et al.*, 2007). According to the conservative theory, the geoid represents the basic reference and all geodetic measurements are reduced to it. However, the constraints of obtaining the gravity field between the geoid and the Earth's surface had inspired Molodensky in 1945 to prove that the physical surface of the Earth can be determined alone without having to know the gravity field below the Earth's surface, which is replaced by the telluroid (quasigeoid) as a concept of normal height system (Molodensky *et al.*, 1962).

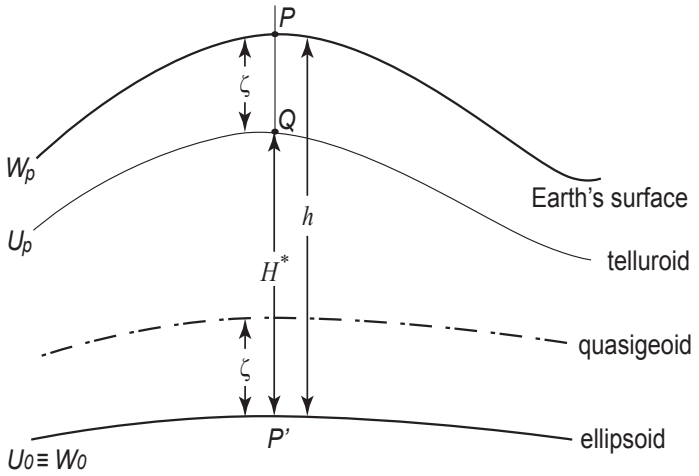

Figure 3.2: The relation between the normal, ellipsoidal and geoid heights.

The main assumption of Molodensky was that the real normal gravity equals the normal gravity potential (Molodensky *et al.*, 1962) $g = \gamma$, $W = U$, and $T = 0$

and re-arranging Equation 3.6 the result will be called the normal height:

$$C = \int_o^{H^N} \gamma \, dh^N = \bar{\gamma} \, H^N \tag{3.17}$$

where H^N is the normal height and $\bar{\gamma}$ is the mean value of the normal gravity along the ellipsoidal normal between the ellipsoid and telluroid: the lower bound of the integral in (Equation 3.17) is referred to the reference ellipsoid.

$$\bar{\gamma} = \frac{1}{H^N} \int_o^{H^N} \gamma \, dh^N \tag{3.18}$$

The normal height H^N can be computed by means of the geopotential number C^N by the following equation (cf. Balasubramania, 1994; Heiskanen and Moritz, 1967)

$$H^N = \frac{C}{\bar{\gamma}} \tag{3.19}$$

and also

$$H^N = \frac{C}{\gamma_\phi} \left[1 + \left(1 + f + m - 2f \, \sin^2\phi \right) \frac{C}{a\gamma_\phi} + \left(\frac{C}{a\gamma_\phi} \right) \right] \tag{3.20}$$

where ω is the angular velocity of the Earth.

The correction term for the normal height OC_{AO} is similarly computed and is given by

$$NC_{AO} = \sum_A^B \frac{\gamma_i - \gamma_\phi}{\gamma_\phi} \, \delta\nu_i + \frac{\bar{\gamma}_A - \gamma_\phi}{\gamma_\phi} \, H_A^N - \frac{\bar{\gamma}_B - \gamma_\phi}{\gamma_\phi} \, H_O^N \tag{3.21}$$

where $\bar{\gamma}_A$ and $\bar{\gamma}_O$ are the average normal gravity values along the plumblines at A

and O, and H_A^N, H_O^N are the normal heights of points A and O.

It was shown by Molodensky *et al.* (1962) that the geodetic height of a point is equal to the sum of normal height and quasigeoid height. Where the normal potential U and the actual potential W have the same value at every point at the telluroid, the distance between the telluroid and the Earth's surface is known as the height anomaly (cf. Amos, 2007; Balasubramania, 1994; Heiskanen and Moritz, 1967). The quasigeoid is similar to the geoid, however, the quasigeoid relates to the telluroid as a basic surface for the normal heights. It only coincides with the geoid on the oceans.

The determination of the normal heights is easy and not requiring considerable effort and time compared with the determination of the orthometric height. Marych and Gudz (1982) studied and investigated the context of Molodensky's first correction concerning quasigeoid height and the gravimetric correction concerning the calculation of normal height. It was found that both terms vanish due to their equivalent values and different signs. This fact makes it possible to simplify the procedure for calculating these corrections.

Despite the similarity between orthometric and the normal height their meaning is completely different (Meyer *et al.*, 2007). Normal heights defined by the normal gravity $\bar{\gamma}$ are in contrast to the orthometric heights that lack a physical meaning and mainly depend on the choice of reference ellipsoid and do not define the equipotential surface, but are still close to the geoid.

3.8 Normal-orthometric height

Normal orthometric height is one of the approximations of the orthometric height. It is regarded as a rough approximation because it is principally used in countries with an acute shortage of surface gravity coverage. In addition, the geopotential numbers are not considered as in the height systems: the normal-geopotential numbers C^n are used instead.

The normal-geopotential numbers are computed from the following formula:

$$C^n = \int_o^{H^{NO}} \gamma \, dh^{NO} \tag{3.22}$$

where dh^{NO} is the height difference

When dividing the normal-geopotential number by the mean value of normal gravity taken along the normal plumbline between the quasigeoid and any arbitrary

point, the normal-orthometric height is computed from the relation (cf. Amos, 2007; Filmer, 2011):

$$H_A^{NO} = \frac{C^{NO}}{\bar{\gamma}} \tag{3.23}$$

Featherstone and Kuhn (2006) indicated that using normal-orthometric heights makes the need for performing gravity measurements, but at the same time the normal-orthometric height will lose the true physical meaning of the orthometric height.

Another way to compute the normal-orthometric heights is by utilising height differences from spirit levelling and the normal-orthometric correction NOC:

$$H^{NO} = \frac{1}{\bar{\gamma}} \sum_{i=1}^{n} \gamma_i \, \Delta h_i + NOC \tag{3.24}$$

where Δh_i are the levelling corrected-height differences.

3.9 New Zealand normal-orthometric correction

The normal-orthometric heights are the current in use heights in the New Zealand geodetic height system. They were mistakenly named as orthometric heights (cf. Gilliland, 1987; DoSLI, 1989; Reilly, 1990). The cumulative normal-orthometric correction NOC was studied by various authors and therefore was translated into different representations, Filmer (2011) analyzed four $NOC's$ introduced by different authors: Rapp (1961), (Bomford, 1971), Heck (1995) and Amos and Featherstone (2009). The cumulative normal-orthometric correction NOC in New Zealand is based on based on GRS67 (IAG, 1971), it is used to derive the NZ normal-orthometric heights to levelling height differences by the following formula (Amos, 2007; Filmer, 2011).

$$NOC = -\left[2\upsilon \, \sin 2\phi_{mid} \left[1 + \left(\nu - 2\frac{\beta}{\nu}\right) \cos 2\phi\right] z\right] H_{av} \delta\phi \tag{3.25}$$

where $\nu = 0.002506$ and $\beta = 0.000007$, ϕ_{mid} denotes the the mid-latitude between the levelling benchmarks. z is $1'$ (in radians), H_{av} is the average height of the instrument at all setups between the benchmarks in metres and $\delta\phi$ the latitude difference between the benchmarks.

3.10 Levelling networks and Ellipsoidal heights

Precise heights above the mean sea level (MSL) are customarily measured by computing height differences using spirit or ordinary levelling. Despite the high precision yielded by traditional levelling methods, these methods are laborious and time-consuming especially for large, remote and mountainous areas. Modern levelling, for example, motorized geometric levelling, motorized trigonometric levelling and 3-dimensional traversing techniques are developed for the sake of reducing time and preserving the accuracy level of the traditional methods (cf. Balasubramania, 1994; Niemeier, 1987)

Traditional levelling methods are divided into two types: direct levelling that straightforwardly describes the method of measuring vertical distance by means of the differences between elevations using precise or semi-precise levelling instruments. And indirect levelling type, which describes the vertical distances by computation and regardless of the points inter-visibility.

Levelling is used for checking the tide gauge stability with regard to different benchmarks (at least three). It is also connected to GPS to evaluate regional gravimetric geoids by computing the differences between the geometrical and undulating heights. Furthermore, the regional levelling networks are connected together with respect to MSL: this sets the possibility of connecting tide gauges together (cf. Becker, 2012). The summation (misclosure) of the height differences is not necessarily equal to zero in the closed levelling lines, no matter the accuracy of the measurements (Heiskanen and Moritz, 1967).

The ellipsoidal height h (see Figure 3.2) is defined as the distance perpendicular to the ellipsoid between the ellipsoid and point P at the Earth's surface (cf. Heiskanen and Moritz, 1967; Jekeli, 2000; Zhang *et al.*, 2005), and it can be derived by different space-geodesy techniques. The ellipsoidal height has no physical meaning: it is a pure geometric length. However, it can be converted to either orthometric H or normal heights H^N through either the geoid height N or the height anomaly ζ (Heiskanen and Moritz, 1967).

Chapter 4

Levelling network analysis

4.1 The unification of LVDs

The unification of LVDs can be done either by a joint adjustment of local levelling networks or by a determination of the gravimetric geoid/quasigeoid model and a subsequent combination of gravity and GPS-levelling data. Two methods were recently applied to unify LVDs in New Zealand based on the latter principle, namely the iterative gravimetric approach and the geopotential-value approach. The iterative gravimetric approach utilises an iterative determination of the regional gravimetric quasigeoid model and its comparison with the geometric quasigeoid model determined using GPS-levelling data for each LVD. The results of this method are provided in terms of the average LVD offsets relative to the regional quasigeoid model. Amos and Featherstone (2009) applied this method to estimate the LVD offsets relative to the NZGeoid05 quasigeoid model. The estimated LVD offsets relative to NZGeoid05 are between 26 cm (for the LVDs One Tree Point 1964, Nelson 1955, and Dunedin-Bluff 1960) and 59 cm (for the LVD Gisborne 1926). Claessens *et al.* (2011) used the same approach to estimate the LVD offsets relative to NZGeoid2009, which is the currently adopted official national quasigeoid model for New Zealand (Amos and Featherstone, 2009). The estimated LVD offsets relative to NZGeoid2009 are between 6 cm (for the LVD One Tree Point 1964) and 49 cm (for the LVD Dunedin 1958). We used the geopotential-value approach in Section 4.3 and in Tenzer *et al.* (2011) to estimate the LVD offsets in New Zealand relative to WHS. WHS is defined by the geoidal geopotential value of W_0, which is adopted by the International Astronomical Union (IAU). The geopotential differences were computed at the GPS-levelling points using the global geopotential model (GGM) coefficients and then averaged for each LVD. The estimated LVD offsets relative to WHS in New Zealand vary between 1 cm (for the LVD Wellington 1953) and 37

cm (for the LVD One Tree Point 1964). A similar method was used by Grafarend and Ardalan (1997b); Ardalan and Garafarend (1999) to calculate the LVD offsets in Baltic countries. It is worth mentioning that different values of W_0 were reported by Sánchez (2007) and Dayoub *et al.* (2011). Sánchez (2007) determined the value of W_0 using different MSL models and different GGMs showing that the choice of MSL and GGM is unimportant for estimating W_0 while the latitude domain of the altimetry-derived MSL models plays a major role. The value of W_0 estimated by Sánchez (2007) differs by 2.5 m^2s^{-2} from the value adopted by IAU. In a more recent study, Dayoub *et al.* (2011) reviewed previous studies using various methods and data sets. They confirmed the conclusions of Sánchez (2007) but reported and recommended a different value of $W_0 = 62636854.2 \pm 0.2$ m^2s^{-2} and established that the dependency of W_0 on the latitude domain is merely due to the mean dynamic topography (MDT).

4.2 Vertical offsets relative to W_0

The geopotential-value approach is utilised to estimate the average offsets of LVDs in New Zealand realised in the system of normal-orthometric heights. The LVD offsets are computed relative to WHS.

The computation of LVD offsets with respect to WHS can be obtained directly from computing the geopotential difference $\delta W_{0,LVD}$ at the collocated GPS and tide-gauge station, which represents the origin for LVD. The geopotential value at the tide-gauge $W_{0,LVD}$ is subtracted from the geoidal geopotential value W_0 to obtain the geoptential difference. The GGM and the ellipsoidal height of the tide-gauge station are utilised to compute the geopotential value $W_{0,LVD}$. Another method to compute the LVD offset was developed by Burke *et al.* (1996) and it is known as the geopotential-value approach. It depends on the resolution of the GGM for averaging the geopotential differences over the GPS-levelling points.

The realisation of the global reference frame was proposed by Burša *et al.* (1999b). Burša *et al.* (1999b, 2001, 2002) applied the geopotential-value approach to estimate the offsets of major LVDs in Europe, North America, and Australia. This method is based on Molodensky's concept of the normal heights according to which the normal gravity potential evaluated at the telluroid equals the actual gravity potential at the Earth's surface (cf. Molodensky *et al.*, 1962). Similarly, a method for computing offsets in Baltic countries was conducted by Grafarend and Ardalan (1997a) and Ardalan and Garafarend (1999).

In the geopotential-value approach, the geopotential difference $\delta W_{0,LVD}$ at GPS-levelling point is obtained from the difference between the normal gravity potential at the telluroid and the actual gravity gravity potential at the Earth's surface. The normal heights of LVD are not realised with respect to the value W_0, but they are referred to MSL at the tide gauge used as the LVD origin (Tenzer *et al.*, 2011). It is very important to consider that the geoid-quasigeoid correction should be added when realising LVD in the system of the orthometric heights For instance, the approximate geoid-quasigeoid correction was applied for instance by Burša *et al.* (1999a) to estimate the average offset of the North American Vertical Datum 1988 (NAVAD 1988) in the system of Helmert's orthometric heights.

4.3 The geopotential-value approach

The principle of this approach is based on estimating the geopotential differences at GPS-levelling points of particular LVD relative to the adopted geoidal geopotential value W_0 (Burša *et al.*, 1997). This method provides the average LVD offsets estimated relative to WHS that is defined by the adopted value of W_0. We applied this method to estimate the LVDs offsets in New Zealand relative to WHS. We used the EGM2008 coefficients complete to degree 2160 of spherical harmonics (in the tide-free system) to compute the gravity potential values at the Earth's surface. The geopotential differences were computed at the GPS-levelling points and then averaged for each LVD. The configuration of the GPS-levelling testing network in New Zealand attributed to 14 LVDs is shown in Figure 4.3.

According to Molodensky's theory of the normal heights (Molodensky *et al.*, 1962), the normal gravity potential U evaluated in the point at the telluroid equals the actual gravity potential W in the corresponding point at the Earth's surface. Hence,

$$U\left(H^N\right) = W(h) \tag{4.1}$$

where H^N denotes the normal height and h the ellipsoidal height. In reality, however, the condition in Equation 4.1 does not hold because the geopotential value $\delta W_{0,LVD}$ at the reference tide-gauge station used as the reference for the normal heights is not the same as the geoidal geopotential value W_0. The geopotential difference $\delta W_{0,LVD}$ between W_0 and $W_{0,LVD}$ is then computed as (cf. Burša *et al.*, 1999b)

$$\begin{aligned} \delta W_{0,LVD} &= W_0 - W_{0,LVD} \\ &= U\left(H^N\right) - W(h) \end{aligned} \tag{4.2}$$

From Equation 4.2, the LVD offset evaluated at the GPS-levelling point is defined as (ibid.)

$$\begin{aligned}\delta H_{0,LVD} &= \frac{\delta W_{0,LVD}}{\bar{\gamma}} \\ &= \frac{U\left(H^N\right) - W(h)}{\bar{\gamma}}\end{aligned} \tag{4.3}$$

where $\bar{\gamma}$ is the integral mean of the normal gravity along the normal plumbline between the level ellipsoid and the telluroid.

The gravity potential W in Equation 4.3 is computed in the point at the Earth's surface from the GGM coefficients complete to degree of spherical harmonics using the following well-known formula (e.g Heiskanen and Moritz, 1967)

$$W = \frac{GM}{r}\sum_{n=0}^{\bar{n}}\sum_{m=-n}^{n}\bar{c}_{nm}\bar{Y}_{nm} + \frac{1}{2}\,\omega^2 r^2 \cos^2\phi \tag{4.4}$$

$$\bar{Y}_{nm} = \left(\frac{a}{r}\right)^n \bar{P}_{nm}(sin\phi)\begin{cases}\cos m\lambda & m \geq 0\\ \sin m\lambda & m < 0\end{cases} \tag{4.5}$$

where r,ϕ,λ are, respectively, the geocentric radius, latitude, and longitude. The normal gravity potential U in Equation 4.3 is computed in the point at the telluroid using Somigliana's formula (Somigliana, 1929; Heiskanen and Moritz, 1967, Eq. 2-62).

$$U = \frac{GM}{ae}\arctan\frac{ae}{u} + \frac{1}{2}\,\omega^2 a^2 \frac{q}{q_0}\left(\sin^2\beta - \frac{1}{3}\right) + \frac{1}{2}\,\omega^2\left(u^2 + a^2e^2\right)\cos^2\beta \tag{4.6}$$

The coefficients q and q_0 in Equation 4.6 read (Heiskanen and Moritz, 1967, Eqns. 2-57, 58)

$$q = \frac{1}{2}\left[\left(1 + 3\frac{u^2}{a^2e^2}\right)\arctan\frac{ae}{u} - 3\,\frac{u}{ae}\right] \tag{4.7}$$

$$q_0 = \frac{1}{2}\left[\left(1 + 3\frac{b^2}{a^2e^2}\right)\arctan\frac{ae}{b} - 3\,\frac{b}{ae}\right] \tag{4.8}$$

The direct transformation of the geocentric spherical coordinates (r,ϕ,λ) to the ellipsoidal coordinates (u,β) is computed using the following equations (Heiskanen and Moritz, 1967, p.228)

$$u^2 = \left(x^2 + y^2 + z^2 - E^2\right)\left[\frac{1}{2} + \frac{1}{2}\sqrt{1 + \frac{4E^2z^2}{\left(x^2 + y^2 + z^2 - E^2\right)}}\right] \tag{4.9}$$

$$\tan\beta = \frac{z\sqrt{u^2 + E^2}}{u\sqrt{x^2 + y^2}} \tag{4.10}$$

where (x,y,z) are the rectangular coordinates, $E = \sqrt{a^2 - b^2}$

The mean value of the normal gravity in Equation 4.3 is evaluated using the following formula (see Heiskanen and Moritz, 1967, Eq. 4-42):

$$\bar{\gamma} \cong \gamma_0 \left[1 - \left(1 + f + m - 2\, f \sin^2\phi\right) \frac{H^N}{a} + \left(\frac{H^N}{a}\right)^2 \right] \tag{4.11}$$

The normal gravity γ_0 at the level ellipsoid is computed from (see Heiskanen and Moritz, 1967, Eq. 2-72)

$$\gamma_0 = \frac{GM}{a\sqrt{a^2 \sin^2\beta + b^2 \cos^2\beta}} \left[1 + \frac{m}{3} \frac{e' q'}{q_0} \sin^2\beta + \left(1 - m - \frac{m}{6} \frac{e' q'}{q_0}\right) \right] \tag{4.12}$$

where $e' = \left(\sqrt{a^2 - b^2}\right)/b$ is the second numerical eccentricity of the level ellipsoid, q_0 is defined in Equation 4.8 and q' reads

$$q' = 3\left(1 + \frac{b^2}{a^2 e^2}\right)\left(1 - \frac{b}{ae} \arctan\frac{ae}{b}\right) - 1 \tag{4.13}$$

4.3.1 Conversion of heights between permanent tide systems

We are aware that the normal-orthometric heights are referred to the mean-tide system and the ellipsoidal heights in the geodetic datum NZGD2000 are defined in the tide-free system. Therefore, we considered the inconsistency of using two different permanent tide systems by converting the normal heights from the mean-tide to tide-free system. We set our analysis to be realised in the zero-frequency tide, tide-free, or the mean-tide system (Report, 1995; Vatrt, 1999). Zadro and Marussi (1973) derived the formula that defines the direct zero-frequency tide-forming gravitational potential $\Delta W_{zero-tide}$ generated by the perturbation body P (Moon and Sun) in the following form

$$\begin{aligned} \Delta W_{zero-tide,P} = {} & \frac{GM}{\bar{r_p}} \sum_{n=2}^{\bar{n}} \left(\frac{r}{r_p}\right)^n P_n(\sin\phi) \\ & \times \sum_{m=0}^{n/2} (-1)^m \frac{(2n-2m)!(n+1)!}{m!(n-m)!} \\ & \times \sum_{i=0}^{n/2} \frac{e_P^i}{(n-i+1)!(i!!)^2} \sum_{j=0}^{n-2m} \frac{\sin^j \varepsilon_0 (\sin\chi_P)^{n-2m-j}}{[(n-2m+j)!!]^2 (j!!)^2} \end{aligned} \tag{4.14}$$

where $GM_{Moon} = 4902.8 \times 10^9\ m^3 s^{-2}$ is the selenocentric gravitational constant; $GM_{Sun} = 13271244 \times 10^{13}\ m^3 s^{-2}$ is the heliocentric gravitational constant and

are the mean geocentric distances of the Moon and Sun; $e_{Moon} = 0.05490$ and $e_{Sun} = 0.01671$ are the eccentricities of their orbits; $\chi_{Moon} = 5.15\ arc - deg$ and $\chi_{Sun} = 0°$ are the inclinations to the ecliptic; $\varepsilon_0 = 23.439278°$ is the obliquity of the ecliptic and i and j are defined for even numbers.

The permanent tide systems are defined by the four fundamental parameters of the Earth: the geocentric gravitational constant GM (Ries *et al.*, 1992; Report, 1995), the mean angular velocity of the Earth's rotation $\omega = 7{,}292{,}115 \times 10^{-11}\ rads^{-1}$ (Report, 1995), the geoidal geopotential value W_0= 62636856±0.5 m^2s^{-2} (Burša *et al.*, 1997) and the second zonal parameter $c_{2,0}$. Whereas the parameters GM, ω and W_0 are not dependent on the tide, the second zonal parameter $c_{2,0}$ is tide-dependent. Alternatively, the permanent tide systems are defined by the set of the following four Earth's parameters: GM, ω and a, and f. The conversion of heights between the permanent tide systems is defined by (Rapp, 1989; Vatrt, 1999)

$$H_{mean-tide} = H_{tide-free} - (1 + k_w - h_w)\frac{\Delta W_{zero-tide}}{g} \tag{4.15}$$

$$H_{zero-tide} = H_{tide-free} - (k_w - h_w)\frac{\Delta W_{zero-tide}}{g} \tag{4.16}$$

$$H_{mean-tide} = H_{zero-tide} - \frac{\Delta W_{zero-tide}}{g} \tag{4.17}$$

where k_w and h_w are the tidal Love numbers. The term ${\hat{I}\check{T}W_{zero-tide}}/{g}$ can be computed with a sub-centimeter accuracy using the following expression (Heikkinen, 1978)

$$\frac{\Delta W_{zero-tide}}{g} \approx -0.198\left(\frac{3}{2}\sin^2\phi - \frac{1}{2}\right) \tag{4.18}$$

The global differences of heights defined in the three permanent tide systems are shown in Figure 4.1. The largest differences up to 20 cm are between the heights defined in the mean-tide and zero-tide systems. The differences between heights defined in the mean-tide and tide-free systems are up to about 14 cm. The smallest absolute differences to about 6 *cm* are between the heights defined in the zero-tide and tide-free systems. The height conversion between the mean-tide and tide-free system is computed using Equation 4.15, the tidal Love numbers $k_w = 0.3$ and $h = 0.6$ were adopted. The differences of the heights in these two tide systems at the points of the GPS-levelling testing network bounded by latitudes (−35.1243° and −46.7950°) vary from 0.0 to 4.1 cm(Tenzer *et al.*, 2011).

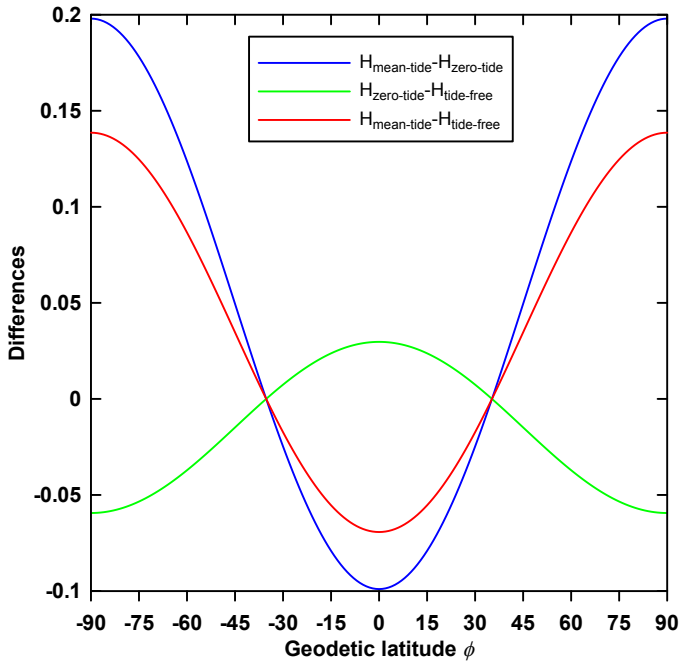

Figure 4.1: The global differences of heights defined in the three permanent tide systems.

4.3.2 Numerical results on the geopotential-value approach

The average LVD offsets in New Zealand are estimated in three stages as follows. Step 1, the conversion of the normal-orthometric heights to the normal heights. Step 2, the tide system was unified to the tide-free system by transforming the tide system of the normal heights to the corresponding tide system of which the ellipsoidal heights at the GPS-levelling points are defined. Step 3, the geopotential-value approach was applied to estimate the LVD offsets.

Table 4.1: The estimated average offsets and their uncertainties (based on LS) of 14 LVDs in New Zealand. The LVD offsets are taken relative to W_0. Unit : 1 cm .

North Island		South Island	
LVD	Offsets	LVD	Offsets
Auckland 1946	12 ± 4	Bluff 1955	17 ± 4
Gisborne 1926	10 ± 4	Deep Cove 1960	30 ± 45
Moturiki 1953	19 ± 9	Dunedin-Bluff 1960	23 ± 7
Napier 1962	24 ± 6	Dunedin 1958	7 ± 18
One Tree Point 1964	37 ± 5	Lyttelton 1937	13 ± 11
Taranaki 1970	12 ± 6	Nelson 1955	20 ± 9
Wellington 1953	1 ± 2	Tarakohe 1982	23 ± 3

The geopotential differences at the GPS-levelling points were computed using Equation 4.2 and then averaged for each of 14 LVDs in New Zealand. The estimated av-

erage geopotential values and the corresponding geopotential differences of 14 LVDs in New Zealand are summarised in Table 4.2.

The estimated average offsets of 14 LVDs within the South and North islands of New Zealand vary from 1 cm (Wellington 1953 LVD) and 37 cm (One Tree Point 1964 LVD). The estimated standard deviations of the average LVD offsets vary from 2 cm (Wellington 1953 LVD) up to 14 cm (Dunedin 1958 LVD). There are different sources contaminating the average LVD offsets with errors due to the commission errors of the EGM2008 coefficients, and additional errors up to several centimetres are expected due to erroneous GPS and levelling measurements. In addition, there are errors due to the tectonic and other unknown vertical deformations of New Zealand's levelling networks beside the omission errors of EGM2008.

Table 4.2: The estimated average geopotential values and the corresponding geopotential differences of 14 LVDs in New Zealand with respect to the geoidal geopotential value. Unit: 1 $m^2 s^{-2}$.

North Island		
LVD	$\overline{W}_{0,LVD}$	$\delta\overline{W}_{0,LVD}$
Auckland 1946	62,636,854.8	1.2
Gisborne 1926	62,636,855.0	1
Moturiki 1953	62,636,854.1	1.9
Napier 1962	62,636,853.6	2.4
One Tree Point 1964	62,636,852.4	3.6
Taranaki 1970	62,636,854.8	1.2
Wellington 1953	62,636,855.9	0.1
South Island		
LVD	$\overline{W}_{0,LVD}$	$\delta\overline{W}_{0,LVD}$
Bluff 1955	62,636,854.3	1.7
Deep Cove 1960	62,636,853.1	2.9
Dunedin-Bluff 1960	62,636,853.7	2.3
Dunedin 1958	62,636,855.3	0.7
Lyttelton 1937	62,636,854.7	1.3
Nelson 1955	62,636,854.0	2.0
Tarakohe 1982	62,636,853.7	2.3

4.4 The joint adjustment approach

The normal-orthometric-corrected loop closures are not independent over the levelling route taken (Featherstone and Kuhn, 2006). However, the accurate computation of the cumulative normal to normal-orthometric height correction to levelled height

differences is restricted (in the absence of observed gravity data along levelling lines) by the cumulative effect of the GGM commission and omission errors especially in mountainous regions of New Zealand with large spatial gravity and elevation gradients. Therefore, the observation equations in the joint adjustment of levelling networks were formed for the normal-orthometric-corrected loop closures, while disregarding the holonomity property (meaning, among other things, that the normal or orthometric corrected loop closures are equal zero independently on the levelling route; cf. Sansò and Vaníček, 2006).

When LVDs are defined in the system of the normal-orthometric heights, the cumulative normal to normal-orthometric height correction $\delta H^{N,NO}$ is applied. The computation of this correction at the surface points along levelling lines is done using the following expression (Tenzer *et al.*, 2011):

$$\begin{aligned}\delta H^{N,NO} &= \frac{1}{\bar{\gamma}}\sum_i g_i\,\delta n_i - \frac{1}{\bar{\gamma}}\sum_i\left[\gamma_{0,i} + \frac{\partial\gamma}{\partial h}\,H_i^{NO}\right]\delta n_i \\ &= \frac{1}{\bar{\gamma}}\sum_i \Delta g_i\,\delta h_i \end{aligned} \tag{4.19}$$

As seen from Equation 4.19, the normal to normal-orthometric height correction is calculated by a summation of the levelled height differences δh_i that are multiplied by the corresponding values of the gravity anomaly Δg_i. In the absence of the observed gravity data the gravity anomalies along levelling lines are generated from GGM. A similar method was used by Filmer *et al.* (2010) for the conversion of the normal-orthometric to normal heights in the Australian Height Datum. They used EGM2008 to reconstruct the observed gravity anomalies at the levelling benchmarks of the Australian National Levelling Network. Filmer *et al.* (2010) computed the correction as a function of the gravity disturbances instead of using the gravity anomalies Δg_i (Tenzer *et al.*, 2011). Since the normal gravity data that used for the definition of the normal-orthometric heights were calculated based on the levelled height differences, the definition of in Equation 4.19 as a function of the gravity anomalies is more rigorous. However, our test results at the New Zealand's levelling networks revealed that the differences in the values of this correction computed using the gravity disturbances δg_i and the gravity anomalies Δg_i are below 0.1 mm and thus completely negligible.

When adopting the Helmert's orthometric heights (see Equation 3.19), the geoid-to-quasigeoid correction $\delta H^{O,N}$ is computed approximately as a function of the (topographic) height H and the simple planar Bouguer gravity anomaly Δg^{SB} at the

observation point using the following formula (Santos *et al.*, 2006)

$$\delta H^{O,N} \cong -H \frac{\Delta g^{SB}}{\gamma_0} \tag{4.20}$$

where γ_0 is the normal gravity evaluated at the surface of the reference ellipsoid. The simple planar Bouguer gravity anomaly Δg^{SB} is computed by (e.g. Heiskanen and Moritz, 1967, p. 131)

$$\Delta g^{SB} = \Delta g - 2\pi G \rho_0 H \tag{4.21}$$

where Δg is the (free-air) gravity anomaly. We note here that either the available normal-orthometric or normal heights can be used in Equation 4.20 as the differences in computed values of the correction $\delta H^{O,N}$ due to using different types of heights are completely negligible.

When LVD is realised in the system of the orthometric heights, the geoid-to-quasigeoid correction is applied. The relation between the normal and (Helmert's) orthometric heights is defined as a function of the simple planar Bouguer gravity anomaly and the topographic height of the computation point (Heiskanen and Moritz, 1967). More rigorous definitions of the orthometric heights and the geoid-to-quasigeoid correction can be found in (Tenzer *et al.*, 2005) and Santos *et al.* (2006).

We have used the levelling and normal gravity data for a joint adjustment of the local levelling networks at the North and South islands of New Zealand fixing the heights of the tide-gauge reference points in Dunedin and Wellington. The choice of these tide-gauge stations was based on the analysis of the GPS-levelling data attributed to 14 LVDs in New Zealand that showed that the LVDs Wellington 1953 and Dunedin 1958 have the smallest average offsets relative to WHS, see Table 4.1. The results of the joint levelling adjustment revealed that the STD of least-squares residuals of normal-orthometric-corrected height differences in New Zealand is 2 mm. The residuals at the levelling benchmarks at the South Island range between ± 1.3 *cm*, while the range of residuals at the North Island's levelling benchmarks is between -2.5 and 2.6 cm.

4.4.1 Input-data description for the joint adjustment

The precise levelling data used in this study comprise 10,150 benchmarks (5,967 levelling benchmarks at the North's Island and 4,183 levelling benchmarks at the South Island). The configuration of the New Zealand's levelling networks is shown in

Figure 4.4. The whole network consists of 14 LVDs (Auckland 1946, Gisborne 1926, Moturiki 1953, Napier 1962, One Tree Point 1964, Taranaki 1970, and Wellington 1953 at the North Island; Bluff 1955, Deep Cove 1960, Dunedin-Bluff 1960, Dunedin 1958, Lyttelton 1937, Nelson 1955 and Tarakohe 1982 at the South Island). As seen in Figure 4.3b, large parts of the South Island are not sufficiently covered by levelling profiles along the mountainous regions of the Southern Alps. Over most of the North Island the coverage of levelling networks is much better except for some irregularities along the mountainous regions of the central and lower North Island.

The cumulative normal-orthometric correction is recomputed using the normal gravity field parameters of the GRS80 reference ellipsoid (Moritz, 1980). Our test results confirmed the finding of Filmer *et al.* (2010) that the differences between the values of the cumulative normal-orthometric correction computed for the GRS67 and GRS80 normal gravity field parameters are completely negligible. The GGM coefficients used in this study to generate the gravity field quantities were taken from EGM2008; see Pavlis *et al.* (2012).

4.4.2 Numerical results on the joint adjustment

The least-squares residuals between the measured and adjusted normal-orthometric-corrected height differences at the levelling benchmarks are shown in Figure 4.4. The histograms of residuals are shown in Figure 4.2. The statistics of the residuals at the levelling networks at the North and South islands are summarised in Table 4.3.

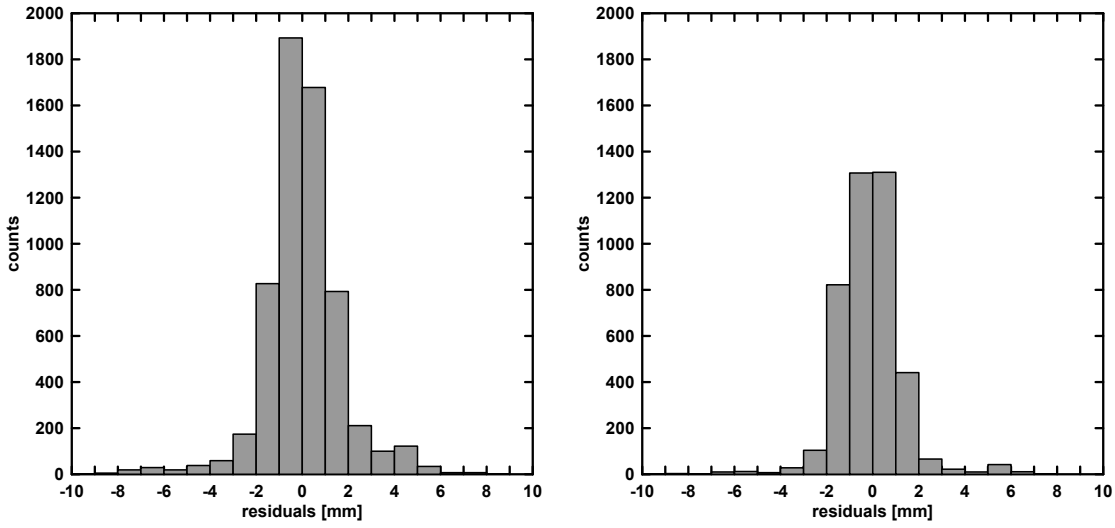

(a) North Island. **(b)** South Island.

Figure 4.2: The histograms of the least-squares residuals between the measured and adjusted normal-orthometric-corrected height differences at levelling benchmarks.

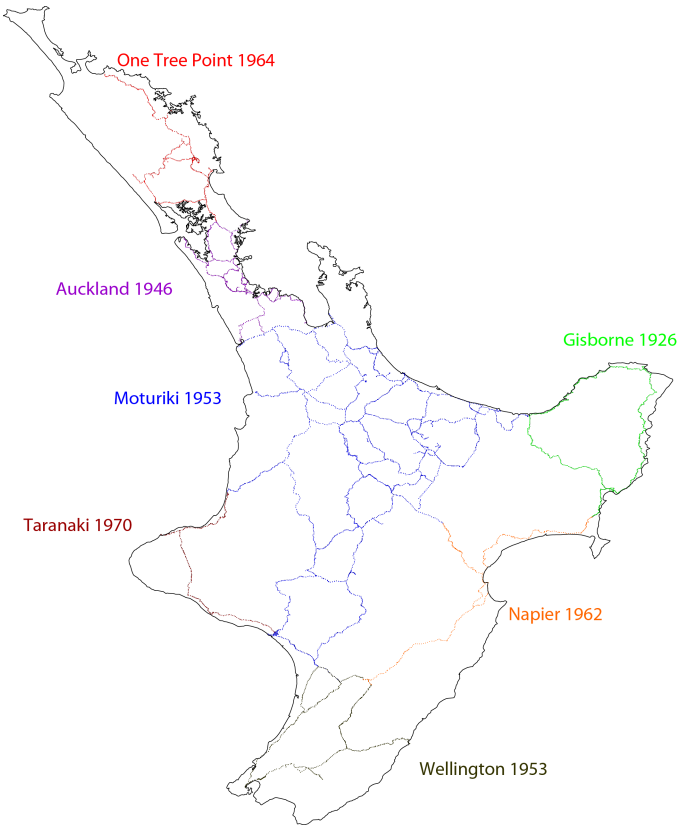

(a) North Island.

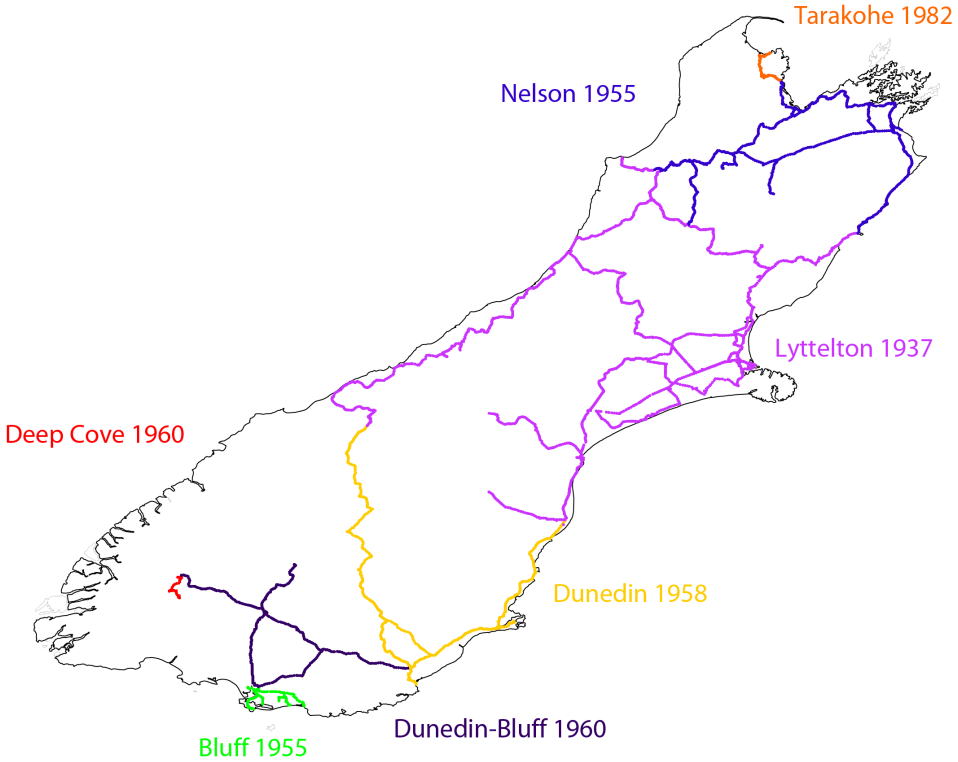

(b) South Island.

Figure 4.3: The levelling networks at the South and North islands of New Zealand attributed to 14 LVDs.

Table 4.3: Statistics of the least-squares residuals between the measured and adjusted normal-orthometric-corrected height differences between the levelling benchmarks at the North and South islands of New Zealand.

North Island			
LVD	Min	Max	Mean
Auckland 1946	-0.8	0.8	0.1
Gisborne 1926	-1.0	0.9	0.2
Moturiki 1953	-0.8	0.0	0.2
Napier 1962	-0.7	0.6	0.1
One Tree Point 1964	-2.5	2.6	0.3
Taranaki 1970	-0.6	0.7	0.1
Wellington 1953	-1.9	1.9	0.2
North Island	**-2.5**	**2.6**	**0.2**
South Island			
Bluff 1955	-0.5	0.5	0.1
Deep Cove 1960	-0.2	1.4	0.1
Dunedin-Bluff 1960	-0.2	0.0	0.1
Dunedin 1958	-1.0	1.0	0.2
Lyttelton 1937	-1.0	1.1	0.2
Nelson 1955	-1.3	1.3	0.2
Tarakohe 1982	-0.3	0.3	0.1
South Island	**-1.3**	**1.4**	**0.2**

The results of the least-squares analysis revealed a good quality of levelling data (by means of the least-squares residuals between the measured and adjusted normal-orthometric-corrected height differences at levelling benchmarks) especially at the local levelling networks Tarakohe 1982 ($\pm$0.3 cm) and Dunedin-Bluff 1960 ($-$0.2 to 0.0 cm) at the South Island. The largest residuals are found at the local levelling networks One Tree Point 1964 ($-$2.5 to 2.6 cm) and Wellington 1953 ($\pm$1.9 cm) at the North Island. The local levelling networks Moturiki 1953 (at the North Island) and Deep Cove 1960 (at the South Island) have a systematic trend (mostly positive or negative) in residuals more likely due to their location in mountainous regions with large horizontal elevation gradients.

4.5 Height conversion

The newly determined normal-orthometric heights were used to determine the normal and (Helmert's) orthometric heights. The height conversion is realised at 10,150 points (5,967 levelling benchmarks at the North Island, and 4,183 levelling benchmarks at the South Island) of the national precise levelling networks. The configuration of the levelling networks at the North and South islands of New Zealand is shown in Figure 4.4. The whole network is attributed to 14 local vertical datums (LVDs) of which the normal-orthometric heights were determined relative to the MSL estimated based on the analysis of tide-gauge records (or connecting to the existing levelling network). For more information we refer the reader to Amos (2007), Amos and Featherstone (2009), Claessens *et al.* (2009, 2011), and Tenzer *et al.* (2011).

4.5.1 Conversion methodology

The theory of heights is commonly used for a practical realisation of the geodetic vertical reference systems worldwide. The orthometric height H is defined in Equation 3.7. However, a true orthometric height cannot be computed exactly (Jekeli, 2000), because the accurate values of the gravity inside the topography cannot be measured (cf. Tenzer *et al.*, 2005). There are a number of different methods of approximating resulting in several variants of orthometric heights as we described it in Chapter 3. The most commonly used type is orthometric height Helmert (1890) that uses the Poincaré-Prey's linear vertical gravity gradient in the definition of the mean gravity (Heiskanen and Moritz, 1967, p. 167) (see Equation 3.8). The commutative normal to normal-orthometric height correction (Equation 4.19) is computed by utilising levelling and gravity anomaly data (cf. Filmer *et al.*, 2010). The correction is then used to convert the normal-orthometric heights to the normal heights.

4.5.2 Numerical results and analysis of height differences

The computation of the cumulative normal to normal-orthometric height correction was done using levelling and gravity anomaly data according to Equation 4.21. The gravity anomalies at the Earth's surface along the levelling lines were calculated using the coefficients taken from EGM2008 complete to degree 2160 of spherical harmonics (Pavlis *et al.*, 2012). The computed values of the EGM2008 gravity anomalies at the levelling benchmarks vary from -157.1 to 115.4 mGal (the gravity

anomalies vary from -84.2 to 115.4 mGal at the South Island's levelling benchmarks, and between -157.1 and 102.5 mGal at the North Island's levelling benchmarks).

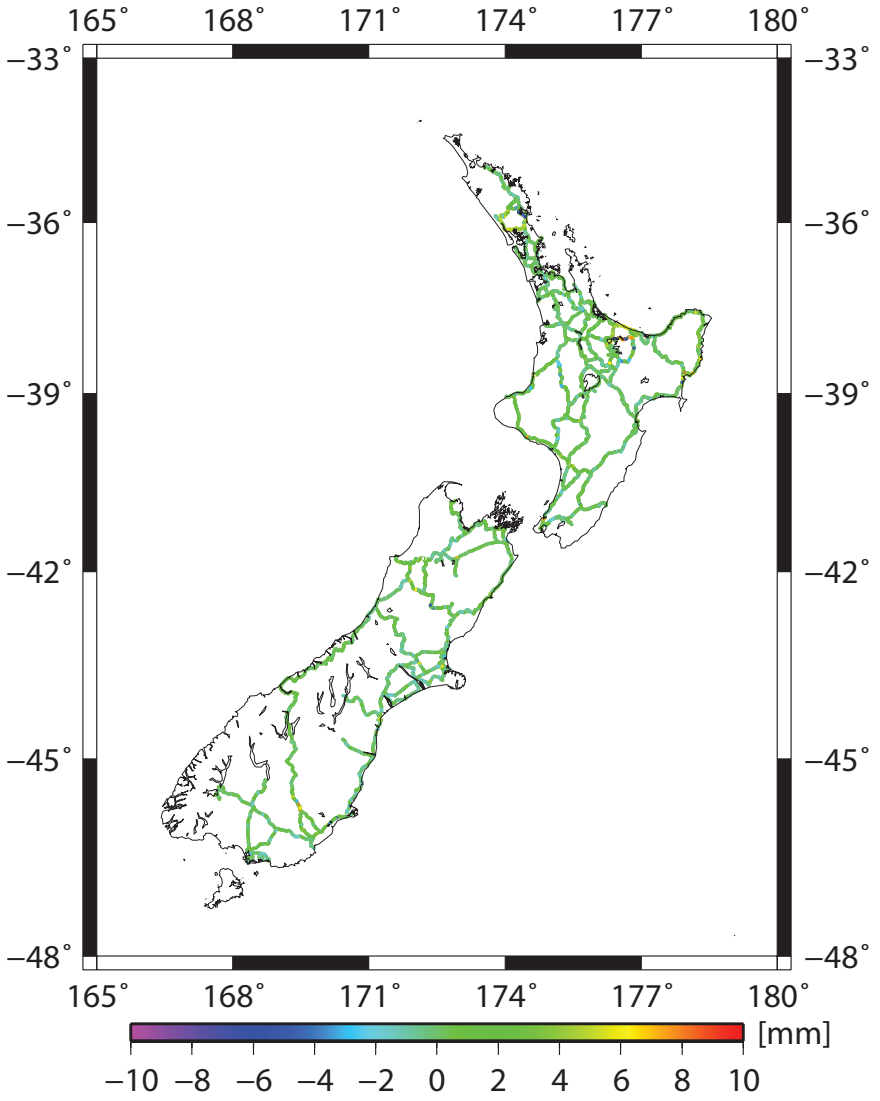

Figure 4.4: The least-squares residuals between the measured and adjusted normal-orthometric-corrected height differences at the levelling benchmarks after the joint adjustment of local levelling networks at the South and North islands of New Zealand. Unit: 1 mm.

The values of the normal to normal-orthometric height correction computed at the levelling benchmarks in New Zealand are shown in Figure 4.5a, and their statistics are given in Table 4.4. At the North Island's levelling benchmarks the correction $H^{N,NO}$ varies from -4.9 to 10.7 cm, while it varies between -2.6 and 5.7 cm at the South Island's levelling benchmarks. The mostly positive values of this correction have their maxima at the levelling lines crossing mountainous regions of the central North Island (LVD Moturiki 1953) and the upper South Island (LVD Lyttelton 1937). The largest negative values of this correction are at the central levelling segment of LVD Napier 1962. Moreover, large negative values of this correction

are also found at levelling lines along the coastline of the west coast of the South Island (LVD Lyttelton 1937) and the east coast of the North Island (LVD Gisborne 1926). Both, the maxima and minima of this correction are situated at the levelling segments with the largest horizontal gravity and terrain elevation gradients.

Table 4.4: Statistics of the normal to normal-orthometric height correction computed at the levelling benchmarks. Unit: 1 cm.

North Island				
LVD	Min	Max	Mean	RMS
Auckland 1946	0.0	1.4	0.3	0.3
Gisborne 1926	-3.3	2.6	-1.6	1.4
Moturiki 1953	-0.5	10.7	2.8	3.2
Napier 1962	-4.9	2.9	-0.9	1.6
One Tree Point 1964	-0.2	2.3	0.3	0.4
Taranaki 1970	-0.1	1.5	0.6	0.4
Wellington 1953	-0.5	2.2	0.7	0.6
North Island	**-4.9**	**10.7**	**0.3**	**0.7**
South Island				
Bluff 1955	-0.1	0.2	0.0	0.1
Deep Cove 1960	-0.1	0.1	0.0	0.01
Dunedin-Bluff 1960	-0.1	1.6	0.0	0.3
Dunedin 1958	-0.1	2.2	0.0	0.3
Lyttelton 1937	-2.6	5.7	-0.5	1.2
Nelson 1955	-0.1	5.6	1.4	0.8
Tarakohe 1982	0.0	5.1	1.0	1.5
South Island	**-2.6**	**5.7**	**0.4**	**0.4**

The computation of the approximate geoid-to-quasigeoid correction $\delta H^{O,N}$ was done according to Equation 4.20. The values of the simple planar Bouguer gravity anomalies Δg^{SB} were computed from the gravity anomalies Δg according to Equation 4.21. The gravity anomalies at the levelling benchmarks were calculated using the EGM2008 coefficients complete to degree 2160 of spherical harmonics. The corresponding values of the simple planar Bouguer gravity anomalies are between -166.0 and 91.4 mGal (from -111.5 to 91.4 mGal at the South Island's levelling benchmarks, and from -166.0 to 73.1 mGal at the North Island's levelling benchmarks). We note here that a smoothing effect of the simple Bouguer reduction on gravity data is not significant due to a low spatial resolution of the EGM2008 gravity anomalies.

The values of the geoid-to-quasigeoid correction computed at the levelling benchmarks in New Zealand are shown in Figure 4.5b, and their statistics are given in Table 4.5. This correction is mostly positive. At the North Island's levelling bench-

marks this correction varies from -1.5 to 9.0 cm, while it varies from -2.5 to 6.5 cm at the levelling benchmarks at the South Island. The maxima of this correction are at the levelling benchmarks located at high elevations in mountainous regions of the Southern Alps (at the South Island) and the central North Island.

Table 4.5: Statistics of the geoid-to-quasigeoid correction computed at the levelling benchmarks. Unit: 1 cm.

North Island				
LVD	Min	Max	Mean	RMS
Auckland 1946	-0.8	0.0	0.1	0.1
Gisborne 1926	0.6	3.7	0.0	1.5
Moturiki 1953	-1.5	6.2	0.6	1.5
Napier 1962	-1.1	9.0	1.0	1.6
One Tree Point 1964	-1.2	0.0	-0.1	-0.2
Taranaki 1970	-0.4	1.7	0.3	0.3
Wellington 1953	-1.0	1.7	0.2	0.3
North Island	**-1.5**	**9.0**	**0.2**	**1.1**
South Island				
Bluff 1955	-0.2	0.0	-0.1	0.0
Deep Cove 1960	0.4	0.8	0.6	0.1
Dunedin-Bluff 1960	-0.6	1.1	0.1	0.4
Dunedin 1958	-1.1	4.1	-0.1	0.1
Lyttelton 1937	-2.5	6.5	0.2	0.5
Nelson 1955	-1.4	2.2	0.1	0.3
Tarakohe 1982	-0.9	2.4	-0.0	0.1
South Island	**-2.5**	**6.5**	**0.2**	**0.6**

The presence of the largest (positive) values of the geoid-to-quasigeoid correction is explained by prevailing negative values of the Bouguer gravity anomalies in mountainous regions. Over the flat regions with low elevations, this correction is mostly negative due to mainly positive values of the Bouguer gravity anomalies in these areas.The differences between the Helmert's orthometric and normal-orthometric heights at the levelling benchmarks in New Zealand are shown in Figure 4.5c and the statistics are given in Table 4.6. At the North Island's levelling benchmarks these differences vary between -3.2 and 13.0 cm, and between -2.9 to 7.9 cm at the levelling benchmarks at the South Island.

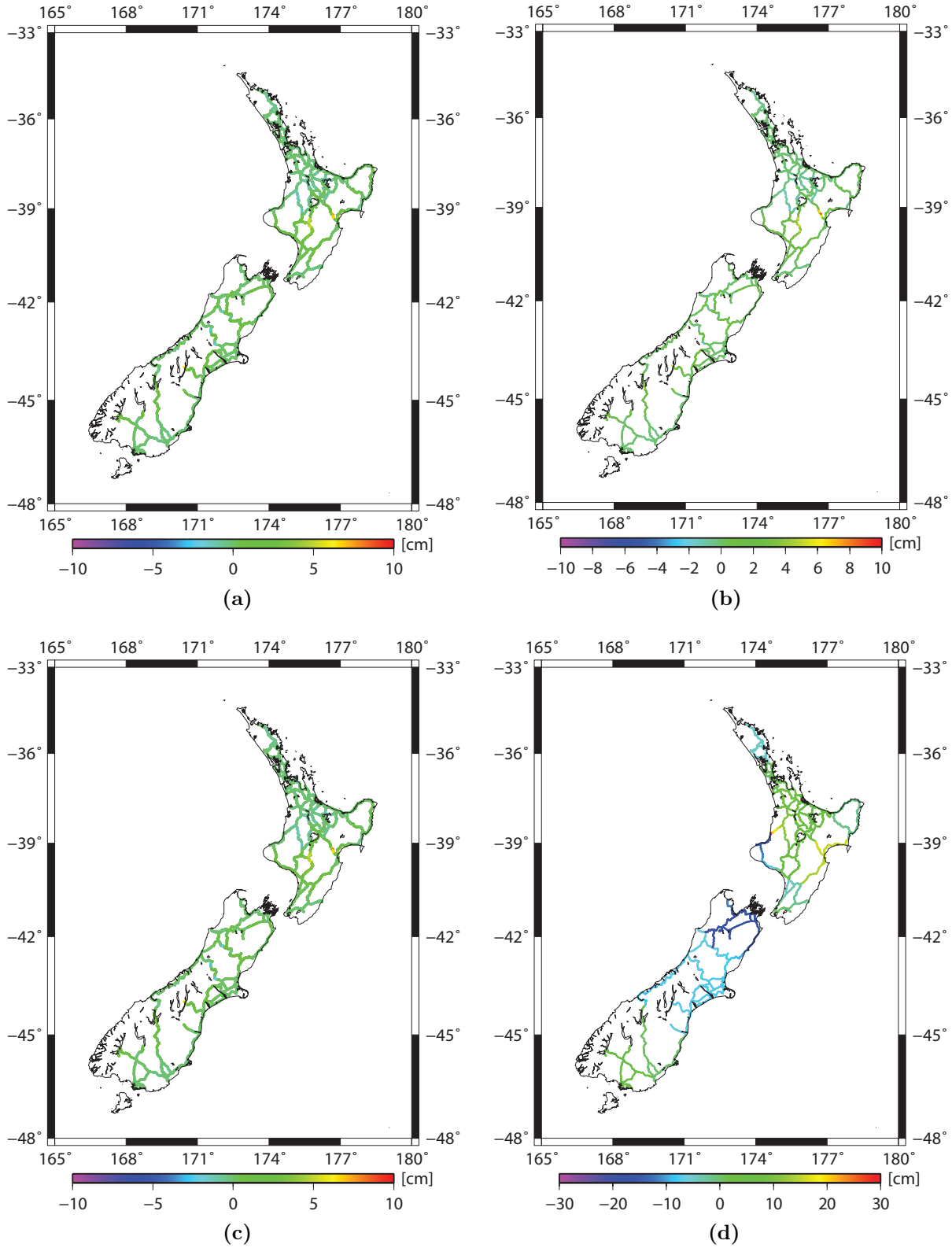

Figure 4.5: a)The normal to normal-orthometric height correction computed at the levelling benchmarks in New Zealand, (b) The geoid-to-quasigeoid correction computed at levelling benchmarks in New Zealand, (c) The differences between the Helmert's orthometric and normal-orthometric heights, (d) Differences between the original and newly determined normal-orthometric heights of the levelling benchmarks at the North and South islands of New Zealand. Unit: 1 cm.

Table 4.6: Statistics of the differences between the Helmert's orthometric and normal-orthometric heights at the levelling benchmarks. Unit: 1 cm.

North Island				
LVD	Min	Max	Mean	RMS
Auckland 1946	-0.8	0.8	0.0	0.2
Gisborne 1926	-3.0	3.7	-0.1	1.3
Moturiki 1953	-1.5	13.0	1.5	3.1
Napier 1962	-3.2	9.0	0.5	1.3
One Tree Point 1964	-1.2	1.3	0.0	-0.2
Taranaki 1970	-0.4	2.2	0.4	0.6
Wellington 1953	-0.9	3.4	0.4	0.6
North Island	**-3.2**	**13.0**	**1.2**	**2.7**
South Island				
Bluff 1955	-0.2	0.0	0.0	0.05
Deep Cove 1960	0.4	0.8	0.5	0.3
Dunedin-Bluff 1960	-0.6	2.3	0.3	0.5
Dunedin 1958	-1.1	4.3	0.3	0.7
Lyttelton 1937	-2.9	7.9	0.1	1.0
Nelson 1955	-1.4	5.9	0.8	1.0
Tarakohe 1982	-0.9	7.6	0.5	1.4
South Island	**-2.9**	**7.9**	**0.4**	**0.6**

The new normal-orthometric heights at the levelling benchmarks were computed from the heights of the fixed tide-gauge reference benchmarks and the adjusted normal-orthometric-corrected height differences. The differences between the newly determined and original normal-orthometric heights of the levelling benchmarks in New Zealand are shown in Figure 4.5d and their statistics are given in Table 4.7. These differences are between -26.5 and 23.4 cm at the North Island's levelling benchmarks and between -21.6 and 6.5 cm at the South Island's levelling benchmarks. The individual comparison of the differences between the newly determined and original normal-orthometric heights at 14 LVDs indicates that these discrepancies are mainly due to the existing LVD offsets and systematic errors in levelling data.

Table 4.7: Statistics of the differences between the original and newly determined normal-orthometric heights of the levelling benchmarks. Unit: 1 cm.

North Island				
LVD	Min	Max	Mean	RMS
Auckland 1946	0.5	0.6	0.5	0.1
Gisborne 1926	-2.2	-1.4	-1.7	0.2
Moturiki 1953	1.5	23.4	7.6	5.5
Napier 1962	1.7	12.4	15.0	1.0
One Tree Point 1964	-4.8	-4.7	-4.8	0.1
Taranaki 1970	-26.5	-0.1	-12.9	6.1
Wellington 1953	-5.9	1.0	-1.8	1.7
North Island	**-26.5**	**23.4**	**3.2**	**6.9**
South Island				
Bluff 1955	6.4	6.5	6.4	0.1
Deep Cove 1960	6.4	6.5	6.4	0.1
Dunedin-Bluff 1960	6.0	6.1	6.1	0.1
Dunedin 1958	-0.4	0.8	0.1	0.3
Lyttelton 1937	-10.7	-5.8	-7.4	0.6
Nelson 1955	-21.6	-13.3	-18.0	1.7
Tarakohe 1982	-11.5	-11.4	-11.5	0.1
South Island	**-21.6**	**6.5**	**-6.5**	**7.4**

The computed corrections $\delta H^{N,NO}$ and $\delta H^{O,N}$ were used for a conversion of the newly derived normal-orthometric heights in New Zealand to the normal and Helmert's orthometric heights. The new database of the normal and Helmert's orthometric heights at the GPS-levelling points will be used for the validation of the gravimetric geoid/quasigeoid models in Section 7.1. The accuracy of the computed corrections $\delta H^{N,NO}$ and $\delta H^{O,N}$ depends mainly on the errors of input gravity data, whereas the errors due to the inaccuracy of the levelled heights are completely negligible. Since the precise levelling in New Zealand was realised without observing the gravity and the GNS Science gravity data base comprises about 40,000 gravity measurements in New Zealand with an irregular spatial distribution, the gravity anomalies at the points of levelling networks were calculated using EGM2008. The comparison of the EGM2008-derived and observed gravity revealed large discrepancies up to several dozens of mGals. A simple error analysis shows that, for example, the error of 10 mGal in the values of the gravity anomaly causes the error of the computed geoid-to-quasigeoid correction of 1 cm at the height of 1000 m, while only 1 mm error at 100 m. On the other hand, large errors are expected in the computed values of the normal to normal-orthometric height correction due to the cumulative contribution of the EGM2008 commission and omission errors.

Chapter 5

Testing GPS-levelling data with GGMs

In this chapter the newly adjusted levelling data at the GPS-levelling testing network in New Zealand are used to compare the accuracy of the recently released satellite-only GGMs compiled using GRACE and GOCE satellite observables. The accuracy of these GGMs is also compared with the combined models EGM2008 and EIGEN-GL04C. The description of the employed GGMs is given in Section 5.1. The accuracy of GGMs is analysed by using the same GPS-levelling data set in Section 5.2, summary and remarks are found in Section 5.3.

5.1 Selection of the models

We selected 9 satellite-only GGMs released during 2010 and 2011. The GOCE and GRACE data were used for the compilation of GOCO-01S (Pail *et al.*, 2010) and GOCO-02S (Goiginger *et al.*, 2011) models complete to spherical harmonic degree 224 and 250, respectively. The GRACE data were used for the compilation of ITG-GRACE2010S (Mayer-Gürr *et al.*, 2010) model complete to spherical harmonic degree 180. The series of the GO-CONS-GCF-2 model versions: DIR-R1 up to degree 240 (Bruinsma *et al.*, 2010), DIR-R2 up to degree 240 (ibid), TIM-R1 up to degree 224 (Pail *et al.*, 2011), TIM-R2 up to degree 250 (Pail *et al.*, 2011), SPW-R1 up to degree 210 (Migliaccio *et al.*, 2011) and SPW-R2 up to degree 240 (Migliaccio *et al.*, 2010) were compiled using the GOCE gravity gradiometry data. In addition we investigated the combined models EGM2008 (Pavlis *et al.*, 2008) and EIGEN-GL04C (Förste *et al.*, 2006), both compiled using GRACE, altimetry and gravity data (including LAGEOS data for EGEN-GL04C). The EGM2008 and EIGEN-GL04C coefficients are available complete to spherical harmonic degree 2160 and

360, respectively. The coefficients of all these GGMs defined in the tide-free system were used for the analysis.

5.2 Testing GGMs

The newly determined normal heights at the GPS-levelling testing network were used to evaluate the accuracy of selected GGMs. We computed the differences between the GPS-levelling and GGM quasigeoid heights equation using the full sets of GGM coefficients. The statistics of these differences calculated at the GPS-levelling testing network for Gravity Observation COmbination (GOCO) (versions: 01S and 02S), ITG-GRACE2010S, GO-CONS-GCF-2 (versions: DIR-R1, DIR-R2, TIM-R1, TIM-R2, SPW-R1 and SPW-R2), EGM2008 and EIGEN-GL04C are summarised in Table 5.1. The computed values of the root mean square (RMS) and mean of the spherical harmonic degree differences are plotted in Figures 5.1 and 5.2.

The RMS of differences between the GPS-levelling and GGM quasigeoid heights are very similar for all investigated GGMs when considering the spherical harmonic degree terms up to about 120 (cf. Figure 5.1). At this interval, the accuracy (in terms of the RMS of differences) gradually increase from more than 3 m to better than 1.3 m (for degree 120). The differences between the RMS values for all GGMs are less than 3 cm. The large discrepancies occur between the RMS values of individual GGMs approximately above degree 120. Here these differences are up to about 20 cm.

The RMS values of EGM2008 and EIGEN-GL04C above the spherical harmonic degree 250 differ more than 20 cm. The mean values of differences between the GPS-levelling and GGM quasigeoid heights for all investigated GGMs are very similar up to degree 20; here the mean values of GGMs differ less than 1 cm from each other. Large differences between these mean values occur above the spherical harmonic degree 20; here the mean values of GGMs differ as much as 20 cm. This is also evident from statistics in Table 5.1. The largest systematic offsets between GGMs and GPS-levelling data were found for EIGEN-GL04C (-25 cm), GOCO-02S (-21 cm), ITG-GRACE2010S (-30 cm) and GO-CONS-GCF-2 versions DIR-R1 (-21 cm) and DIR-R2 (-20 cm). The best agreement between the GPS-levelling and GGM quasigeoid heights (by means of the RMS fit) was achieved when using the GRACE and GOCE satellite-only model GOCO-02S.

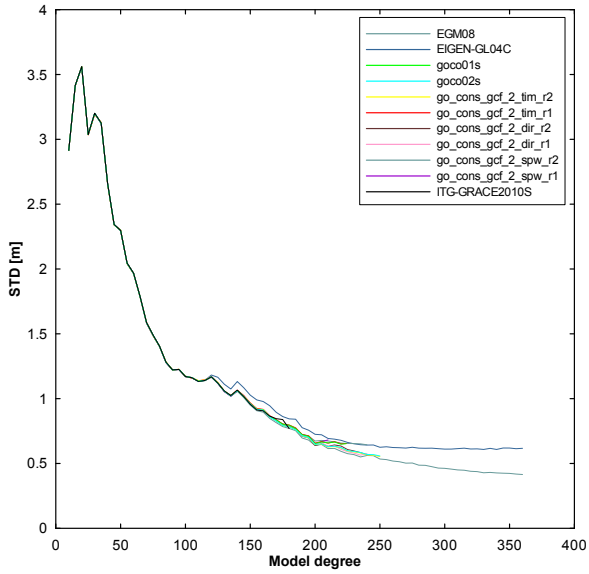

Figure 5.1: The RMS of the spherical harmonic degree differences between the GPS-levelling and GGM quasigeoid heights computed at the GPS-levelling testing network in New Zealand for. Note that the values for EGM2008 are provided only up to degree/order 360.

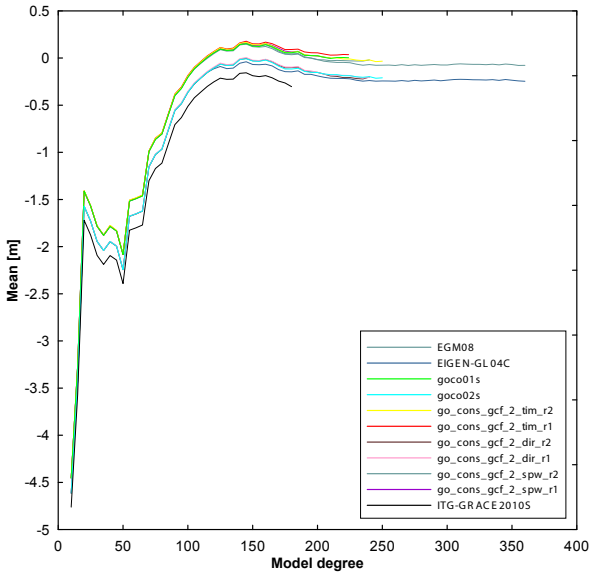

Figure 5.2: The mean of the spherical harmonic degree differences between the GPS-levelling and GGM quasigeoid heights computed at the GPS-levelling testing network in New Zealand. Note that the values for EGM2008 are provided only up to degree/order 360.

Table 5.1: Statistics of the differences between the GPS-levelling and GGM quasigeoid heights computed at the GPS-levelling testing network in New Zealand for GOCO (versions: 01 S and 02 S), ITG-GRACE2010S, GO-CONS-GCF-2 (versions: DIR-R1, DIR-R2, TIM-R1, TIM-R2, SPW-R1 and SPW-R2), EGM2008 and EIGEN-GL04C. Unit: 1 m.

Model	Degree	Min	Max	Mean	RMS
EGM2008	2160	1.37	4.29	-0.16	0.35
EIGEN-GL04C	360	-2.47	4.09	-0.25	0.62
GOCO					
01S	224	-1.57	4.28	0.00	0.65
02S	250	-1.41	4.22	-0.21	0.56
GO-CONS-GCF-2					
TIM_R1	224	-1.62	4.35	0.04	0.65
TIM_R2	240	-1.28	4.42	-0.02	0.57
DIR_R1	240	-1.62	4.18	-0.21	0.58
DIR_R2	240	-1.48	4.32	-0.20	0.57
SPW_R1	210	-1.87	4.17	0.00	0.68
SPW_R2	240	-1.81	4.29	-0.02	0.64
ITG-GRACE2010S	180	-2.71	3.91	-0.30	0.77

A good agreement was also attained for the satellite-only GOCE models GO-CONS-GCF-2 versions DIR-R1, DIR-R2 and TIM-R2 (cf. Table 5.1). The RMS fit of these GGMs with GPS-levelling data is similar and vary from 56 cm (for GOCO-02S) to 58 cm (for GO-CONS-GCF-2 version DIR-R1). The best agreement of GGMs with GPS-levelling data by means of the mean value of differences was attained for GOCO-01S (0 cm) and for GO-CONS-GCF-2 version TIM-R2 (-2 cm). When taking into consideration both, the RMS and mean of differences, the satellite-only model GO-CONS-GCF-2 version TIM-R2 has the best fit with GPS-levelling data in New Zealand; the RMS fit is 57 cm and the mean of differences is -2 cm. The EGM2008 has the best RMS fit with GPS-levelling data of 35 cm (and the mean of differences -16 cm) when using its coefficients complete to degree/order 2160. This is expected due to using terrestrial gravity and altimetry data that significantly improved the regional fit. The combined model EIGEN-GL04C complete to spherical harmonic degree 360 has a much lower accuracy; the RMS fit is 62 cm and the mean of differences is -25 cm. For the same spectral resolution, the RMS fit of EGM2008 is 42 cm (and the mean of differences is -8 cm).

5.3 Remarks on testing GGMs

The GRACE and GOCE model GOCO-02S has, among all tested satellite-only GGMs, the best RMS fit with GPS-levelling data in New Zealand of 56 cm. When

taking into consideration the minimum RMS fit, GOCE satellite-only model GOCO-02S (Goiginger *et al.*, 2011) has the best agreement with GPS-levelling data: the RMS fit is 56 cm and the mean of differences is -21 cm (ibid). On the other hand, three GO-CONS-GCF-2 satellite only models namely TIM-R2 (computed using the time-wise approach), DIR-R1 and DIR-R2 (computed using the direct approach) are found to be very close to each other and GOCO-02S. TIM-R2 has the best agreement with GPS-levelling data with regard to the mean of differences; the mean of differences is 2 cm.

All investigated satellite-only GGMs have better agreement with GPS-levelling data than the combined model EIGEN-GL04C. On the other hand, the combined model EGM2008 has the best regional agreement with GPS-levelling data (ibid). All investigated GGMs have a very similar RMS fit with GPS-levelling data for the spherical harmonic terms up to degree/order of about 120. They have also very small disagreements between the mean values of differences up to spherical harmonic degree 20. At higher-degree terms, however, large inconsistencies were found between individual GGMs. The differences between the RMS fits of individual GGMs above degree 120 reach as much as 20 cm. The corresponding differences in the mean values, again to about 20 cm, were confirmed above the spherical harmonic degree terms of 20.

Based on minimum RMS fit selection from the numerical analysis shown in Table 5.1, GOCO-02S satellite only model is found to be suitable for the geoid/quasigeoid computation in this study. The comparison was made based on the minimum mean value of differences and the minimum RMS, that's why the model SPW-R1 was not selected despite of having mean value of differences of zero, but a contradictory RMS value (68 cm) which is larger than that of GOCO-02S (57 cm).

Chapter 6

Regional gravimetric geoid/quasigeoid modelling

In this chapter, three methodologies of geoid/quasigeoid modelling are applied to compute the improved gravimetric model in New Zealand. The three methods are least-squares modification of stokes formula (known as KTH method), boundary element method and discretised integral-equation approach (DIEA).

The objectives of this chapter is to demonstrate and review three different geoid/quasigeoid methods and analyse their results. Three gravimetric solutions are compiled in this chapter, namely NZGM2010, NZQM2010 and OTG12 using KTH, BEM and DIE methods, respectively. The KTH method and BEM methods are reviewed in Sections 6.4 and 6.6. The new DIEA has been carefully investigated as shown in Section 6.9, the investigation is applied to test four discretised integral equations and their behaviours before and after gravity data smoothing.

6.1 Stokes formula

The geoid heights can be computed from the terrestrial gravity anomalies Δg using the well-known Stokes formula. The classical form of Bruns-Stokes formula is written as (Stokes, 1849)

$$N = \int_{\alpha=0}^{2\pi} \int_{\psi=0}^{\pi} S(\psi)\, \Delta g \sin\psi \, d\alpha \, d\psi \tag{6.1}$$

where R is the Earth's mean radius, γ_0 is the normal gravity evaluated at the surface of the reference ellipsoid GRS80 (Moritz, 1980), ψ is the geocentric angle, $S(\psi)$ denotes original Stokes function and α is the azimuth .

Stokes function reads

$$S(\psi) = \sum_{n=2}^{\infty} \frac{2n+1}{n-1} P_n(\cos\psi) \tag{6.2}$$

The original Stokes function can be written in a closed form as follows:

$$S(\psi) = \frac{1}{\sin\left(\frac{\psi}{2}\right)} - 6\sin\left(\frac{\psi}{2}\right) + 1 - 5\cos\left(\frac{\psi}{2}\right) - 3\cos\left(\frac{\psi}{2}\right)\ln\left[\sin\left(\frac{\psi}{2}\right) + \sin^2\left(\frac{\psi}{2}\right)\right] \tag{6.3}$$

6.2 Modification of Stokes formula

Based on Stokes theory (Stokes, 1849), the Stokes surface integration (Equation 6.1) has to be applied over the whole Earth. But in fact, the global coverage of the gravity data is very poor to fulfill this requirement. Due to this limitation it was suggested that Equation 6.1 has to be applied where terrestrial gravity data are available, meaning that the surface integral will be limited or truncated to small cap σ_0 around the computation point. Once we cannot restrict our computation to Equation 6.1 due to lack of gravity data, errors will stem as a consequence.

By confining the computation area into small cap ψ_0 Equation 6.1 can be presented by Bruns-Stokes formula:

$$N = \int_{\alpha=0}^{2\pi} \int_{\psi=0}^{\psi_0} S(\psi)\, \Delta g \sin\psi \, d\alpha \, d\psi \tag{6.4}$$

where N denotes the geoid estimator. The near-zone surface integration domain $\int_{\alpha=0}^{2\pi}\int_{\psi=0}^{\psi_0}\sin\psi \, d\alpha \, d\psi$ is limited by the spherical distance ψ_0.

The difference between the geoid height in Equation 6.1 and the new estimator in Equation 6.4 is called the truncation error of Stokes formula:

$$\delta N = \int_{\alpha=0}^{2\pi} \int_{\psi=0}^{\pi-\psi_0} S(\psi)\, \Delta g \sin\psi \, d\alpha \, d\psi \tag{6.5}$$

where $(\pi - \psi_0)$ represents far zone (the area outside the gravity area).

When using local gravity data, Stokes formula will be truncated to inner zone, which causes truncation errors due to the lack of the gravity data in remote zones.

Equation 6.5 can be written as

$$\delta N = \frac{R}{2\gamma}\sum_{n=2}^{\infty} Q_n(\cos\psi)\,\Delta g_n$$

Molodensky *et al.* (1962) proposed that the inclusion of the terrestrial gravity data and long wavelength gravity data generated from global geopotential model coefficients (up to degree M) will help to reduce the effects of the remote zone.

After the advent of satellites it has become easy to compute the geoid height globally, which will give a compensation for the truncation effects in addition to the modification of Stokes kernel.

Equation 6.1 can be written in following form

$$N = \hat{N} + \delta N \tag{6.6}$$

by combining terrestrial gravimetric data Δg with the satellite gravity data from the GGM spherical harmonic coefficients Δg_n and supposing that both data sets do not contain errors we obtain the geoid estimator

$$N = \frac{\mathrm{R}}{4\pi\gamma_0}\int_{\alpha=0}^{2\pi}\int_{\psi=0}^{\psi_0} S^{\bar{n}}(\psi)\,\Delta g\,\sin\psi\,d\alpha\,d\psi + \frac{R}{2\gamma}\sum_{n=2}^{M} Q_n(\cos\psi)\,\Delta g_n \tag{6.7}$$

The coefficients $Q_n(\cos\psi)$ determine the effects of remote areas due to the truncation. Δg_n are determined by the GGM up to the maximum degree M, $S^{\bar{n}}(\psi)$ is the modified of Stokes function.

6.3 Modification methods

The aim of modifying the Stokes function is to reduce errors of the geoid estimator (Equation 6.4). The combination of terrestrial and satellite gravity data has been studied by a large number of scientists for a long time. In these sections an overview of two principal methods is given.

6.3.1 Deterministic methods

The deterministic methods intend to decrease the effects of the remote zone resulting from the truncation of the original Stokes formula (Equation 6.1) and therefore

improving their convergence through using lower-degree geopotential coefficients. The deterministic methods were broadly studied by many scientists, for instance, Molodensky *et al.* (1962); Wong and Gore (1969); Meissl (1971); Vincent and Marsh (1974); Jekeli (1980, 1981); Heck and Grüninger (1987); Vaníček and Kleusberg (1987); Kearsley (1988); Vaníček and Sjöberg (1991); Vaníček *et al.* (1996); Forsberg *et al.* (1997); Omang and Forsberg (2002).

Some authors employed RCR approach using high-degree coefficients of the GGM for generating a higher-degree reference field and the residual field is computed from the integral formula (see e.g. Jeffreys, 1953, 1962; De Witte, 1967; Wong and Gore, 1969). Another type of deterministic modifications to Stokes functions based on RCR approach were discussed and investigated by Featherstone *et al.* (1998); J. Evans (2000); Featherstone (2003); Vaníček and Featherstone (1998).

From the above paragraphs we can understand that the deterministic methods are confined to resolve errors of the remote zone by focusing only on terrestrial gravity component which basically denotes the first term term in Equation 6.7 which contains the Stokes kernel while the GGM term was not addressed.

6.3.2 Stochastic methods

In contrast to the deterministic modification, the stochastic modification of Stokes kernel aims to reduce the errors of the terrestrial gravity and spherical harmonic coefficients of GGM by combining both of them optimally in the least-squares sense (see e.g. Sjöberg, 1979, 1980, 1981, 1984, 1991b, 2003c; Wenzel, 1981, 1982).The stochastic methods were investigated and discussed in (Sjöberg and Fan, 1986; Fan, 1989; Sjöberg and Hunegnaw, 2000; Ellmann, 2001, 2004; Ågren, 2004; Ellmann, 2005d,c,a; Nahavandchi and Sjöberg, 2001).

Since the deterministic methods were investigated for gravimetric solutions in New Zealand by (Amos, 2007; Amos and Featherstone, 2009) and (Claessens *et al.*, 2009, 2011) to compute NZGeoid05 and NZGeoid2009, we confine ourselves only to one kind of the stochastic methods that uses the least-squares modification (LSM) to Stokes formula. The LSM was proposed by Sjöberg (1984, 1991a, 2003c) and was properly derived in three comparable versions (biased, unbiased and optimum). Each of the three versions can be adopted for obtaining the final gravimetric model. In the following section we will show how we adopted LSM to compute the first experimental gravimetric geoid model of New Zealand (Abdalla and Tenzer, 2011) by providing description, results and analysis.

The selection of the parameters $\psi_0 = 3°$ and $n = 65$ was done empirically, based on finding the optimal compatibility between the error variance $C(0)$ of the terrestrial gravity, ψ_0 and n that makes $S^n(\psi)$ edge to zero. As demonstrated in Figure 6.1, the modified Stokes kernel $S^n(\psi)$ converges to zero for $\psi \to 3°$ and thus minimises the truncation bias for the chosen parameter $\psi_0 = 3°$. For more details we refer readers to studies by (Ellmann, 2004, 2005a). The example of truncation bias of the original Stokes function $S(\psi)$ is also illustrated in Figure 6.1. For comparison, the parameters $\psi_0 = 1.5°$ and $n = 40$ were adopted in computing the regional quasigeoid model NZGeoid05 (cf. Amos, 2007). Claessens *et al.* (2009, 2011) used $\psi_0 = 2.5°$ and $n = 40$ in computing NZGeoid2009. It was noted that Amos (2007) and Claessens *et al.* (2009, 2011) used the deterministic modification of the Bruns-Stokes formula.

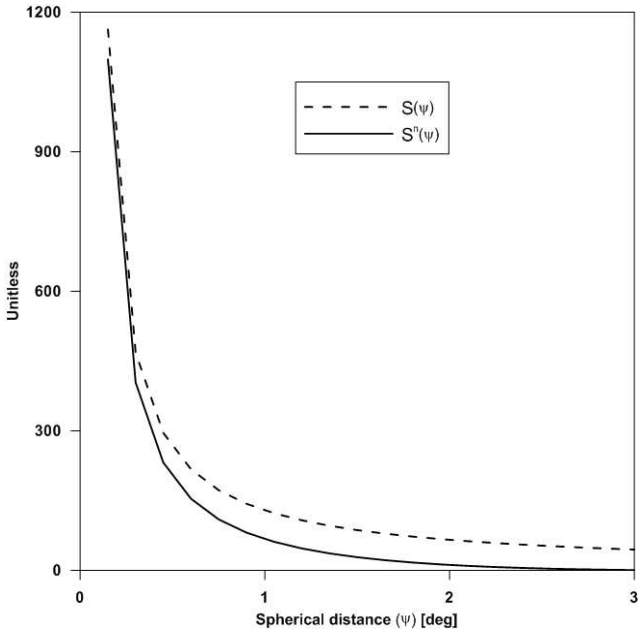

Figure 6.1: The comparison of the modified Stokes function $S^n(\psi)$ computed for the parameters $\psi_0 = 3°$ and the original Stokes function $S(\psi)$ at the interval of $0 \leq \psi \leq 3°$.

6.4 Geoid determination by stochastic LSM

In this section we will use the stochastic least-square modification of Stokes formula (LSM) to compute the first experimental gravimetric geoid model of New Zealand called hereafter NZGM2010; the LSM of Stokes formula is widely known as the KTH method. The KTH method utilises the least-squares modification of the Stokes integral for the biased, unbiased, and optimum stochastic solutions. The principle of this modification is to minimise the truncation errors, while the near-zone surface integration area around the computation point is often limited to a few hundred kilometres. The far-zone contribution is estimated using the satellite-only GGM.

Various least-squares stochastic solutions are applied to estimate the maximum spherical distance of the near-zone surface integration area and the maximum degree of the satellite-only GGM coefficients based on empirical models for the harmonic and terrestrial gravity anomaly degree variances. The integral convolution of the modified Stokes kernel with the observed gravity anomalies over the near-zone integration area and the far-zone gravity field contribution estimated from GGM yields the approximate geoid heights. The final gravimetric geoid is then obtained after applying four additive corrections to the approximate geoid heights. These additive corrections account for the gravitational effects of topography and atmosphere, the downward continuation reduction, and the ellipsoidal approximation of the Earth's shape.

The main difference between the KTH method and conventionally used approaches for the gravimetric geoid determination thus comes from a different treatment of the gravity corrections and consequently different types of gravity anomaly data used in the Stokes integral convolution. In conventional Stokesian approaches, the observed gravity anomalies are first corrected for the topographic and atmospheric gravitational effects and subsequently reduced to the geoid surface. The integral convolution of the (modified)-Stokes kernel with the corrected and reduced gravity anomalies provides the final gravimetric geoid after subtracting the primary indirect topographic effect on the geoid.

In the KTH method, the Stokes integration is applied directly to the observed gravity anomaly data at the Earth's surface. The integral convolution of the (modified)-Stokes kernel with the observed gravity anomalies provides the approximate geoid heights. The complete contribution of the direct and secondary indirect effects of topography and atmosphere on the gravity anomalies and consequently the primary indirect effects of topography and atmosphere on the geoid heights are treated as the combined topographic and atmospheric corrections applied to the approximate geoid heights (Sjöberg, 2003a).

Similarly, the contribution of the downward continuation of the gravity anomalies from the Earth's surface onto the geoid surface is treated as the downward continuation correction to the approximate geoid heights. The formulation of the modified Bruns-Stokes formula in spherical approximation yields the correction for the ellipsoidal approximation of the Earth's shape. The theoretical and numerical aspects of the KTH method are described in Sjöberg (1984, 1991a, 2003d,b,c). This method was successfully applied to compile regional geoid in different countries by several authors: Nsombo (1996); Nahavandchi (1998); Hunegnaw (2001b); Ellmann (2001, 2004); Ågren (2004); Ågren *et al.* (2009); Kiamehr (2006); Daras (2008); Ulotu (2009); Abdalla and Fairhead (2011).

6.4.1 NZGM2010 geoid model based on modification of Stokes formula

According to the KTH method, the gravimetric geoid height N is computed as a sum of the following components (Sjöberg, 2003a):

$$N = \tilde{N} + \delta N^{T} + \delta N^{A} + \delta N^{dwc} + \delta N^{ell} \tag{6.8}$$

where $\tilde{N}$ is the approximate geoid height, δN^{T} the combined topographic correction, δN^{A} the combined atmospheric correction, δN^{dwc} the downward continuation correction and δN^{ell} the ellipsoidal correction for the formulation of the Bruns-Stokes formula in the spherical approximation to the problem. The approximate geoid height in Equation 6.8 is computed using the modified Bruns-Stokes formula in the following form (Sjöberg, 2003c).

The surface integration element $d\sigma_0 = \sin\psi \, d\alpha \, d\psi$ in Equation 6.7 can be defined in the polar spherical coordinates (α,ψ) with the spherical azimuth α and the spherical distance ψ and it reads

$$\tilde{N} = \frac{\mathrm{R}}{4\pi\gamma_0} \int_{\alpha=0}^{2\pi} \int_{\psi=0}^{\psi_0} S^{\bar{n}}(\psi) \, \Delta g \sin\psi \, d\alpha \, d\psi + \frac{\mathrm{R}}{2\gamma_0} \sum_{n=2}^{\bar{n}} b_n \, \Delta g_n^{GGM} \tag{6.9}$$

The first constituent on the right-hand side of Equation 6.9 represents the terrestrial gravity anomaly contribution to the approximate geoid heights. This contribution is computed by the integral convolution of the observed gravity anomalies at the Earth's surface with the modified Stokes kernel $S^{\bar{n}}(\psi)$ that is defined as (*ibid*)

$$S^{\bar{n}}(\psi) = S(\psi) - \sum_{n=2}^{\bar{n}} \frac{2n+1}{2} b_n P_n(\cos\psi) \tag{6.10}$$

where $S(\psi)$ is the (original) Stokes kernel, $P_n(\cos\psi)$ are the Legendre polynomials of degree n for the argument of cosine of the spherical distance ψ. The second constituent on the right-hand side of Equation 6.9 represents the GGM contribution to the approximate geoid heights. This contribution is computed from the GGM coefficients up to a maximum degree $\bar{n}$ of spherical harmonics and from a set of the least-squares modification parameters $\{b_n : n = 2,3,...,\bar{n}\}$. The Laplace spherical harmonics Δg_n^{GGM} for the gravity anomalies of degree n in Equation 6.9 are defined as (e.g., Heiskanen and Moritz, 1967, page 89)

$$\Delta g_n^{GGM} = \frac{\mathrm{GM}}{a^2} \left(\frac{a}{r}\right)^{n+2} (n-1) \sum_{m=-n}^{n} c_{n,m} \mathrm{Y}_{n,m} \tag{6.11}$$

where $c_{n,m}$ are the GGM coefficients of the disturbing potential T . The least-squares

modification parameters b_n are defined by the following linear system of observation equations (cf. Sjöberg, 2003c):

$$\sum_{r=2}^{\bar{n}} b_r \, a_{k,r} = h_k \;\; (k = 2,3,...,\bar{n}) \tag{6.12}$$

The coefficients $\{a_{k,r} \;: k, r,...,\bar{n}\}$ of the design matrix read

$$a_{k,r} = \left(\sigma_r^2 + \mathrm{dc_n^{GGM}}\right) \delta_{k,r} - E_{\mathrm{k,r}} \, \sigma_r^2 - E_{\mathrm{r,k}} \, \sigma_k^2 + \sum_{n=2}^{\infty} E_{n,k} \, E_{n,k} \left(\sigma_n^2 + C_n\right) \tag{6.13}$$

The coefficients $\{h_k \;: k = 2,3,...,\bar{n}\}$ of the observation vector are given by

$$h_k = \Omega_k - Q_k \, \sigma_k^2 + \sum_{n=2}^{\infty} E_{n,k} \left[Q_{n,k} \left(\sigma_k^2 + C_n\right) - \Omega_k \right] \tag{6.14}$$

The parameters Ω_k, $E_{n,k}$, $\delta_{k,r}$ and C_n in Equations 6.13 and 6.14 read

$$\Omega_k = \frac{2\sigma_k^2}{k-1} \tag{6.15}$$

$$E_{n,k} = \frac{2k+1}{2} e_{n,k} \tag{6.16}$$

$$\delta_{k,r} = \begin{cases} 1 & \text{if } k = r \\ 0 & \text{otherwise} \end{cases} \tag{6.17}$$

$$C_n = \sigma_n^2 + \begin{cases} \dfrac{c_n^{GGM} dc_n^{GGM}}{(c_n^{GGM} + dc_n^{GGM})} & \text{if } 2 \le n \le \bar{n} \\ c_n^{GGM} & \text{if } n > \bar{n} \end{cases} \tag{6.18}$$

where σ_n^2 are the terrestrial gravity anomaly error degree variances, c_n^{GGM} and dc_n^{GGM} are the GGM gravity anomaly degree variances and their error degree variances. Molodensky's truncation coefficients Q_k and the function $e_{n,k}$ are defined in Equations 6.26 and 6.34.

The upper limit of expansion (Equations 6.13 and 6.14) is truncated at $n_{max} = 2000$.

The GGM gravity anomaly degree variances c_n^{GGM} are computed from the GGM coefficients $C_{n,m}$ and $S_{n,m}$ of the disturbing potential as follows

$$c_n^{GGM} = \frac{(\mathrm{GM})^2}{a^4} (n-1)^2 \sum_{m=0}^{n} \left(C_{n,m}^2 + S_{n,m}^2\right) \tag{6.19}$$

In practice, the infinite series in Equations 6.13 and 6.14 are truncated at a chosen upper limit of the expansion. In this study, we used the maximum degree of $n_{max} = 2000$. The GGM gravity anomaly degree variances c_n^{GGM} of degree $\bar{n} < n \le n_{max}$

are generated synthetically using the analytical model developed by Tscherning and Rapp (1974), see alsoÅgren (2004); Ellmann (2005a). It reads

$$c_n^{GGM} = \alpha \frac{(n-1)}{(n-2)(n+24)} \left(\frac{\mathrm{R_B}}{\mathrm{R}} \right)^{n+4} \tag{6.20}$$

where $\alpha = 425.28\mathrm{mGal}^2$,$\mathrm{R} = 6371 \times 10^3$ m, and $\mathrm{R_B} = \mathrm{R} - 1225$ m. The GGM gravity anomaly error degree variances $dc_n^{GGM}$of degree ($\bar{n} < n$) are calculated from the standard errors $dC_{n,m}$ and $dS_{n,m}$ of the GGM coefficients as follows (cf. Rapp and Pavlis, 1991)

$$dc_n^{GGM} = \frac{(\mathrm{GM})^2}{a^4} (n-1)^2 \sum_{m=0}^{n} \left(dC_{n,m}^2 + dS_{n,m}^2 \right) \tag{6.21}$$

The GGM gravity anomaly error degree variances dc_n^{GGM} of degree $\bar{n} < n$ are usually neglected. The terrestrial gravity anomaly error degree variances σ_n^2 are calculated according to the procedure described in Ågren (2004) and Ågren *et al.* (2009).

The system of observation equations in Equation 6.12 is formed for the biased least-squares solution. The corresponding system of normal equations is then solved directly, for instance, by applying the Gauss elimination method. Alternative methods of solving the system of normal equations for finding the modification parameters b_n are discussed in Sjöberg (1984). When forming the system of observation equations for either the optimum or unbiased least-squares solutions, the system of normal equations becomes ill-conditioned (cf. Sjöberg, 1991a, 2003c). The regularisation techniques are applied. The determination of the unbiased and optimum least-squares modification parameters and the regularisation techniques are discussed in Ågren (2004) and Ellmann (2005b).

6.4.2 Additive corrections

The Stokes formula presupposes that the disturbing potential is harmonic outside the geoid. This simply implies that there are no masses outside the geoid surface, and that they must be moved inside the geoid or completely removed in order to apply Stokes formula. This assumption of the forbidden masses outside the geoid (bounding surface) is necessary when treating any problem of physical geodesy as a boundary-value problem in potential theory. The difficulties encountered by the removal of the mass effects stem from their irregular distribution above the geoid.

Additionally, the application of Stokes formula needs gravity to be observed or reduced at sea level, which represents the bounding surface or the integral boundary.

The gravity reduction to the sea level surface implies a change of gravity corresponding to topographic and atmospheric direct effect on the geoid. After applying Stokes formula to determine the gravimetric geoid, the effect of restoring the topography and atmospheric masses (the indirect effect) is accounted for. Stokes formula applies to spherical reference surface. Therefore, the entering is given on the sphere. In the approximation of the geoid given by a global reference ellipsoid, there is a deviation of about 100 m, which causes a systematic error of about several decimetres in geoid height when neglecting the flattening of the ellipsoid. The correction of the gravity anomaly for the direct effect must be analytically downward continued (reduced) to the sea level. This step is called downward continuation (DWC).

In the KTH computational scheme for geoid determination (Sjöberg, 2003a) on the surface, the gravity anomalies and GGM are used to determine the approximate geoid height. All the corrections are then added to separately. In contrast to conventional methods by means of gravity reductions, the forbidden masses are treated before using Stokes formula, which is the purpose of the various reductions to gravity anomalies.

The combined topographic correction in Equation 6.8 is computed approximately using the following simple expression (cf. Sjöberg, 2001):

$$\delta N^T \approx -\frac{2\pi}{\gamma_0} G\rho^T H^2 \tag{6.22}$$

where $\rho^T = 2670\ kgm^{-3}$ is the adopted value of the topographic density (Hinze, 2003), and the height of the computation point above sea level. The combined atmospheric correction in Equation 6.8 is defined as (cf. Sjöberg and Nahavandchi, 2000)

$$\delta N^A = -\frac{2\pi R}{\gamma_0}\rho_0^A \sum_{n=2}^{\bar{n}} \left(\frac{2}{n-1} - b_n - Q_n^{\bar{n}}\right) H_n - \frac{2\pi R}{\gamma_0}\rho_0^A \sum_{n=\bar{n}+1}^{\infty} \left(\frac{2}{n-1} - \frac{n+2}{2n+1} Q_n^{\bar{n}}\right) H_n \tag{6.23}$$

where ρ_0^A is the adopted nominal value of the atmospheric density at sea level, that is, $\rho_o^A = 1.230\ kg\,m^{-3}$ (cf Sjöberg, 2001). The surface (topographic) height functions of degree n in Equation 6.23 read

$$H_n = \sum_{m=-n}^{n} H_{n,m} Y_{n,m} \tag{6.24}$$

where $H_{n,m}$ are the numerical coefficients of the global elevation model (GEM) of degree n and order m.

The modified Molodensky's truncation coefficients $Q_n^{\bar{n}}$ are given by Sjöberg and Nahavandchi (2000)

$$Q_n^{\bar{n}} = Q_n - \sum_{k=2}^{\bar{n}} \frac{2k+1}{2} b_k \, e_{n,k} \tag{6.25}$$

where Q_n the Molodensky's truncation coefficients read (Molodensky *et al.*, 1962)

$$Q_{\mathrm{n}} = \int_{\psi_0}^{\pi} S(\psi) \, P_n(\cos\psi) \sin\psi \, d\psi \tag{6.26}$$

Molodensky's truncation coefficients Q_n are computed recurrently according to formulas derived by Hagiwara (1976)

$$\begin{aligned} Q_n = & -\frac{1}{(n-1)(n+2)} \\ & \times \left\{ nS(t)[P_{n-1}(t) - tP_n(t)] - (1-t)^2 P_n(t) \frac{dS(t)}{dt} + 2K_n(t) + 2I_n(t) + 9J_n(t) \right\} \end{aligned} \tag{6.27}$$

Equation 6.3 can be transformed a function of t to the form $S(t)$ as by considering $t = \cos\psi$:

$$S(t) = \sqrt{\frac{2}{1-t}} - 6\sqrt{\frac{1-t}{2}} + 1 - 5t - 3t\ln\left(\sqrt{\frac{1-t}{2}} + \frac{1-t}{2}\right) \tag{6.28}$$

$\frac{dS(t)}{dt}$ is the derivative of Stokes kernel and represents the isotropic part of Vening Meinesz kernel:

$$\frac{dS(t)}{dt} = -8 + \frac{1}{\sqrt{2}(1-t)^{3/2}} - \frac{3\left(\sqrt{2} - \sqrt{1-t}\right)}{\sqrt{2}(1-t^2)} - 3\ln\left(\sqrt{\frac{1-t}{2}} + \frac{1-t}{2}\right) \tag{6.29}$$

$K_n(t)$are recursively evaluated as:

$$K_n(t) = 2k_{n-1}(t) - k_{n-2}(t) - \frac{P_n(t) - P_{n-2}(t)}{(2n-1)\sqrt{2(1-t}} \tag{6.30}$$

Zero and first degree terms of $K_n(t)$are evaluated as:

$$K_0(t) = -\frac{1}{2} + \sqrt{\frac{1}{2(1-t)}}, \quad K_1(t) = -\frac{3}{2} + \sqrt{\frac{1}{2(1-t)}} + \sqrt{\frac{1-t}{2}} \tag{6.31}$$

$I_n(t)$ and $J_n(t)$ are computed from Legendre polynomials:

$$\begin{aligned} I_n(t) &= \int_{\psi_0}^{\pi} P_n(\cos\psi)\sin\psi \, d\psi \\ &= \frac{1}{2n+1}[P_{n+1}(t) - P_{n-1}(t)] \end{aligned} \tag{6.32}$$

$$J_n(t) = \int_{\psi_0}^{\pi} \cos\psi P_n(\cos\psi)\sin\psi \, d\psi$$
$$= \frac{1}{2n+1}\left[\frac{n+1}{2n+3}P_{n+2}(t) + \frac{2n+1}{(2n-1)(2n+3)}P_n(t) - \frac{n}{2n-1}P_{n-2}(t)\right] \quad (6.33)$$

Alternatively, they can be computed using Paul (1973a) algorithm. The functions $e_{n,k}$ of the spherical distance ψ_0 are defined in the following integral form (cf. Sjöberg and Nahavandchi, 2000)

$$e_{n,k} = \int_{\psi_0}^{\pi} P_n(\cos\psi)\ P_k(\cos\psi)\ \sin\psi \, d\psi \quad (6.34)$$

The downward continuation correction δN^{dwc} in Equation 6.8 consists of three terms that are computed individually (cf. Ågren, 2004):

$$\delta N^{dwc} = \delta N^{dwc,1} + \delta N^{L1,Far} + \delta N^{dwc,L2} \quad (6.35)$$

The first term $\delta N^{dwc,1}$ in Equation 6.35 is defined as (Sjöberg, 2003a)

$$\delta N^{dwc,1} = \frac{\Delta g}{\gamma_0}H + 3\frac{\tilde{\zeta}}{r}H - \frac{1}{2\gamma_0}\left.\frac{\partial \Delta g}{\partial r}\right|_{r=R+H} H^2 \quad (6.36)$$

where $\tilde{\zeta}$ denotes the approximate value of the height anomaly at the computation point. Due to the diminutive value of $\delta N^{dwc,1} = 1mm$ that corresponds to an error of about $1m$ for the height of the computation point of $H = 2000$ m, it is convenient to compute $\tilde{\zeta}$ in Equation 6.36 using the following simplified formula (Sjöberg, 2003e):The linear vertical gravity anomaly gradient $\left.\frac{\partial \Delta g}{\partial r}\right|$ at the computation point is calculated according to the expression for the analytical continuation given in Heiskanen and Moritz (1967).

It reads

$$\left.\frac{\partial \Delta g}{\partial r}\right|_{r=R+H} = \frac{R^2}{2\pi}\int_{\alpha=0}^{2\pi}\int_{\psi=0}^{\psi_0} \frac{\Delta \mathrm{g}(\alpha,\psi) - \Delta \mathrm{g}}{\ell_0^3(\psi)} \sin\psi \, d\alpha \, d\psi - \frac{2}{R}\Delta g_P \quad (6.37)$$

where Δg and $\Delta g(\alpha,\psi)$ are the values of the surface gravity anomaly at the positions of the computation and running integration points, respectively. The Euclidean spatial distance $\ell_0^3(\psi)$ in Equation 6.37 reads

$$\ell_0^3(\psi) = 2\ R \sin\frac{\psi}{2} \quad (6.38)$$

The downward continuation correction terms $\delta N^{L1,Far}$ and $\delta N^{dwc,L2}$ in Equation

6.35 are computed using the following expressions

$$\delta N^{L1,Far} = \frac{R}{2\gamma_0}\sum_{n=2}^{\bar{n}}\left(b_n + Q_n^{\bar{n}}\right)\left[\left(\frac{R}{\mathrm{r}}\right)^{n+2} - 1\right]\Delta g_n^{GGM} \tag{6.39}$$

and

$$\delta N^{dwc,L2} = \frac{R}{4\pi\gamma}\int_{\alpha=0}^{2\pi}\int_{\psi=0}^{\psi_0} S^{\bar{n}}(\psi)\left.\frac{\partial \Delta g}{\partial r}\right|_{r=R+H}[H - H(\alpha,\psi)]\sin\psi d\alpha d\psi \tag{6.40}$$

where H and $H(\alpha,\psi)$ are the topographical heights at the positions of the computation and running integration points, respectively.

The ellipsoidal correction δN^{ell} in Equation 6.8 is computed approximately as (cf. Sjöberg, 2004b)

$$\delta N^{ell} \approx \psi_0\left[\left(0.12 - 0.38\sin^2\varphi\right)\Delta \mathrm{g} + 0.17\,\tilde{N}\cos^2\varphi\right] \tag{6.41}$$

where δN^{ell} is given in millimetres, Δg in mGals, $\tilde{N}$ in metres and φ is the geocentric spherical latitude of the computation point.

6.5 Numerical results on NZGM2010

The $2' \times 2'$ gravity anomalies at the Earth's surface over the data area bounded by the parallels of 25° and 60° southern geodetic latitude and the meridians of 160° and 190° western longitude were used to determine the gravimetric geoid heights. The $2' \times 2'$ gravity anomalies were reconstructed from the gravity measurements provided by the GNS Science gravity database (onshore) according to the procedure described in Janák and Vaníček (2005) and extracted from the DNSC08 marine gravity database (offshore). The DNSC08 marine gravity database is provided by the Danish National Space Centre (Andersen *et al.*, 2009). The values of gravity anomalies vary from 252.6 to 310.7 mGal with the mean of 2.0 mGal, and the standard deviation (STD) is 35.1 mGal. Based on analysis conducted in Chapter 5, the satellite-only model GOCO-02S (Goiginger *et al.*, 2011) was used to model the GGM contribution. The topographic heights were generated from the 1" × 1" detailed DTM of New Zealand and from the 30" × 30" global elevation data of SRTM30_PLUS V5.0 (Becker *et al.*, 2009).

Various least-squares stochastic solutions are applied in the KTH method to estimate the maximum spherical distance ψ_0 of the near-zone surface integration area and the maximum degree n of the GGM coefficients based on empirical models for

the harmonic and terrestrial gravity anomaly degree variances. The GGM gravity anomaly degree variances c_k^{GGM} and their error degree variances dc_k^{GGM} were computed from the GOCO-02S coefficients according to Equations 6.19 and 6.21. The inaccuracy of modelling the GGM contribution increases proportionally with increasing degree of the GGM coefficients, the error degree variances of GOCO-02S significantly increases above the degree 77 of spherical harmonics.

Since the accuracy of marine and terrestrial gravity data used in this study is unknown, we assessed the accuracy of input gravity data according to the approach described in detail in Tenzer (2008). This approach utilises the variance component estimation (VCE) technique (see e.g. Förste, 1979; Koch and Kusche, 2002; Kusche, 2003) for observation groups weighting. The gravity data were separated into two data sets consisting of the terrestrial and marine gravity data from the GNS Science and DNSC08 databases. The parameterisation of gravity field was done in terms of the spherical radial basis functions (SRBF). The representative value of the variance $C(0) = 2\ mGal^2$ of the entire input gravity data was obtained as the weighted mean of the corresponding values estimated for these two observation groups. We note here that this value is more likely unrealistic, especially in mountainous regions where the accuracy of the gravity anomalies is much lower due to the errors in determined heights of the observation points.

The $2' \times 2'$ surface gravity anomaly data up to $\psi_0 = 3°$ of the spherical distance around the computation point and the GOCO-02S coefficients up to degree $n = 65$ of spherical harmonics were used to calculate the approximate geoid heights N according to Equation 6.9. The spherical harmonics of the normal gravity field were computed for the parameters of the GRS80 reference ellipsoid. The discrete values of the combined topographic correction δN^T were computed according to Equation 6.22 on a $1" \times 1"$ geographical grid using the $1" \times 1"$ detailed DTM of New Zealand and adopting the average topographical density of kgm^{-3} (cf. Hinze, 2003). The $2' \times 2'$ mean values of the combined topographic correction were then computed by a spatial averaging of the corresponding $1" \times 1"$ discrete values. The $2' \times 2'$ mean values of the combined topographical correction vary from -69.0 to 0.0 cm with the mean of -0.2 cm, and the standard deviation is 2.1 cm (see Figure 6.2a). The $30" \times 30"$ global elevation data of SRTM30_PLUS V5.0 were used to generate the GEM coefficients $H_{n,m}$. These coefficients complete to degree and order 2160 were used to compute the combined atmospheric correction δN^A at the $2' \times 2'$ geographical grid according to Equation 6.23.

The combined atmospheric correction is shown in Figure 6.2c. It varies from 0.0 to 1.2 cm with the mean of 0.6 cm, and the standard deviation is 0.3 cm. The $2' \times 2'$

gravity anomalies and the mean topographical heights averaged for $2' \times 2'$ geographical grid cells were used to compute the near-zone contribution to the downward continuation correction δN^{DWC} according to Equations 6.35 to 6.40. The corresponding long-wavelength contribution was computed using the GOCO-02S coefficients complete to degree 65 of spherical harmonics. The downward continuation correction is shown in Figure 6.2b. It varies from -3.7 to 58.7 cm with the mean of 2.5 cm, and the standard deviation is 3.2 cm. The ellipsoidal correction δN_{ell} was computed using Equation 6.41. Over the study area of New Zealand this correction is negligible; the maxima of this correction are less than 1 mm.

The gravimetric geoid model compiled on a $2' \times 2'$ geographical grid at the computation area of New Zealand and its continental shelf bounded by the parallels of 28° and 57° southern geodetic latitude and the meridians of 163° and 187° eastern longitude is shown in Figure 6.3. The geoid heights vary from -39.69 to 49.58 m with the mean of 8.03 m, and the standard deviation is 24.57 m.

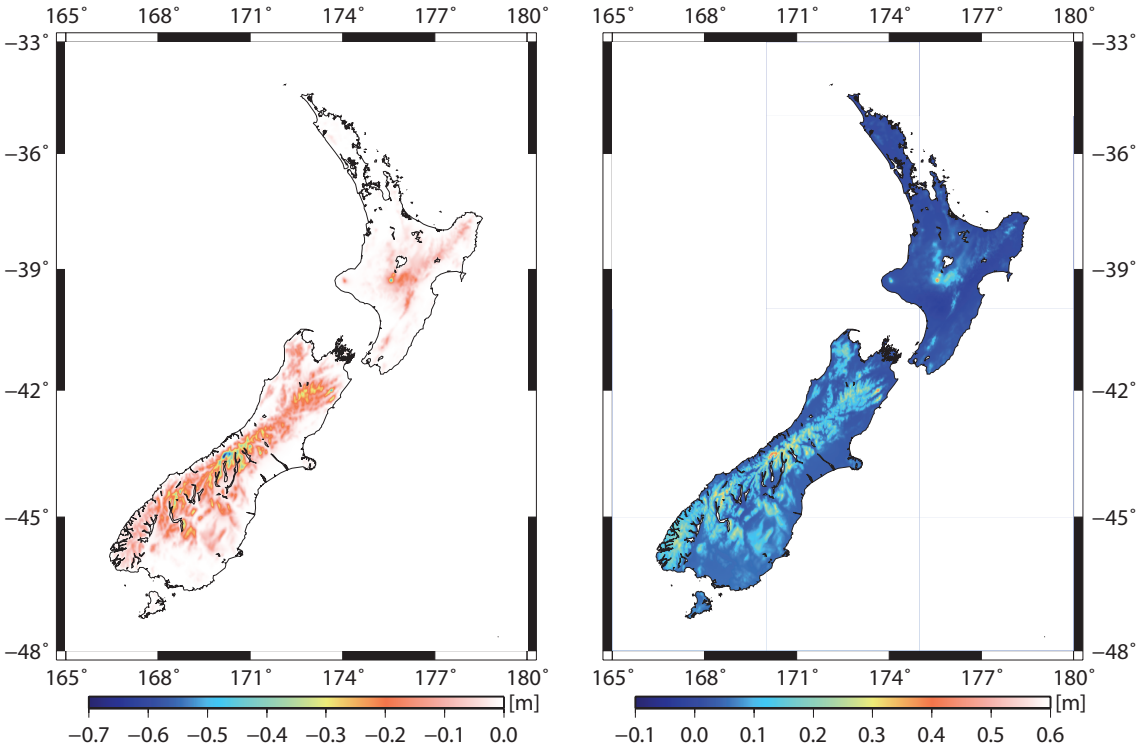

(a) Topographic correction. **(b)** Downward continuation correction.

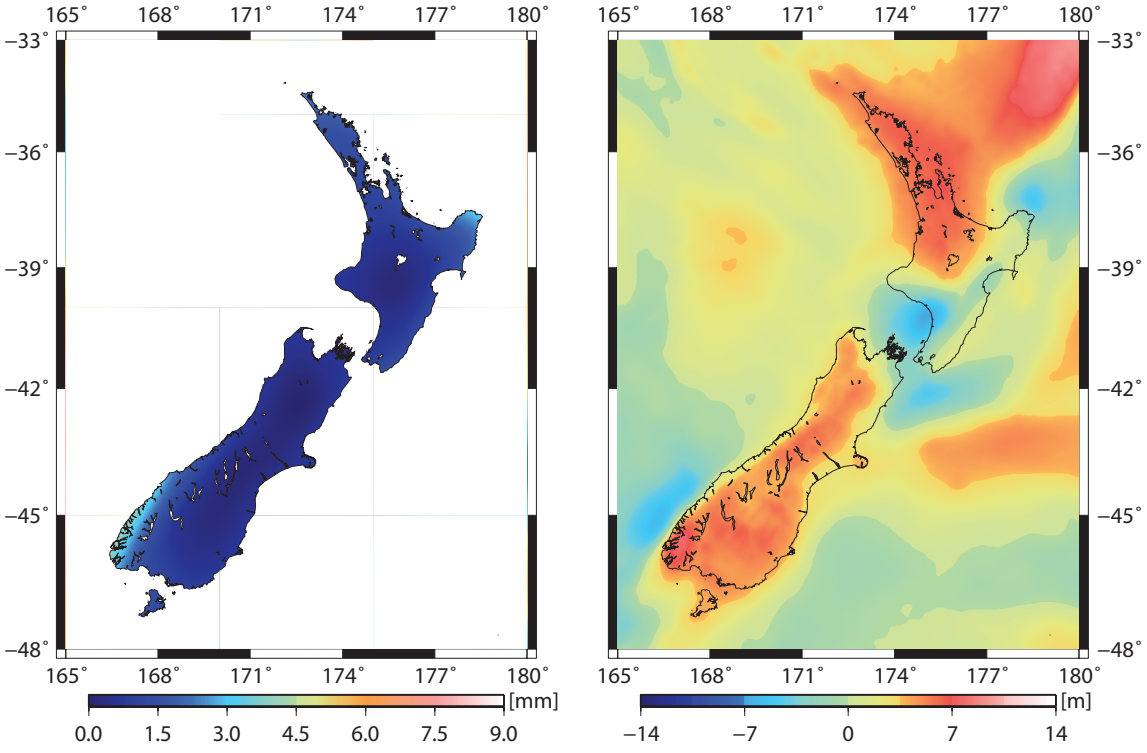

(c) Atmospheric correction. **(d)** Stokesian solution.

Figure 6.2: The additive corrections compiled over the computation area of New Zealand.

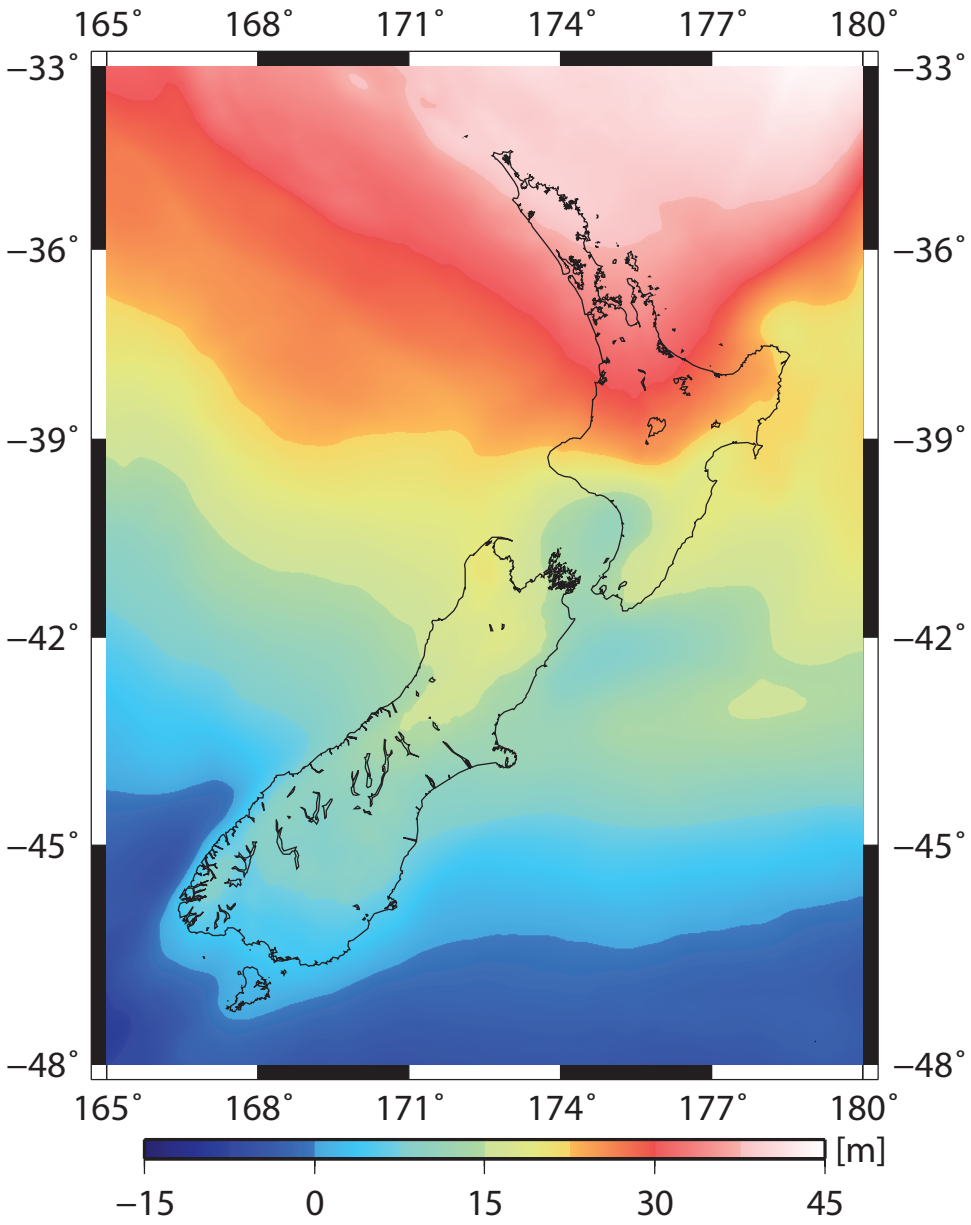

Figure 6.3: The NZGM2010 compiled on a $2' \times 2'$ geographical grid at the computation area of New Zealand and its continental shelf.

6.6 Quasigeoid determination by Boundary Elements Method (BEM)

In this section, BEM has been applied to determine the gravimetric quasigeoid model for New Zealand (Čunderlík *et al.*, 2010; Tenzer *et al.*, 2012). The direct BEM formulation for the Laplace equation is applied to obtain a numerical solution to the linearised fixed gravimetric boundary-value problem in points at the Earth's surface. The numerical scheme uses the collocation method with linear basis functions. It involves a discretisation of the Earth's surface, which is considered as a fixed boundary. The theoretical and numerical aspects of this method are discussed in Čunderlík *et al.* (2007) and Čunderlík and Mikula (2010).

With the current development of high-performance computing facilities, numerical methods such as BEM, finite element method (FEM), and finite volume method (FVM) are used more often in precise global and regional gravity field modelling. The first applications of FEM to the gravity field modelling were given by Meissl (1981) and Shaofeng and Dingbo (1991). Recently, FEM and FVM, applied in physical geodesy, have been discussed in (Fašková, 2008; Fašková *et al.*, 2009). The first application of BEM in physical geodesy was given by (Klees and Silverstein, 1992). This approach based on the indirect BEM formulation and the Galerkin BEM was further developed by Lehmann and Klees (1996); Klees (1996); Lehmann (1997); Klees and Lehmann (2001). Čunderlík *et al.* (2007) formulated the direct BEM for the fixed gravimetric boundary-value problem based on the collocation with linear basis functions. This approach was later completed by developing an iterative procedure for the elimination of far-zone interactions in Čunderlík and Mikula (2010). In this section, we will apply the BEM approach developed by Čunderlík *et al.* (2007) and Čunderlík and Mikula (2010) to determine the detailed gravimetric quasigeoid at the study area of New Zealand.

6.7 Direct BEM for the linearised fixed gravimetric BVP

The linearised fixed gravimetric boundary-value problem represents an exterior oblique derivative problem for the Laplace equation. It is defined as (cf. Koch and Pope, 1972; Bjerhammar and Svensson, 1983; Grafarend, 1989).

$$\triangle^2 T(\mathbf{r}) = 0, \tag{6.42}$$

$$\langle \nabla T(\mathbf{r}), \boldsymbol{s}(\mathbf{r}) \rangle = -\delta g(\mathbf{r}), \tag{6.43}$$

$$T(x) = O(|\mathbf{r}|)^{-1}, \tag{6.44}$$

where (r,Ω) is an arbitrary point and domain Ω represents the body of the Earth with its boundary Γ given by the Earth's surface. $\langle \nabla T, \mathbf{s} \rangle$ is the inner product of two vectors ∇T and $\mathbf{s}$, where the unit vector $\boldsymbol{s}$ is defined as follows:

$$\boldsymbol{s}(\mathrm{r}) = -\frac{\nabla U(\mathrm{r})}{|\nabla U(\mathrm{r})|} \tag{6.45}$$

Equation 6.43 represents the oblique derivative boundary condition as the normal to the Earth's surface Γ does not coincide with the vector defined in Equation 6.45. The direct BEM formulation for the Laplace equation leads to a boundary integral equation (BIE) that can be derived using Green's third identity or through the method of weighted residual (Brebbia *et al.*, 1984; Schatz *et al.*, 1990). A main advantage arises from the fact that only the boundary of the solution domain requires a subdivision into its elements. Thus, the dimension of the problem is effectively reduced by one. The application of the direct BEM to the linearised fixed gravimetric boundary-value problem Equations 6.42, 6.43 and 6.44 yields BIE in the following form (Čunderlík *et al.*, 2007):

$$\frac{1}{2}T(\mathbf{r}) + \int_{\Gamma} T(\mathbf{r}') \frac{\partial G}{\partial \mathbf{n}_{\boldsymbol{\Gamma}}}(\mathbf{r},\mathbf{r}'_{\mathbf{i}}) dy = \int_{\Gamma} \frac{\partial T}{\partial \mathbf{n}_{\boldsymbol{\Gamma}}}(\mathbf{r}'_{\mathbf{i}}) G(\mathbf{r},\mathbf{r}'_{\mathbf{i}}) dy, \tag{6.46}$$

where x and $\mathbf{y}$ are the geocentric position vectors of the computation and moving (integration) points, respectively, $\mathbf{n}_{\boldsymbol{\Gamma}}$ is the normal to the boundary Γ, and the kernel function G represents the fundamental solution to the Laplace equation:In order to handle the oblique derivative problem we use the same simplification as proposed by Čunderlík *et al.* (2007). According to the oblique derivative boundary condition in Equation 6.43, the negative value of the gravity disturbance δg is defined as a projection of the vector $\nabla T(\mathbf{r})$ onto the direction of $\mathbf{s}(\mathbf{r})$. The normal derivative term $\partial T/\partial n_{\Gamma}$on the right-hand side of BIE in Equation 6.46 approximately equals $\partial T/\partial \mathbf{n}_{\boldsymbol{\Gamma}} \cong \partial g(\mathbf{r}) \cos\mu(\mathbf{r})$, where $\mu(\mathbf{r})$ is the angle $\angle(\mathbf{n}_{\boldsymbol{\Gamma}}(\mathbf{r}),\mathbf{s}(\mathbf{r}))$. This term represents the projection of the vector onto the normal. In this way the oblique derivative boundary condition in Equation 6.43 is incorporated in the direct BEM formulation in Equation 6.46. The boundary integral equation in Equation 6.46 is discretised by means of using the collocation method. It involves a discretisation of the complicated Earth's surface by a triangulation of the topography and approximations of the boundary functions by linear functions on each triangular panel using linear basis functions. This is realised by the piecewise linear polynomials defined on the planar triangular panels, where vertices of this triangulation represent the colloca-

tion points. BIE in Equation 6.46 is then rewritten to the following discrete form (Čunderlík, Mikula, and Mojzeš, 2007; Faškovà, 2008):

$$c_i T_i \psi_i + \sum_{j=1}^{N} \int_{supp\psi_j} T_j \frac{\partial G_{i,j}}{\partial \mathbf{n_\Gamma}} \psi_j \mathrm{d}\Gamma_j = \sum_{j=1}^{N} \int_{supp\psi_j} \delta g_j G_{i,j} \mathrm{d}\Gamma_j (i = 1,2,....,N), \qquad (6.47)$$

where c_i represents the spatial segment bounded by the panels joined at the i-th collocation point, and N is the total number of nodes. The discretised boundary integral equations 6.47 form the linear system of observation equations

$$\mathbf{Mt} = \mathbf{L}\delta\mathrm{g} \qquad (6.48)$$

where $\mathbf{t}$ is the vector of unknown disturbing potential T at the collocation points, and δg is the vector of observed gravity disturbances δg. The elements of matrices $\mathbf{M}$ and $\mathbf{L}$ represent the integrals of the discrete form of BIEs in Equation 6.47. The discretisation of the integral operators is affected by the weak singularity of the kernel functions. The integrals with regular integrands are approximated by the Gaussian quadrature and non-regular integrands (singular elements) require a special treatment. For more details see Čunderlík *et al.* (2007). In case of the oblique derivative boundary condition in Equation 6.43, or the Neumann boundary condition using the aforementioned projection, the matrix $\mathbf{M}$ represents a system matrix, while the known vector $\mathbf{f} = \mathbf{L}\delta\mathbf{g}$ is given on the right-hand side of Equation 6.48.

6.8 BEM quasigeoid computation

In quasigeoid determination with regard to boundary element method (e.g. Čunderlík *et al.*, 2010), a regional refinement of the collocation points, is extracted from the global rough topography triangulation network with a resolution of 0.2°. The collocation points network over New Zealand and surrounding marine area from the global are refined at a resolution of 1.5°. The collocation points over the continental areas were located by employing a set of data, the topographical heights derived from regional and global DEMs, gravity disturbances (cf Figure 6.4a) derived from the existing gravity anomaly data sets and height anomalies derived from derived from GGM. With regard to the surrounding marine areas, the improved mean sea surface height DNSC08 (Andersen *et al.*, 2009) was utilised to locate the geocentric positions of sea surface heights on the collocation network. The MSS was derived from a combination of 12 years of satellite altimetry from a total of eight different satellites covering the period 1993 - 2004. It is the time-averaged physical height of the oceans surface. It represents the summation of the geoid height and the temporal

mean of the ocean dynamic topography (MDT). The 30”×30” SRTM30PLUS_V5.0 (Becker *et al.*, 2009) global DEM was used beside the local 1” × 1” New Zealand DEM for the topographic areas. Height anomalies over the collocation points were computed using EGM2008 coefficients complete to the degree and order 2160 of spherical harmonics. Having height anomalies and topography heights allows us to derive the ellipsoidal (geodetic) heights over the computation area (Figure 6.4b).

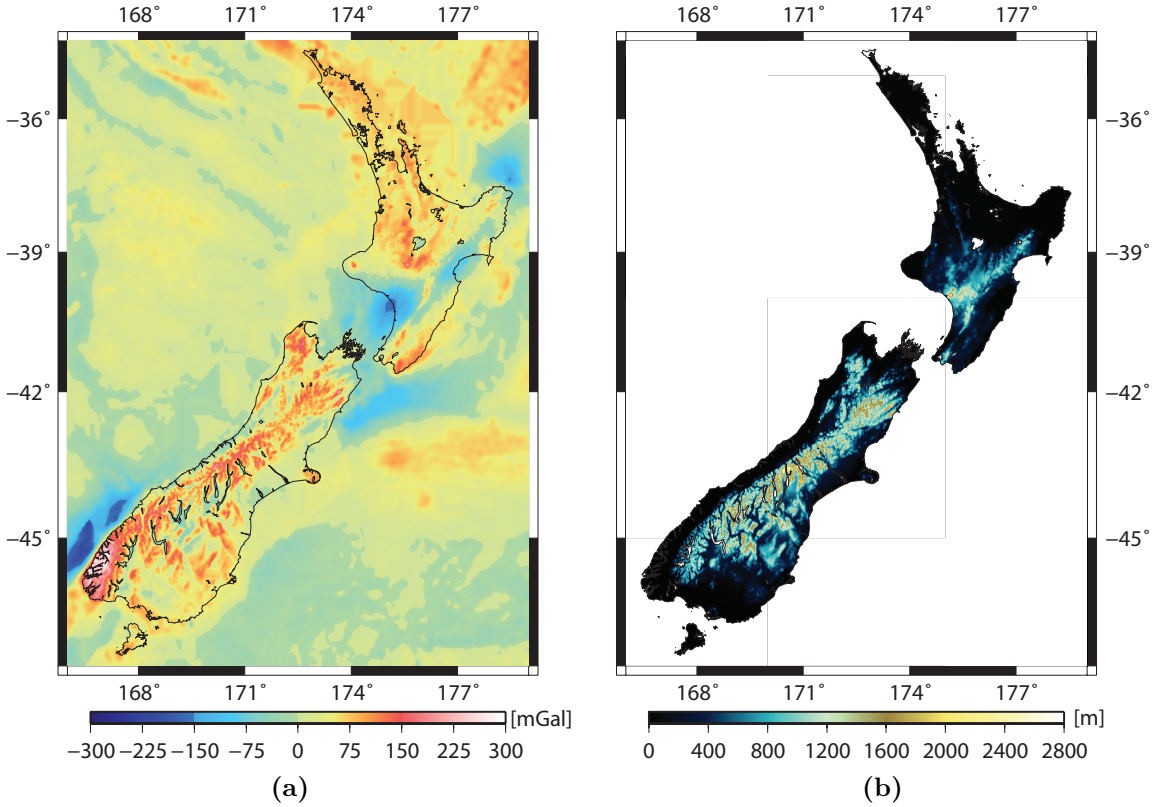

Figure 6.4: (a) The gravity disturbances, and (b) The ellipsoidal heights of the collocation points over the study area of New Zealand

The last step before the determination of the gravimetric quasigeoid by BEM is to transfer the gravity anomaly data to gravity disturbances through the following equation (Heiskanen and Moritz, 1967).

$$\delta g = \Delta g - \frac{\delta \gamma}{\delta h} \varsigma \tag{6.49}$$

The height anomalies ς in Equation 6.49 were calculated using the EGM2008 coefficients complete to degree 2160. The gravity anomalies Δg were compiled from the GNS Science gravity data (onshore) and extracted from the DNSC08 marine gravity database (offshore) provided by the Danish National Space Centre (Andersen *et al.*, 2009).

The gravimetric quasigeoid model NZQM2010 compiled at the study area of New

Zealand is shown in Figure 6.5. The computed values of the quasigeoid heights vary from -5.91 to 41.85 m with the mean of 18.29 m, and the standard deviation is 11.68 m. Within onshore New Zealand, the quasigeoid heights are everywhere positive with minima located at Steward Island and along the south coast of the South Island and maxima at the upper part of the North Island.

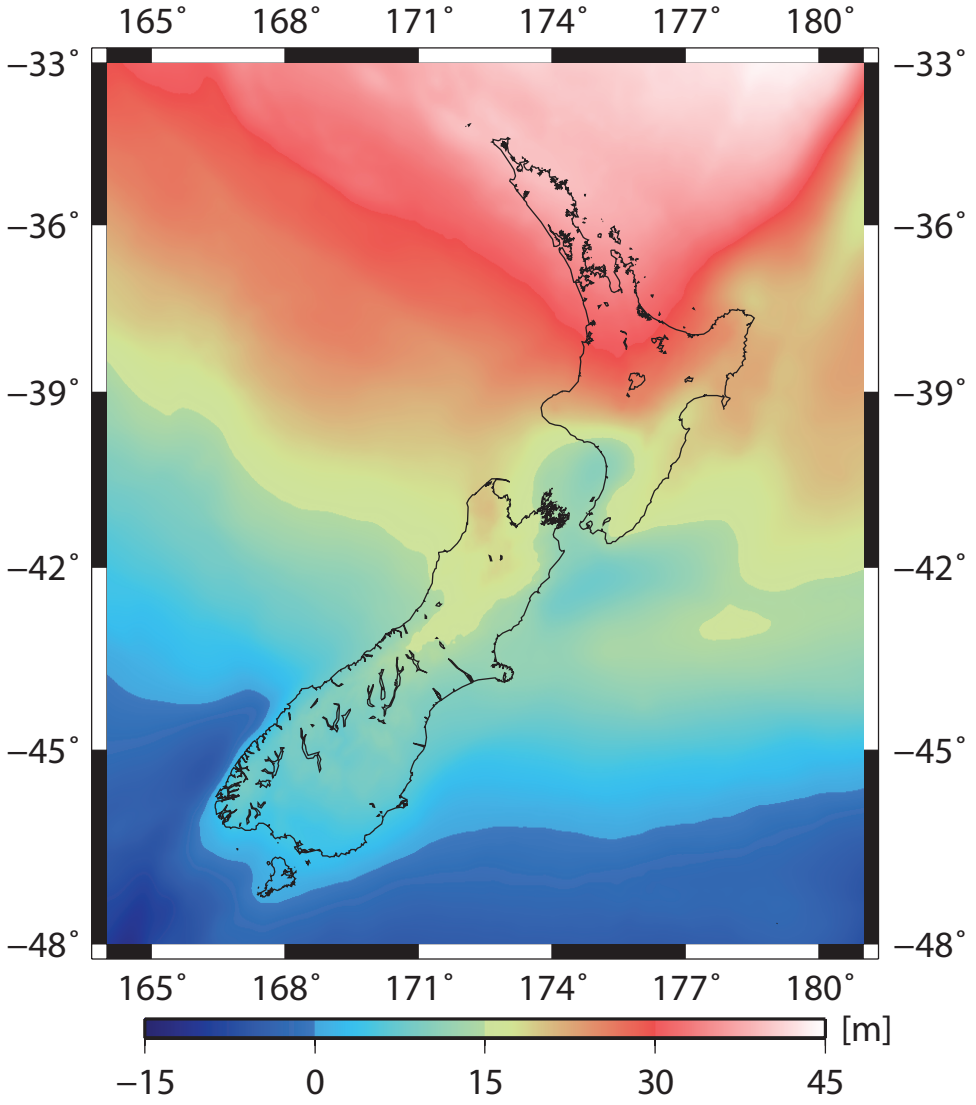

Figure 6.5: The gravimetric quasigeoid model NZQM2010 compiled at the study area of New Zealand.

6.9 Discretised integral-equation-based approaches

The determination of the residual gravimetric geoid is normally carried out on the basis of converting the local terrestrial gravity data into disturbing potential either on the geoid or the ellipsoid. This conversion is based on a widely known procedure called two-step approach (Bjerhammar, 1962, 1969; Bjerhammar and Svensson, 1983; Sideris, 1987; Martinec and Vaníček, 1996). It involves the Poisson's downward gravity continuation followed by the Stokes/Hotine integration. The performance of the two-step approach is typically conducted by reducing the terrestrial data to the geoid/ellipsoid surface and removing all topography above them. The second step is to convert the reduced anomalies into the disturbing potential in association with Green's integral. This procedure is complex due to the inverse problem of the discrete gravity data in the integral equation.

The unstable and unrealistic variances between the input and predicted gravity data cause the inverse problem (cf. Martinec, 1998), particularly, the high-frequency part of the predicted data (Martinec, 1998; Tenzer and Klees, 2008). It was demonstrated in Martinec (1996, 1998) that the ill-posed downward continuation is governed by the Fredholm's integral of the 1^{st} kind Fredholm (1900)and the solution is obtained by solving the Fredholm's integral formula of the 2^{nd} kind, which is yielded by adding Tikhinov regularisation to the Fredholm's first kind formula (cf. Schaffrin *et al.*, 1977; Engels *et al.*, 1993).

The regularisation procedures are extensively found in literature, for instance in Tikhonov and Arsenin (1977), and Lavrentev *et al.* (1986). Furthermore, various regularisation methods were reviewed and presented by Hansen (1987, 2008). Regarding downward continuation, regularisation methods were studied by several geodesists, for example, (Rummel *et al.*, 1979; Moritz, 1980; Tarantola, 1987; Sideris and Forsberg, 1991; Xu, 1992; Rauhut, 1992; Ilk, 1993; Vaníček *et al.*, 1996; Bouwman, 1998; Kern and Schwartz, 2002). The iterative scheme which was introduced by Martinec (1996) is based on finding the smallest grid step of data discretisation that could keep the downward continuation well-posed

To simplify the inversion problem in two-step approach, a new and more efficient method that can directly compute the disturbing potential from the terrestrial gravity data was presented by Novák (2003). This method combines the solution of the first and second/third boundary-value problems and directly relates observed gravity with the disturbing potential values by means of the Green integrals. Novák (2003) applied this method to geoid modelling from airborne gravity data. Alberts and

Klees (2004) compared various integral-equation-based approaches with the least-squares collocation in context of the quasigeoid modelling from airborne gravity data. Another version of one-step procedure was used by Novák and Heck (2002) to convert gravity disturbances at flight level into disturbing gravity potential.

The discretised integral equations are formulated for the gravity anomaly data (Δg,Δg^{r}, $\triangle g^{\mathrm{t}}$ and $\Delta g^{\mathrm{r,t}}$) at the data point $\mathbf{r}$ in the following form:

$$\Delta g(\mathbf{r}) = \sum_{i=1}^{l} \beta(\mathbf{r}'_{\mathbf{i}}) \Psi(\mathbf{r},\mathbf{r}'_{\mathbf{i}}) \tag{6.50}$$

where $\{\Psi(\mathbf{r},\mathbf{r}'_{\mathbf{i}}) : i = 1,2,...,I\}$ are the discretised integral equation functionals, and $\beta(\mathbf{r}'_{\mathbf{i}})$ are the coefficients that parameterise the gravity field at the positions $\mathbf{r}'_{\mathbf{i}}$.

In the Poisson integral approach , $\Psi(\mathbf{r},\mathbf{r}'_{\mathbf{i}})$ is given by the Poisson kernel P (see e.g. Kellogg, 1929):

$$\Psi(\mathbf{r},\mathbf{r}'_{\mathbf{i}}) = P(\mathbf{r},\mathbf{r}'_{\mathbf{i}}) = \left|\mathbf{r}'_{\mathbf{i}}\right| \frac{|\mathbf{r}|^2 - \left|\mathbf{r}'_{\mathbf{i}}\right|^2}{\left|\mathbf{r} - \mathbf{r}'_{\mathbf{i}}\right|^3}, \tag{6.51}$$

where $\left|\mathbf{r} - \mathbf{r}'_{\mathbf{i}}\right|$ is the Euclidean spatial distance; and $\hat{\mathbf{r}} = \mathbf{r}/|\mathbf{r}|$ and $\hat{\mathbf{r}}' = \mathbf{r}'/\left|\mathbf{r}'\right|$ are unit vectors in the direction $\mathbf{r}$ and $\mathbf{r}'$, respectively. In the Green integral approach, $\Psi(\mathbf{r},\mathbf{r}'_{\mathbf{i}})$ reads Novák (2003)

$$\Psi(\mathbf{r},\mathbf{r}'_{\mathbf{i}}) = G(\mathbf{r},\mathbf{r}'_{\mathbf{i}}) = -\frac{\partial P(\mathbf{r},\mathbf{r}'_{\mathbf{i}})}{\partial |\mathbf{r}|} - \frac{2}{|\mathbf{r}|} P(\mathbf{r},\mathbf{r}'_{\mathbf{i}}), \tag{6.52}$$

In the point-mass approach, $\Psi(\mathbf{r},\mathbf{r}'_{\mathbf{i}})$ is the reciprocal Euclidean distance (e.g. Tenzer and Klees, 2008):

$$\Psi(\mathbf{r},\mathbf{r}'_{\mathbf{i}}) = N(\mathbf{r},\mathbf{r}'_{\mathbf{i}}) = |\mathbf{r} - \mathbf{r}'_{\mathbf{i}}|^{-1} \tag{6.53}$$

The first order radial multipole approach, is defined as (Marchenko, 1998)

$$\Psi(\mathbf{r},\mathbf{r}'_{\mathbf{i}}) = M(\mathbf{r},\mathbf{r}'_{\mathbf{i}}) = \left|\mathbf{r}'_{\mathbf{i}}\right| \frac{\left|\mathbf{r}'_{\mathbf{i}}\right| - |\mathbf{r}| \left(\hat{\mathbf{r}}^{\mathrm{T}} \hat{\mathbf{r}}'\right)}{\left|\mathbf{r} - \mathbf{r}'_{\mathbf{i}}\right|^3} \tag{6.54}$$

The parameterisation of gravity anomaly data for all four types of the discretised integral equations is done at the positions located below data points at the chosen constant depth beneath the Bjerhammar sphere. The radius of the Bjerhammar sphere is set equal to 6371 km. The choice of the optimal depth is done based on minimising the RMS fit between the observed and predicted gravity data (Tenzer and Klees, 2008). The number of unknown parameters is identical to the number of

input gravity data. To reduce the size of the design matrix, the system of discretised integral equations is formed only for the near zone, while the distant-zone contribution is disregarded. The near zone is limited by the maximum spherical distance of 3°. The systems of discretised integral equations for the near zone are solved using the Jacobi iteration scheme (e.g. Young, 1971) as follows:

Considering SRBF kernel $\Psi(\mathbf{r},\mathbf{r}'_\mathbf{i})$, the relation between gravity anomaly Δg_g at the geoid when a prior knowledge of gravity anomaly at the topography surface Δg_t is available, is given by the following equation (Heiskanen and Moritz, 1967):

$$\Delta g_t = \Psi(\mathbf{r},\mathbf{r}'_\mathbf{i}) \times \Delta g_g \tag{6.55}$$

where Δg_t, $\Delta g_g \in \mathbb{R}^n$; $\Psi \in \mathbb{R}^{n\times n}$, $\psi_{ii} \neq 0$

Although Equation 6.55 could be ill-posed, the inversion of $\Psi(\mathbf{r},\mathbf{r}'_\mathbf{i})$ is a requisite to obtain Δg_g. Practically, there is a direct correlation between the ill-posedness of $\Psi(\mathbf{r},\mathbf{r}'_\mathbf{i})$ and the maximum height of elevations of the points of interest, and there is an inverse correlation between the ill-posedness and the block size of the geoid grid, especially when it goes denser (Martinec *et al.*, 1996).

The linear system of Equations (6.55) is similar to the classic matrix equation of the form

$$\mathbf{Ax} = \mathbf{L} \tag{6.56}$$

where $\mathbf{A}$ is an $n \times n$ matrix, $\mathbf{x}$ is a vector of unknowns with n elements, and $\mathbf{L}$ is a vector with n elements.

Reformulating Jacobi's iteration in terms of SRBF reads

$$\mathbf{\Delta g_g} = [\mathbf{\Psi}(\mathbf{r},\mathbf{r}'_\mathbf{i})]^{-\mathbf{1}}\mathbf{\Delta g_t} \tag{6.57}$$

$\Psi(\mathbf{r},\mathbf{r}'_\mathbf{i})$ can be written as

$$\mathbf{\Psi}(\mathbf{r},\mathbf{r}'_\mathbf{i}) = \mathbf{I} + [\mathbf{\Psi}(\mathbf{r},\mathbf{r}'_\mathbf{i}) - \mathbf{I}] \tag{6.58}$$

where $\mathbf{I}$ is the unit matrix of order n (cf. Martinec, 1998)

inserting Equation 6.58 in 6.55 we get

$$\Delta \mathbf{g}_t = \mathbf{I} \times \Delta \mathbf{g}_g + \Delta \mathbf{g}_g[\Psi(\mathbf{r},\mathbf{r}'_\mathbf{i}) - \mathbf{I}] \tag{6.59}$$

rearranging Equation 6.59 and starting the iteration with an initial value ($i = 0$)

$$\Delta \mathbf{g}_g^{(i)} = \Delta \mathbf{g}_t + [\mathbf{I} - \mathbf{\Psi}(\mathbf{r},\mathbf{r}'_\mathbf{i})]\Delta \mathbf{g}_g^{(i-1)} \tag{6.60}$$

where i is the number of iterations, $(i-1)$ means the present level and (i) represents the new level. By substituting iterated values at $(i-1)$ into the equation, the new values at iteration (i) can be estimated.

The iterations are subject to the condition $\left|\Delta \mathbf{g}_g^{(i)} - \Delta \mathbf{g}_g^{(i-1)}\right| \approx \varepsilon$, where ε is the acceptable error: iterations will be stopped when ε approaches the predetermined value, this way of stop criterion is discrepancy principle.

6.10 Study area and data sets

In this section, the accuracy of the local gravity field modelling is investigated using the integral-equation-based approaches described in the previous section. In particular, the investigation is based on testing the performance of the local gravity data when the gravity data are corrected for the residual terrain model (RTM-correction) and for the reference gravity field (remove-restore scheme) to analyse the accuracy of approximating the (irregularly distributed) gravity data corrected for the residual terrain model (RTM-correction) and for the reference gravity field (in the remove-restore scheme). Tenzer and Klees (2008) applied these approaches in order to compare the accuracy of approximating the topography-corrected and uncorrected (regularly distributed) mean gravity data in rugged terrain of the Canadian Rocky Mountains. All integral equations are discretised below data points at the chosen constant depth relative to the Bjerhammar sphere. The choice of the optimal depth is done based on minimising the RMS fit between the observed and predicted gravity data. In all four approaches the number of unknown parameters is identical to the number of input gravity data and the systems of discretised integral equations are solved using Jacobi iteration.

The chosen study area is situated in rugged terrain of the Southern Alps and flat coastal regions at the South Island of New Zealand including offshore areas. This study area is bounded by the parallels of 40° and 45° southern latitudes and the meridians of 170° and 175° eastern longitudes. The topographic heights at the study area, obtained from the 1" × 1" detailed DTM of New Zealand (Columbus *et al.*, 2011), reach 2384 m (see Figure 6.6a). The offshore (altimetry-derived) gravity anomaly data used for the numerical experiment were extracted from the DNSC08 marine gravity database (Andersen *et al.*, 2009). The DNSC08 marine gravity data are made available by the Danish National Space Centre (DNSC). Within New Zealand, we used the (observed) terrestrial gravity anomaly data from the GNS Science gravity database. The complete data set of 69605 gravity anomalies comprises 57603 marine gravity anomaly data distributed on a $1' \times 1'$ regular geographical

grid and the additional 12002 irregularly distributed observed terrestrial gravity anomaly data from the GNS Science gravity database. The map of gravity anomaly data distribution is shown in Figure 6.6b.

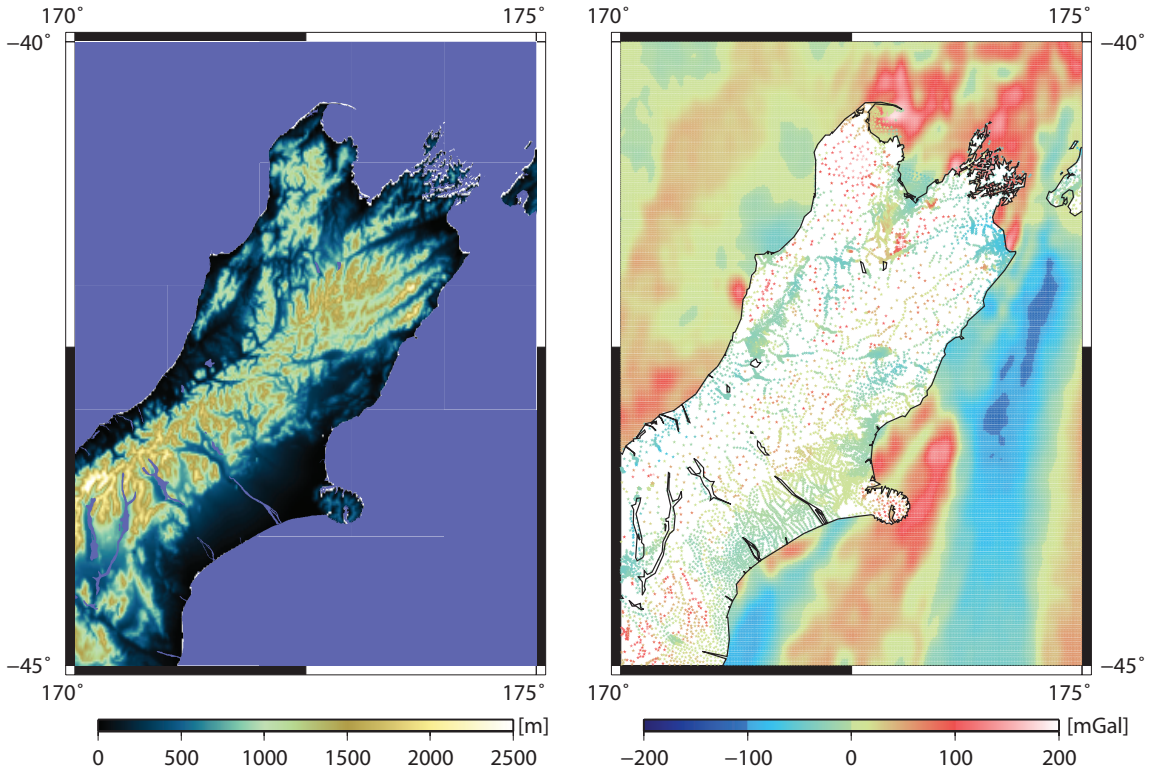

(a) Topography. **(b)** Gravity anomaly data.

Figure 6.6: The input data sets over the study area

The reference gravity field was evaluated using GOCO-02S global geopotential model (Goiginger *et al.*, 2011) complete to spherical harmonic degree 65. The choice of this maximum degree of the global geopotential model was based on the previous selection in Section 6.5. The performance of GOCO-02S at spherical harmonic degree 65 and 250 with respect to the local gravity data was tested over the study and the results were very similar. Therefore, using GOCO-02S at spherical harmonic degree 65 is satisfactory at this stage. However, the maximum degree 250 will be applied in the final quasigeoid computations in Section 6.13. The procedure of computing and applying the RTM-correction to gravity data is described by Forsberg and Tscherning (1997). The gravity data sets within the study area prepared for the numerical experiments are shown in Figure 6.7 and statistics are summarised in Table 6.1.

These gravity data sets consist of: (i) the observed (onshore) and altimetry-derived (offshore) gravity anomalies Δg, (ii) the residual gravity anomalies Δg^{r}, (iii) the

RTM-corrected gravity anomalies $\triangle g^{\mathrm{t}}$, and (iv) the RTM-corrected residual gravity anomalies $\Delta g^{\mathrm{r,t}}$. The differences among the data sets in Table 6.1 are based on using the original gravity anomalies Δg without making any changes. Then the data set Δg^{r} is corrected from reference field by subtracting gravity anomalies computed from GOCO-02S geopotential model at spherical harmonic degree 65 from Δg. The RTM-corrected residual gravity anomalies Δg^{t} are obtained by by removing the topographic correction from the gravity anomalies Δg. The RTM-corrected residual gravity anomalies $\Delta g^{\mathrm{r,t}}$ are obtained by removing reference field Δg^{r} and RTM correction Δg^{t} from the gravity anomaly data set.

Table 6.1: Statistics of four gravity anomaly data sets within the study area used for the numerical experiment. Unit 1 mGal.

Gravity data	**Min**	**Max**	**Mean**	**STD**
Δg	-114.4	182.7	6.2	47.1
Δg^{r}	-174.6	125.4	8.4	47.8
Δg^{t}	-159.8	158.1	-6.0	35.0
$\Delta g^{\mathrm{r,t}}$	-151.8	152.2	-20.5	30.5

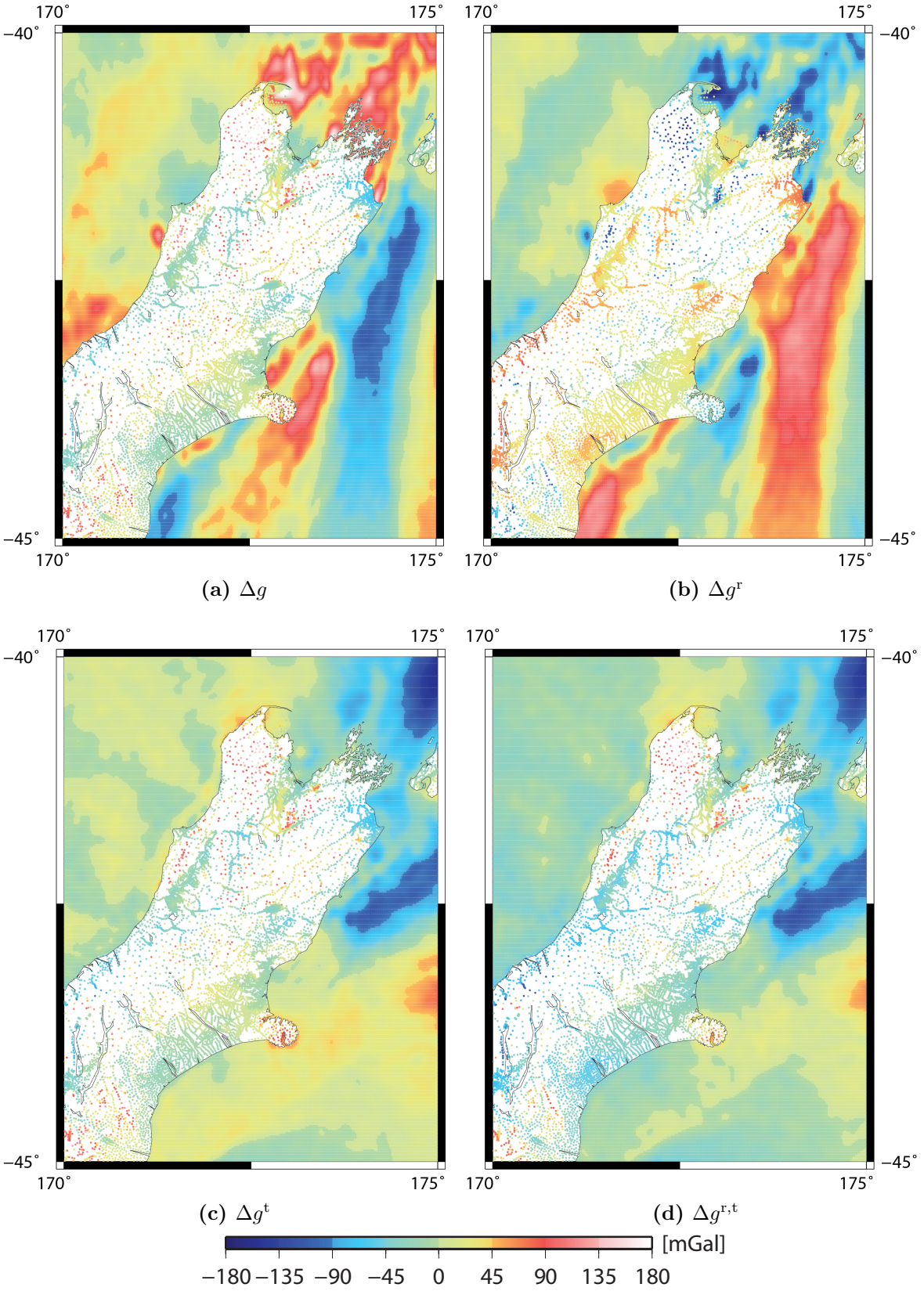

Figure 6.7: Gravity data sets: (a) gravity anomalies, (b) residual gravity anomalies, (c) RTM-corrected gravity anomalies, and (d) RTM-corrected residual gravity anomalies. Unit: 1 mGal.

The correlation of the gravity anomaly data with the topography is shown in Figure 6.8. The smoothing effect of the RTM-correction applied to gravity anomaly data is about 26 in terms of the RMS of gravity data dispersion.

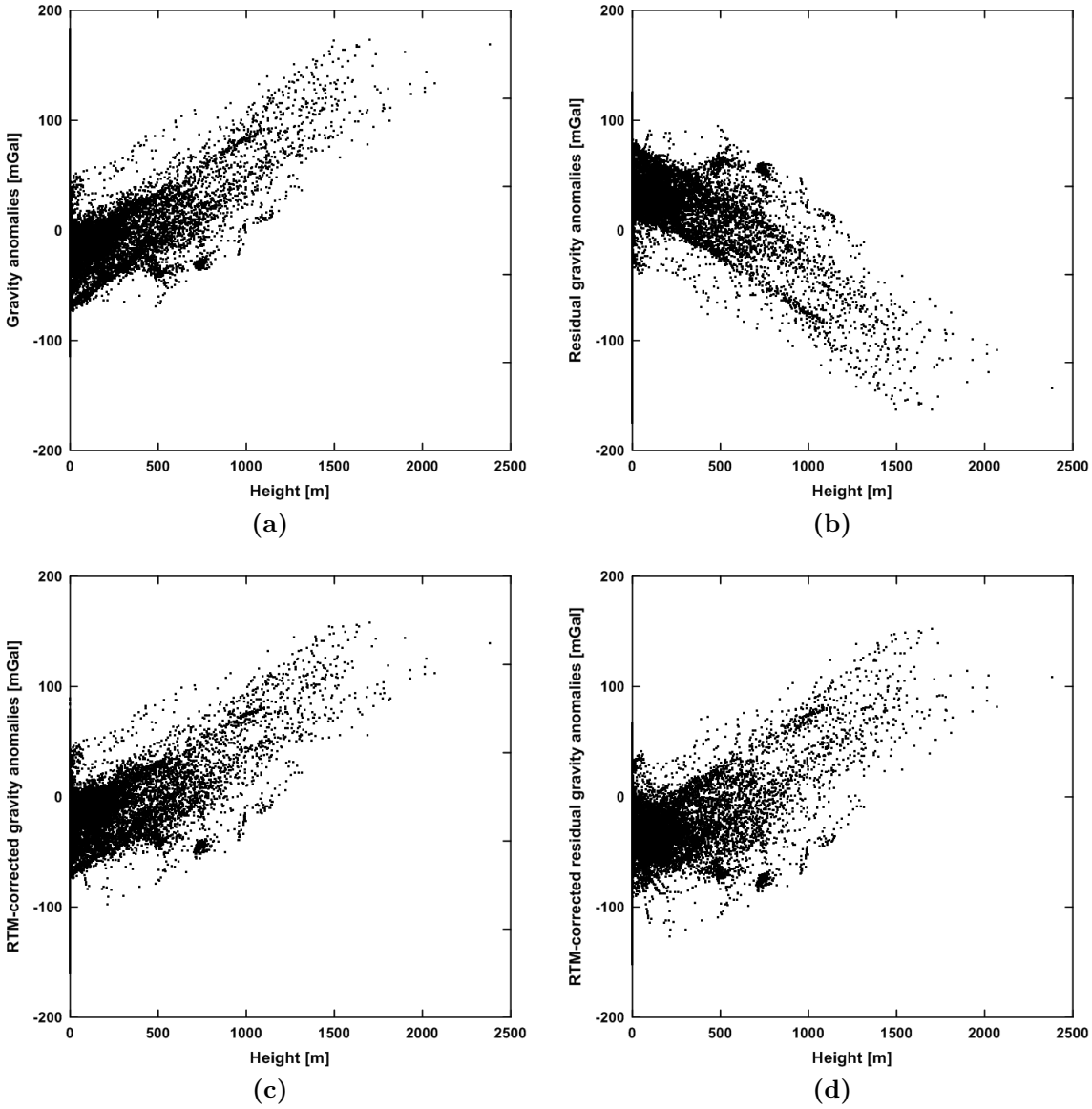

Figure 6.8: Correlation between the input gravity data and topography shown for (a) gravity anomalies, (b) residual gravity anomalies, (c) RTM-corrected gravity anomalies, and (d) RTM-corrected residual gravity anomalies.

6.11 Numerical results: integral-equation approaches

We applied the RMS minimisation technique for finding the optimal depth (between 0 and 10 km below the Bjerhammar sphere with a step of 0.1 km) of the parameterisation of gravity field by the Poisson, Green, point-mass, and radial multipole kernels. The SRBFs were applied with gravity anomaly, residual gravity anomalies after removing reference field, RTM-corrected anomalies and RTM-corrected residual anomalies. The results are shown in Figures 6.9, 6.9b, 6.9c and 6.9d.

The accuracy of gravity field approximation is assessed at the data points within the study area. The geographical maps of the residuals between observed and predicted gravity anomaly data sets for the optimal depths of the parameterisation for these four approaches are shown in Figures 6.10a to 6.10d, and statistics of residuals are summarised in Table 6.2. The RMS fit improves with decreasing depth of the parameterisation until the solution becomes ill-posed. The accuracy of the Green and point-mass approaches improves almost proportionally with decreasing depth. On the other hand, the RMS fit of the Poisson and radial multipole approaches is very sensitive with respect to the choice of the depth. Already several hundred metres significantly changes the accuracy. A similar accuracy was attained (for all four input gravity data sets) when applying the Poisson, point-mass, and radial multipole approaches. This result confirmed the finding of Tenzer and Klees (2008) that almost the same accuracy of local gravity field modelling can be achieved while using different types of integral kernels.

On the other hand, the accuracy of the Green integral approach is much higher. This significant accuracy improvement is because the Green integral approach utilises the gravity anomaly operator (of the Poisson kernel) instead of the identity kernel operators utilised in the Poisson, point-mass, and radial multipole approaches. The results also revealed that the optimal depths of the Poisson, point-mass, and radial multipole kernels are very similar, ranging between 0.1 and 0.2 km. Moreover, the optimal depths are almost unchanged when using different gravity data sets. On the other hand, the optimal depth of the Green kernel is 3.0 km when approximating Δg, Δg^{t} and $\Delta g^{\mathrm{r,t}}$, while it decreased to 2.5 km for Δg^{r}. Green, red and blue colours in Figures 6.9, 6.9b, 6.9c and 6.9d stand for the offset of 1,2 and 3 degree, respectively, around the computation area.

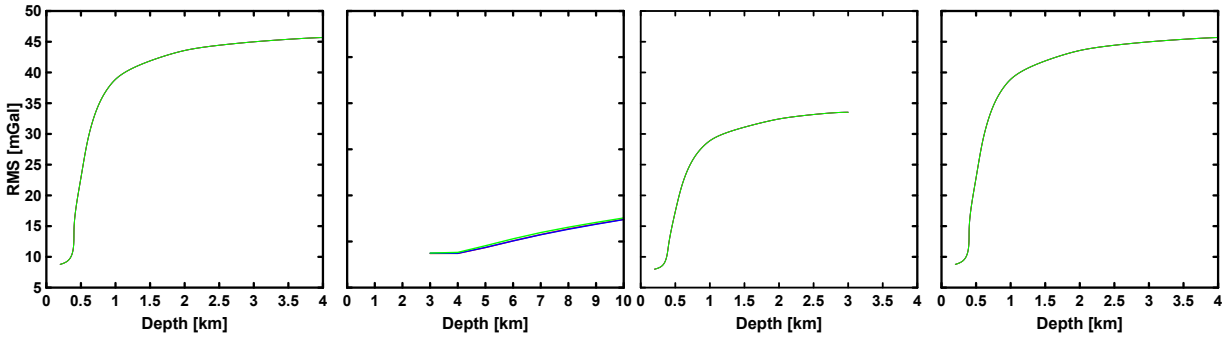

(a) Poisson

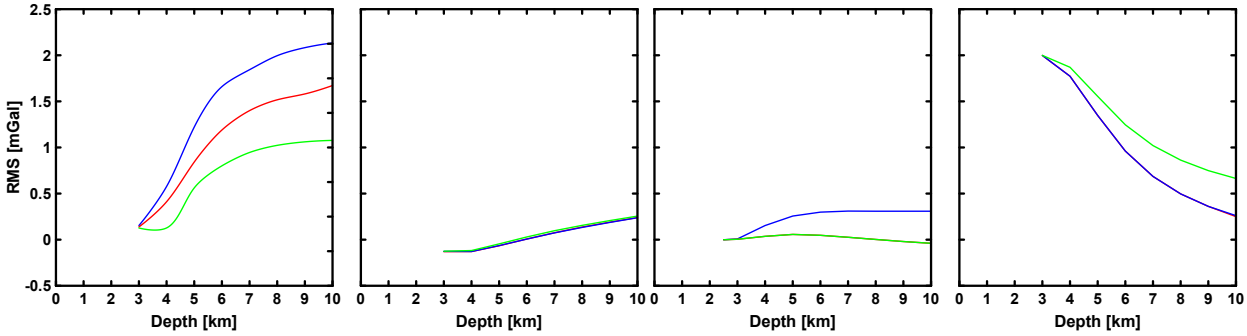

(b) Green

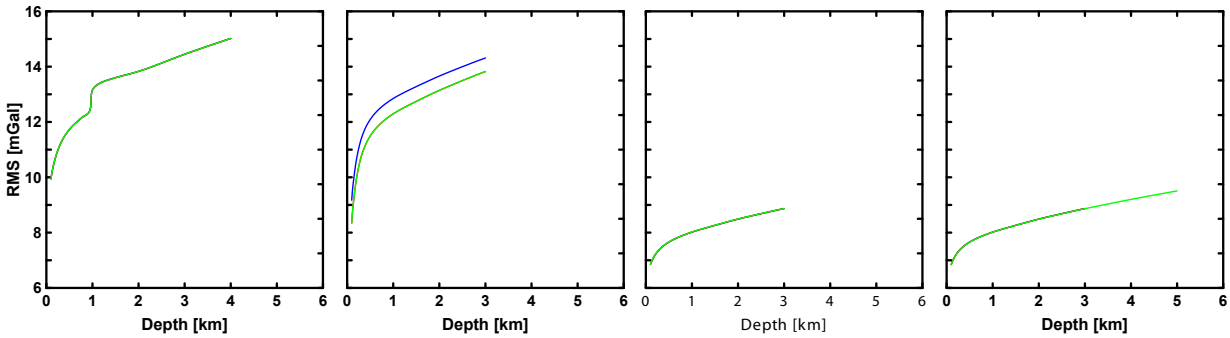

(c) Point mass

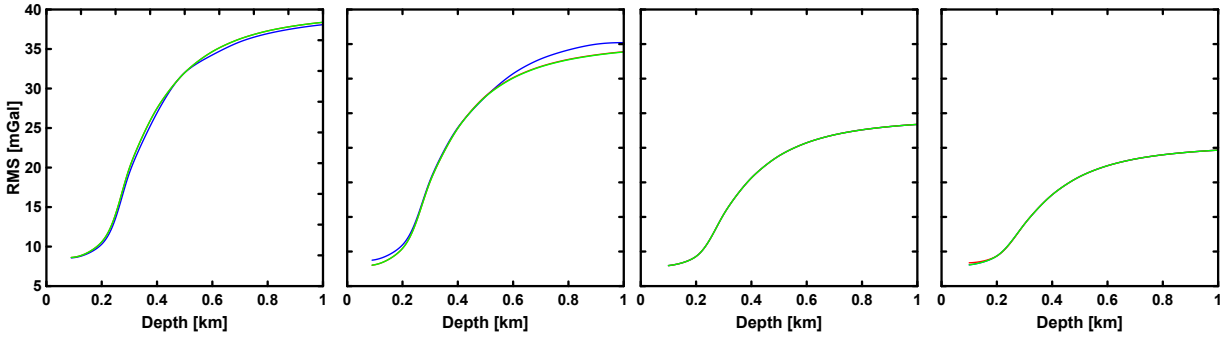

(d) Radial multipole

Figure 6.9: RMS minimisation technique for finding the optimal depth of the parameterisation by (a) Poisson, (b) Green, (c) Point mass and (d) Radial multipole kernels

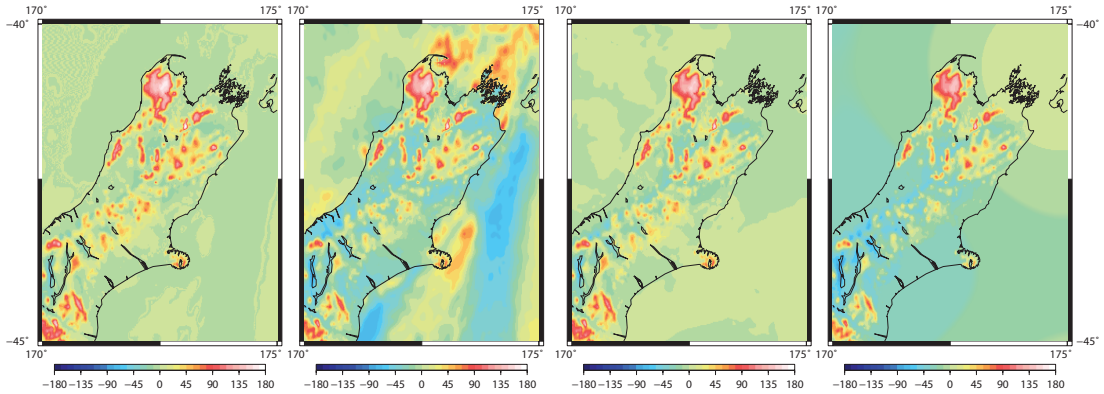

(a) Poisson approach. Unit: 1 mGal

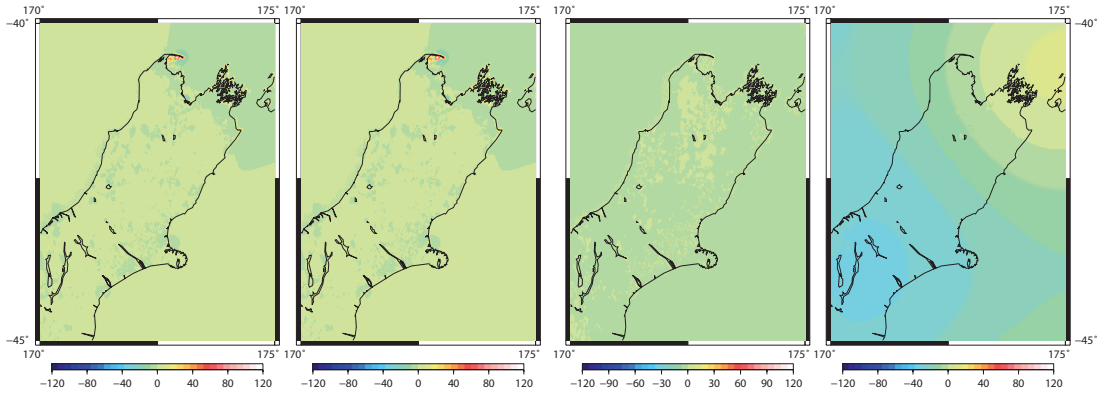

(b) Green approach. Unit: 1 mGal

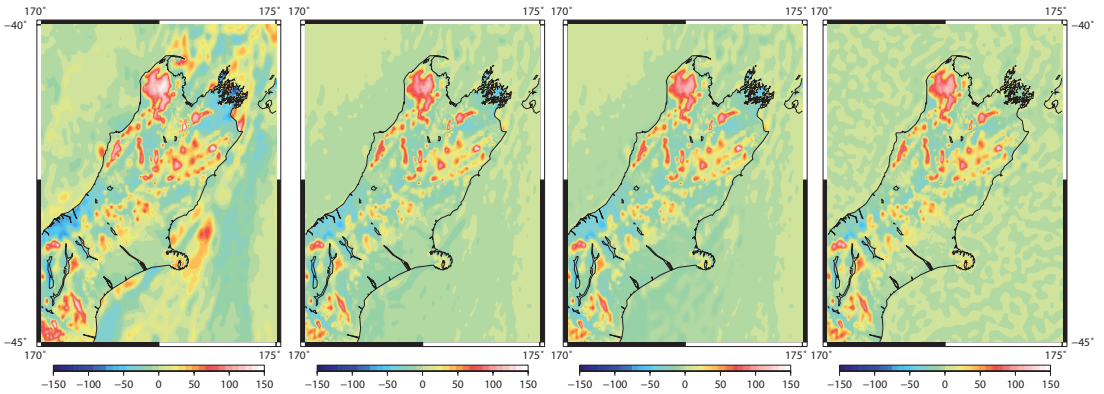

(c) Point mass approach. Unit: 1 mGal.

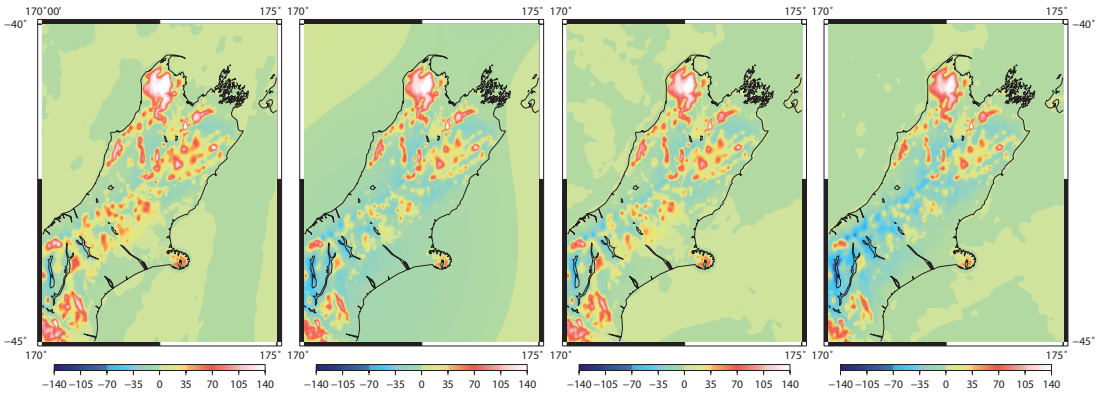

(d) Radial mulipole approach. Unit: 1 mGal

Figure 6.10: Geographic maps of the residuals between the observed and predicted data (from left) Δg, Δg^{r}, Δg^{t} and $\Delta g^{\mathrm{r,t}}$ after applying four discretised integral approaches.

Table 6.2: Statistics of the residuals between the observed and predicted gravity anomalies, residual, RTM-corrected and RTM-corrected residual gravity anomalies for the optimal depths of the parameterisation by the integral kernels. Unit: 1 mGal.

Gravity anomalies				
kernel	**Min**	**Max**	**Mean**	**RMS**
Poisson	-53.0	168.8	0.8	8.7
Green	-43.9	201.9	0.2	4.7
Point-mass	-102.9	157.8	0.2	9.9
Radial multipole	-53.4	165.7	0.7	8.6
Residual gravity anomalies				
Poisson	-159.4	72.2	0.0	8.0
Green	-197.7	-83.5	-0.1	4.6
Point-mass	-155.3	70.9	2.0	9.0
Radial multipole	-61.7	149.1	0.4	8.0
RTM-corrected gravity anomalies				
Poisson	-60.5	151.9	0.50	8.0
Green	-22.7	-31.2	0.0	0.7
Point-mass	-61.8	149.1	0.1	6.9
Radial multipole	-61.7	149.1	0.4	8.0
RTM-corrected residual gravity anomalies				
Poisson	-87.4	146.4	-0.3	7.9
Green	-24.7	25.5	0.0	0.9
Point-mass	-64.6	150.5	0.0	6.8
Radial multipole	-61.7	149.1	0.4	8.0

Figures 6.10a to 6.10d show the impact of using SRBF approaches on the four gravity data sets within the study area (Figure 6.7). The residuals between the observed and predicted anomalies are large in the regions where gravity measurements are few e.g. Tasman, Marlborough, Mount Cock and Southern Alps, Banks Peninsula and Central Otago (Figure 6.6b). These large residuals have the same trend when all SRBF approaches (Figures 6.10a, 6.10c and 6.10d) except the Green approach (Figure 6.10b). The Green integral approach shows small residuals of about ±20 mGal in all anomaly data sets.

From the numerical results illustrated in Table 6.2, the application of the RTM correction and consequently the smoothing of the high-frequency part of gravity signal improved the accuracy of the gravity field approximation by the Poisson and radial multipole approaches only slightly; the relative improvement of the RMS fit

is less than 10%. The application of the RTM correction to gravity anomaly data improved the RTM fit by 30% when using the point-mass approach.

Table 6.2 shows that most significant improvement of the RMS fit by applying the RTM correction was achieved when using the Green integral approach, from 4.7 mGal (for the uncorrected gravity anomalies) to 0.7 mGal (for the RTM-corrected gravity anomalies in Table). It represents more than 6.5 times better RMS fit. Obviously, the subtraction of the reference gravity field from the gravity anomalies does not significantly improve the accuracy of the gravity field approximation due to removing the long-wavelength part of the gravity signal. The presence of the small negative systematic bias due to the non-uniqueness of the solution of Green's integral equation (caused by transforming gravity to potential and consequently introducing a low-frequency component of which radial derivative equals zero) is completely removed when subtracting the reference gravity field.

In contrast, the application of the RTM correction introduced the systematic bias to Green's solution. The clarification of the systematic bias in the solutions obtained by the Poisson, point-mass, and radial multipole approaches is not simple as there is not a clear behaviour when applying the RTM correction and subtracting the reference field from gravity anomalies. The residuals between the observed and predicted gravity anomalies for the original gravity anomaly data and after removing the reference field and RTM correction are shown in Figures 6.10a, 6.10b, 6.10c and 6.10d. The numerical results revealed a very poor quality of the local gravity field approximation in some parts of mountainous regions where the residuals reach several dozens of mGals. The accuracy over the flat terrain and offshore areas is significantly better. We explain this low accuracy by the over-parameterisation of the solution in areas of large spatial elevation and gravity gradient variations together with irregular gravity data distribution.

Furthermore, we tested the effect of using the residual gravity Δg^{r} and RTM-corrected gravity $\Delta g^{\mathrm{r,t}}$ data on the quasigeoid computation over the tested area. The comparison between the geometric and the gravimetric heights revealed that computing the quasigeoid heights from the residual gravity anomalies has given better accuracy and consistency than using the RTM-corrected anomalies. RTM correction to the residual gravity did not add any improvement with respect to the GPS-levelling data. Restoring high frequency signal in terms of disturbing potential in the computation of the quasigeoid has introduced an ambiguous systematic error in the eastern coastal areas enclosed by red ovals (Figure 6.11b) because RTM-corrected residuals are expected to be smoother than the residual gravity. Hence, the residual gravity Δg^{r} will be used currently to undertake the quasigeoid computation and the RTM-corrected residuals will be investigated in the future studies.

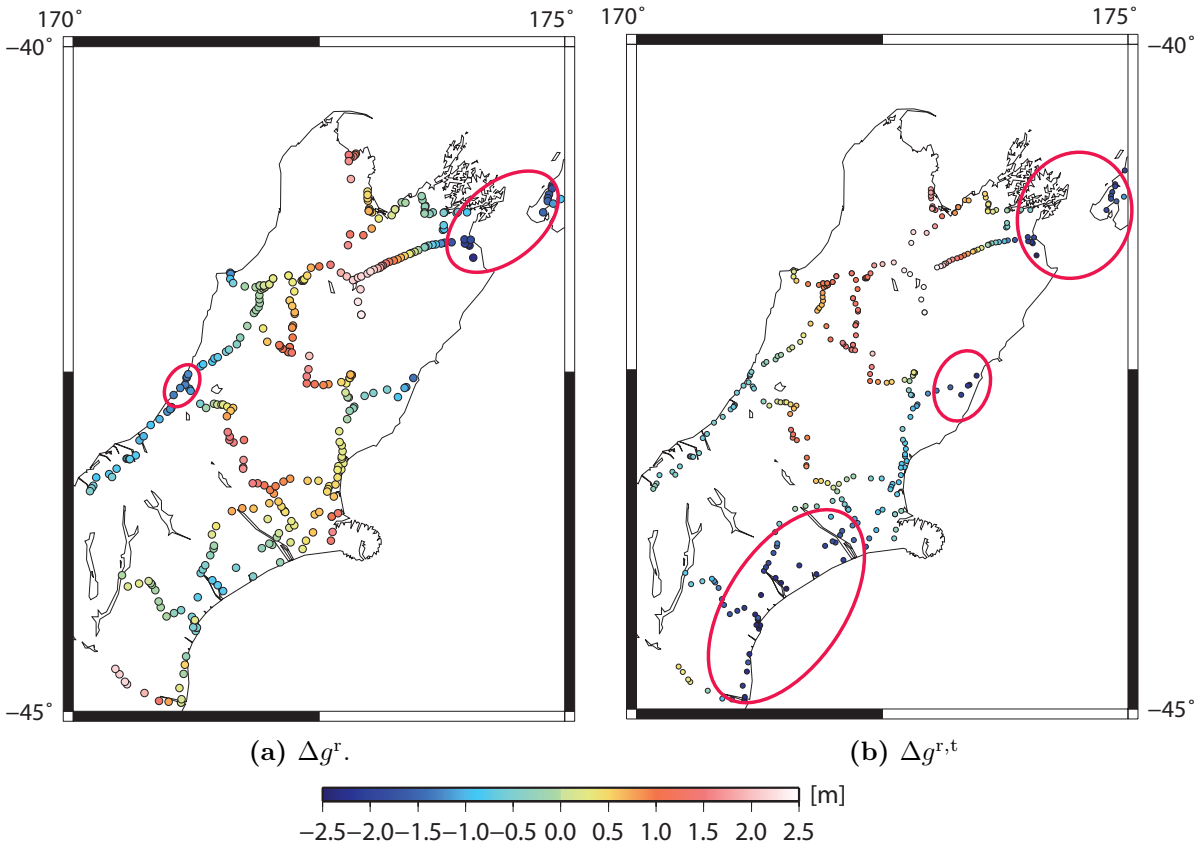

(a) Δg^{r}. **(b)** $\Delta g^{\mathrm{r,t}}$

Figure 6.11: Least-squares residuals between the geometric quasigeoid heights derived from GPS-levelling and the gravimetric quasigeoid heights computed using (a) residual gravity anomalies and (b) RTM-corrected gravity.

6.12 Remarks on the accuracy of local gravity data

The most accurate approximation of the observed (onshore) and altimetry-derived (offshore) gravity anomaly field is attained when using Green's integral approach (cf. Figure 6.9b). For the optimal parameterisation depth of 3.0 km, the RMS fit is 4.7 mGal at the data points. This RMS fit is almost two times better than the corresponding RMS fits obtained after using Poisson's, Point-mass, and Radial multipole approaches. The RMS fit of these three integral approaches is very similar ranging between 8.6 mGal (for Radial multipole approach) and 9.9 mGal (for Point-mass approach). The application of the RTM-correction to gravity anomaly data significantly improves the RMS fit of Green's integral approach, from 4.7 mGal for the uncorrected gravity anomaly data to 0.7 mGal for the RTM-corrected gravity anomaly data (cf. statistics in Figures 6.9b and 6.10b). The RMS fit of the Point-mass approach improved about 30% from 9.0 mGal (for the uncorrected gravity anomaly data) to 6.9 mGal (for the RTM-corrected gravity anomaly data). On

the other hand, the application of the RTM-correction to gravity anomaly data improved the RMS fit of the Poisson and radial multipole approaches less than 10%. The application of the RTM-correction to gravity anomaly data thus significantly improved only the RMS fit of the Green integral approach. In contrast, no improvement was obtained when using RTM-corrected gravity data in the computation of the quasigeoid comparing to the residual gravity data. The quasigeoid solution derived from residual gravity data has better accuracy in terms of RMS (cf. Figure 6.11 and Table 6.3)

Table 6.3: Statistics of the least-squares residuals between the geometric and gravimetric quasigeoid determined using residual and RTM-corrected gravity data. Unit: 1 m.

	residual anomalies	RTM-corrected
Min	-0.97	-1.94
Max	1.00	2.43
RMS	0.61	0.90

6.13 Compilation of the regional quasigeoid model for New Zealand

In this section, we determine our final experimental quasigeoid model for New Zealand (hereafter called OTG12). We implement the RCR numerical scheme. The residual gravity data obtained from observed gravity data after subtracting the reference gravity field are treated individually for the near and far zones. The discretised integral-equation approach (see Tenzer *et al.*, 2012) is applied to compute the near-zone (residual) contribution to gravity field. The far-zone (residual) contribution to gravity field is evaluated in spectral domain utilising the far-zone modified spherical harmonics (see Tenzer *et al.*, 2009, 2011).

6.13.1 Methodology

For the implementation of the RCR we employ a combination of terrestrial gravity and satellite-based gravity data derived from the global geopotential model. The residual gravity anomalies are obtained by removing reference field of gravity anomalies derived from the GGM. Furthermore, the effects of far-zone contribution on the gravity anomalies (Tenzer *et al.*, 2011) are also removed. The resulting residual gravity are used to compute residual disturbing potential. For the computation of the high-frequency disturbing potential, we use Green's integral approach. For the

restore step in RCR procedure, in addition to the residual potential we also compute the disturbing potential from the GGM spherical harmonics coefficients (Heiskanen and Moritz, 1967), and the effect of far-zone contribution on the disturbing potential is also computed. All potential quantities are added and by applying Bruns theory (ibid.) the quasigeoid heights are finally acquired.

In short, the RCR scheme was used to compute the gravimetric quasigeoid model combining information from detailed terrestrial gravity data sets and satellite-only GGM. The reasons for using the satellite-only GGM in gravimetric geoid/quasigeoid modelling are discussed, for instance, by Vaníček and Sjöberg (1991). Among these reasons the most important factor is that the satellite-derived GGMs provide a homogenous description of long-wavelength gravity field with well-defined stochastic properties. The gravity field quantities were divided into the reference (long-wavelength) and residual (high-frequency) components. The reference gravity field is defined by the maximum degree of spherical harmonics. The residual gravity field quantities were treated individually for the near- and far-zone surface integration sub-domains. The near zone is defined as $\psi \in \langle 0,\psi_0\rangle$, and $\psi \in \langle \psi_0,\pi\rangle$ defines the far zone; where ψ is the spherical distance and ψ_0 is the upper bound of the near zone.

6.13.2 Reference field and near-zone contribution

The computation of the reference disturbing potential T_{ref} and respective gravity anomaly Δg_{ref} at a surface point from the GGM coefficients is done using the following well-known expressions (e.g., Heiskanen and Moritz, 1967):

$$T_{\text{ref}}(r,\Omega) = \frac{GM}{R}\sum_{n=2}^{\bar{n}}\left(\frac{R}{r}\right)^{n+1}\sum_{m=-n}^{n} T_{nm}Y_{nm} \tag{6.61}$$

$$\Delta g_{\text{ref}}(r,\Omega) = \frac{GM}{R^2}\sum_{n=2}^{\bar{n}}\left(\frac{R}{r}\right)^{n+2}\sum_{m=-n}^{n} T_{nm}Y_{nm} \tag{6.62}$$

The computation of the near-zone (residual) disturbing potential T_{nz} at a surface point (r,Ω) from the corresponding near-zone (residual) gravity anomalies Δg_{nz} is done in two successive numerical steps. First, the gravity data analysis is applied to find the parametric solution in terms of the disturbing potential values at the parametric surface. The parameterisation of the local gravity field is done by forming the observation equation for each gravity value Δg_{nz} in the following form:

$$\Delta g_{nz}(r,\Omega) = \sum_{i=1}^{l} T_{nz}\left(r',\Omega_i'\right)G(\mathbf{r},\mathbf{r}_\mathbf{i}') \tag{6.63}$$

where T_{nz} are the disturbing potential values that parameterise the gravity field at positions $\left(r',\Omega'\right)$ within the near zone, and l is the total number of discretisation elements within the near zone.

In the second step, the gravity synthesis is applied to compute the near-zone (residual) disturbing potential values T_{nz} at the surface points (r,Ω) from the parameterised solution.

The parameterised solution is found by inverse solving the system of observation equations formed over the near zone according to Equation 6.63. The gravity synthesis is then carried out using the following expression:

$$T_{nz}(r,\Omega) = \sum_{i=1}^{l} T_{nz}\left(r',\Omega_i'\right) P(\mathbf{r},\mathbf{r_i'}) \tag{6.64}$$

The expression in Equation 6.64 is the discretised Poisson's integral equation. It allows computing the disturbing potential at the surface point from the respective values that parameterise the gravity field in terms of disturbing potential.

The Green's kernel G for defining the relation between Δg_{nz} and T_{nz} (e.g. Novák, 2003) has been demonstrated in Equation 6.52. The Poisson kernel in Equation 6.51 is given by (e.g. Heiskanen and Moritz, 1967, Chap. 1-16).

6.13.3 Far-zone contribution

The far-zone (residual) disturbing potential value and respective gravity anomaly at a surface point are computed using the following expressions (cf. Tenzer *et al.*, 2009):

$$\begin{aligned} T_{fz}(r,\Omega) = T_{fz}(R,\Omega) &- \left[\frac{r-R}{R}\right]\sum_{n=2}^{\bar{n}}(n+1)\tilde{T}_n(\Omega,\psi_0) \\ &+ \frac{1}{2}\left[\frac{r-R}{R}\right]^2\sum_{n=2}^{\bar{n}}(n+1)(n+2)\tilde{T}_n(\Omega,\psi_0) \end{aligned} \tag{6.65}$$

where $\delta g_{fz}(\Omega)$ are the surface spherical harmonics of the gravity disturbance δg. Similarly, Green's integral modified for computing the far-zone contribution to the gravity anomaly Δg_{fz} was obtained after applying the relation between $T_n(\Omega)$ and $\Delta g_n(\Omega)$ in the following form:

$$\begin{aligned} r\Delta g_{fz}(r,\Omega) = R\Delta g_{fz}(R,\Omega) &- \frac{r-R}{R}\sum_{n=2}^{\bar{n}}(n-1)(n+1)\tilde{T}_n(\Omega,\psi_\circ) \\ &+ \frac{1}{2}\left[\frac{r-R}{R}\right]^2\sum_{n=2}^{\bar{n}}(n-1)(n+1)(n+2)\tilde{T}_n(\Omega,\psi_\circ) \end{aligned} \tag{6.66}$$

where $\bar{n}$ is the maximum degree of the GGM coefficients used for generating the far-zone residual gravity field quantities. The far-zone modified surface spherical function $\tilde{T}_n(\Omega,\psi_\circ)$ in Equation 6.66 is related to the surface spherical functions $T_n(\Omega)$ by means of the Molodensky's truncation coefficients as follows (ibid.)

$$\begin{aligned}\tilde{T}_n(\Omega,\psi_0) &= (n-1)\frac{Q_n(\psi_0)}{2}T_n(\Omega) \\ &= (n-1)\frac{Q_n(\psi_0)}{2}\sum_{m=-n}^{n} T_{nm}Y_{nm}(\Omega)\end{aligned} \tag{6.67}$$

The disturbing potential components T_{ref}, T_{nz} and T_{fz} are converted into the respective components ς_{ref}, ς_{nz} and ς_{fz} of the height anomaly ς by applying the Bruns formula, while using the normal gravity value γ computed at the telluroid.

6.14 Numerical results

In order to solve the near-zone contribution, we first subtracted the reference gravity field from the terrestrial gravity anomaly data (shown in Figure 6.7). The computation of T_{ref} and Δg_{ref} was realised according to the expressions given in Equations 6.61 and 6.62, respectively. The reference gravity field was considered up to the maximum degree 250 of spherical harmonics. We used the maximum degree of the geopotential model in the quasigeoid computation to utilise the advantage of GRACE/GOCE combination in GOCO-02S combined satellite-only model, particularly in the medium-short-wavelength Earth's gravitational field (see Figure 5.1 and Table 5.1). The reference gravity anomalies and height anomalies computed using the GOCO-02S coefficients complete to spherical harmonic degree 250 are shown in Figures 6.12a and 6.12b. Over the study area, the reference gravity anomalies vary from -17.4 to 52.5 mGal, with the mean of 10.5 mGal and the STD is 13.4 mGal. The reference height anomalies are within -8.92 and 44.78 m, with the mean of 17.93 m and the STD is 13.43 m.

Furthermore, the far-zone contribution was subtracted from the residual gravity anomalies. The far-zone contributions to residual gravity field quantities were computed according to the expressions given in Equations 6.65 and 6.66. The far-zone contributions were generated using the EGM2008 coefficients from degree 251 up to 2160 of spherical harmonics, to 2160 consider far zone contribution on the quasigeoid. The results are shown in Figure 6.12b. The far-zone residual gravity anomalies vary from -43.3 to 47.6 mGal, with the mean of 0.0 mGal and the STD is 7.3 mGal. The far-zone residual height anomalies are within -2.31 and 1.77 m, with the mean of -0.01 m and the STD is 0.37 m.

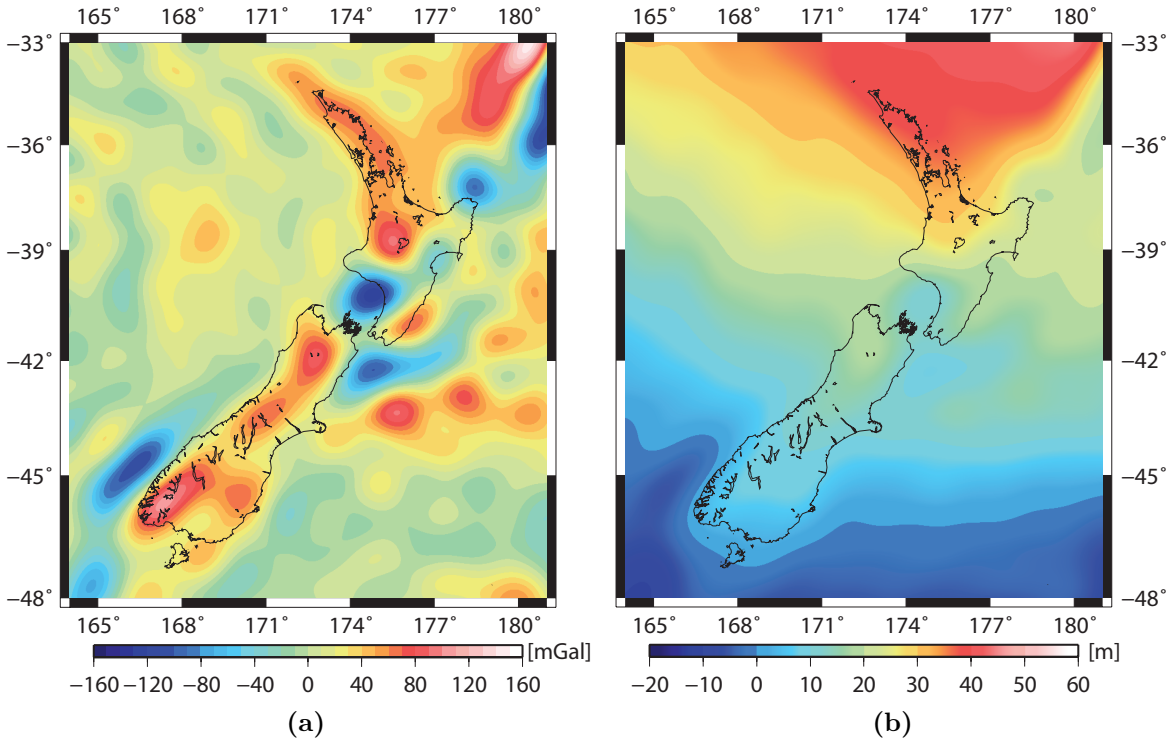

Figure 6.12: (a) The reference gravity field quantities and (b) height anomaly computed on a $1' \times 1'$ grid of surface points using the GOCO-02S coefficients complete to degree 250 of spherical harmonics.

The near-zone residual gravity anomalies are shown in Figure 6.13a. They vary from -236.3 to 315.2 mGal, with the mean of 0.0 mGal and the STD is 41.4 mGal. These gravity anomaly data were used to compute the near-zone residual disturbing potential at surface points and subsequently the height anomalies. The solution was obtained after applying the discretised integral-equation approach. The parameterisation of gravity anomaly data was done at the positions located below data points at the chosen constant depth beneath the Bjerhammar sphere. The radius of the Bjerhammar sphere was set equal to 6371 km. We used the depth of 3 km. The choice of the optimal depth was done based on minimising the RMS fit between the observed and predicted gravity data (Tenzer, 2008; Tenzer and Klees, 2008).

The computation was carried out in two steps. First, the system of observation equations was formed for the near-zone residual gravity anomaly data according to Equation 6.63. The vector of observations was formed by the values of the near-zone residual gravity anomalies at the surface points. The unknown parameters are the corresponding disturbing potential values on the parametric surface. The design matrix was formed by Green's kernels (defined in Equation 6.52). The number of unknown parameters is identical to the number of input gravity data. We applied

the mask matrix to account only for the values within the near-zone area. For more details the reader is referred to Tenzer and Novák (2008). The system of observation equations was solved iteratively using the Jacobi scheme (e.g. Young, 1971).

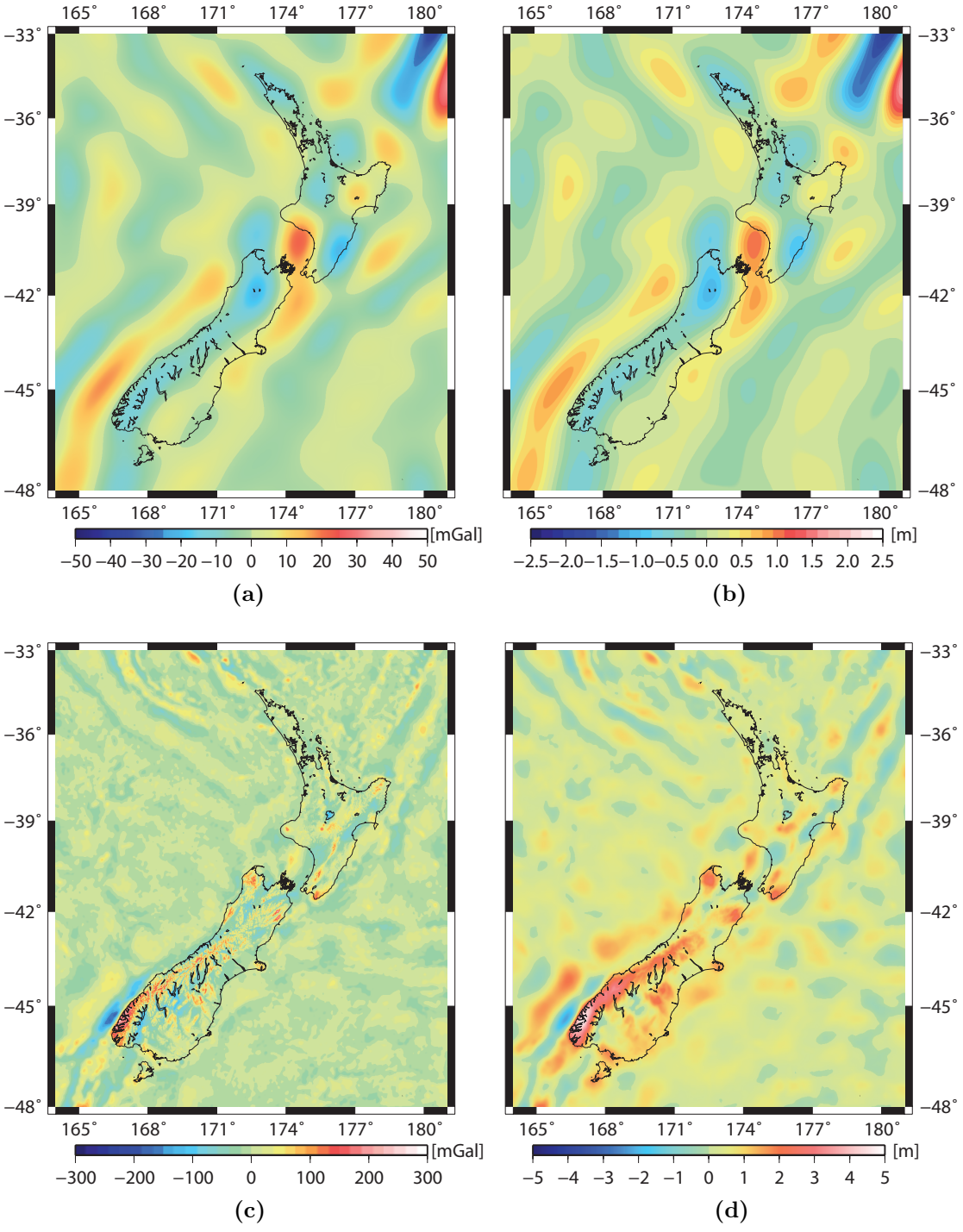

Figure 6.13: (a) The far-zone (residual) gravity anomalies and (b) The far-zone residual height anomalies computed using the EGM2008 coefficients within degrees from 251 up to 2160 of spherical harmonics, (c) The near-zone (residual) gravity field Δg_{nz}, (d) The near-zone (residual) height anomalies ζ_{nz} computed on a $1' \times 1'$ grid of surface points.

After finding the solution that parameterises the gravity field in terms of the disturbing potential values, the gravity synthesis was applied according to Equation 6.64. In this numerical step, the parametric solution was used to calculate the near-zone residual disturbing potential values at surface points. The respective height anomalies were obtained after applying the Bruns formula. The near-zone residual height anomalies are shown in Figures 6.13c and 6.13d. They vary between -9.63 and 11.42 m, with the mean of 0.25 m and the STD is 2.17 m. The final regional gravimetric quasigeoid model is shown in Figure 6.14. The gravimetric height anomalies vary between -12.29 and 45.48 m, with the mean of 18.17 m and the STD is 13.70 m.

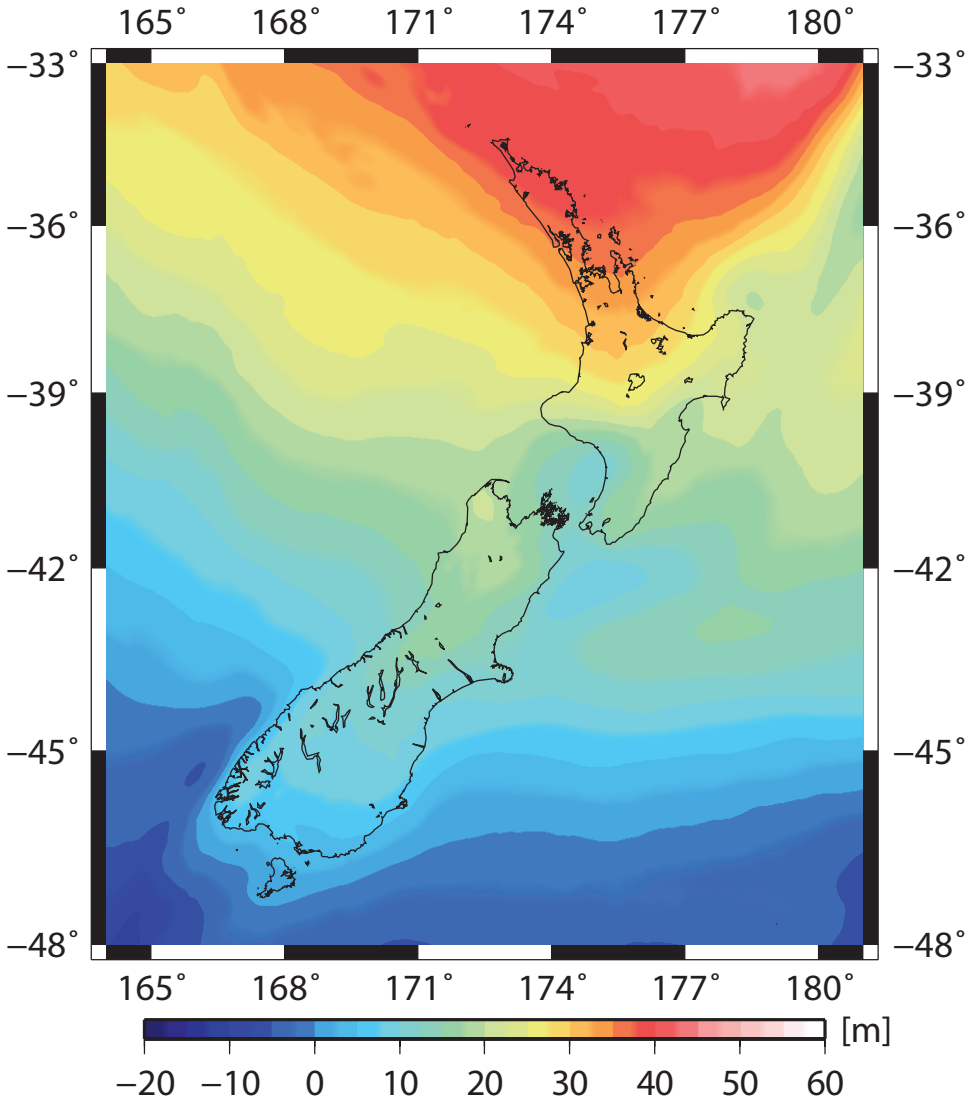

Figure 6.14: The regional gravimetric quasigeoid model for New Zealand computed on a $1' \times 1'$ geographical grid.

Chapter 7

Analysis of results

7.1 Validation of regional gravimetric models

The newly determined orthometric and normal heights at the GPS-levelling testing network were used to assess the accuracy of the regional geoid and quasigeoid models (NZGM2010, NZGeoid2009, NZQM2010 and OTG12). The geometric geoid heights were calculated from the NZGD2000 geodetic heights by subtracting the (Helmert's) orthometric heights. The geometric quasigeoid heights were obtained from the NZGD2000 geodetic heights by subtracting the normal heights. The differences between the geometric and gravimetric geoid heights were computed for the regional geoid model NZGM2010. The corresponding differences between the geometric and gravimetric quasigeoid heights were computed for the regional quasigeoid models NZGeoid2009, NZQM2010 and OTG12.

We further analysed the accuracy of the regional geoid/quasigeoid models in New Zealand using the original normal-orthometric heights defined in 12 major LVDs and converted to systems of the normal and orthometric heights by applying the cumulative normal to normal-orthometric height correction and subsequently the geoid-to-quasigeoid correction. We then added the average values of LVD offsets relative to WHS and NZGeoid2009 to these heights. The average offsets of major LVDs at the North and South islands of New Zealand are given in Tables 1.1 and 4.1. The LVD offsets relative to WHS (Tenzer *et al.*, 2011) range from 1 cm (Wellington 1953 LVD) to 37 cm (One Tree Point 1964 LVD). The reported LVD offsets relative to NZGeoid2009 (Claessens *et al.*, 2009, 2011) range from 6 cm (One Tree Point 1964 LVD) to 49 cm (Dunedin 1958 LVD). The NZGD2000 geodetic heights and the orthometric/normal heights corrected for the LVD offsets relative to WHS and NZGeoid2009 were compared with the gravimetric geoid/quasigeoid heights of NZGM2010, NZGeoid2009 and NZQM2010.

7.1.1 Validation before fitting

Statistics of the differences between the geometric and gravimetric geoid/quasigeoid heights at the GPS-levelling testing network (for the newly adjusted levelling networks and LVD offsets relative to NZGeoid2009 and WHS) are given in Table 7.1. As seen in Table 7.1, the RMS fit of all gravimetric solutions with GPS-levelling data is up to 80 cm or better. The best agreement between the geometric and gravimetric solutions is attained between OTG12 and the geometric quasigeoid heights applying newly determined orthometric/normal heights; the RMS of differences is 42 cm. OTG12 shows more consistency and less biases than the other models. The reduction of the offsets's number has decreased the expected errors from different LVD offsets. The RMS fit of (NZGM2010, NZQM2010 and NZGeoid2009) gravimetric solutions with GPS-levelling data is in a similar range (45 cm to 56 cm), when applying the LVD offsets relative to newly determined normal/orthometric height, NZGeoid2009 or WHS (cf. Table 7.1).

Table 7.1: Statistics of the differences (in metres) between the geometric and gravimetric geoid/quasigeoid heights at the GPS-levelling testing network calculated for NZGM2010, NZQM2010, NZGeoid2009 and OTG12 using the newly determined orthometric/normal heights, normal-orthometric heights defined in LVDs and corrected for the LVD offsets relative to NZGeoid2009 and WHS.

Newly determined orthometric/normal heights				
Model	**Differences**			
	Min	**Max**	**Mean**	**RMS**
NZGM2010	-1.05	0.66	-0.54	0.57
NZQM2010	-0.98	0.67	-0.43	0.46
NZGeoid2009	-0.99	0.61	-0.52	0.54
OTG12	-0.80	0.42	-0.37	0.42
LVD relative to NZGeoid09				
NZGM2010	-1.00	0.65	-0.52	0.55
NZQM2010	-1.06	0.81	-0.42	0.45
NZGeoid2009	-1.04	0.65	-0.50	0.52
OTG12	-0.99	-0.60	-0.66	0.82
LVD relative to WHS				
NZGM2010	-1.00	0.65	-0.52	0.55
NZQM2010	-1.05	0.80	-0.42	0.46
NZGeoid2009	-1.03	0.64	-0.50	0.52
OTG12	-1.00	0.60	-0.65	0.68

These solutions have also a better RMS fit when compared with the solutions obtained after applying the newly determined orthometric/normal heights (Table 7.1)

except for NZQM2010 and OTG12 for which the RMS fit slightly improved. All results confirmed the presence of large systematic offsets between the gravimetric and geometric solutions; the mean values of differences range from 37 up to 66 cm. The differences between NZQM2010 and GPS-levelling data have the largest distortions for both applied LVD offsets; the range of differences between the geometric and gravimetric quasigeoid heights is 1.87 m (for the LVD offset relative to NZGeoid2009) and 1.85 m (for the LVD offset relative to WHS, see Table 7.1). The smallest range of differences of 1.22 m was found between the OTG12 and newly adjusted GPS-levelling data.

7.1.2 Validation after fitting

The gravimetric geoid/quasigeoid solutions were further combined with GPS-levelling data in order to reduce the large systematic distortions found between the geometric and gravimetric geoid/quasigeoid heights. These systematic distortions were modelled by a 3-parameter model (Kotsakis and Sideris, 1999), the 3-parameter model is given as

$$\mathbf{a_i x} = (\cos\phi_i \cos\lambda_i)x_1 + (\cos\phi_i \sin\lambda_i)x_2 + (\sin\phi_i)x_3 \tag{7.1}$$

The matrix system of observation is solved as

$$\mathbf{Ax} = \mathbf{\Delta N} - \varepsilon \tag{7.2}$$

applying least-square approach the parameters $\hat{\mathbf{x}}$ are obtained by

$$\hat{\mathbf{x}} = (\mathbf{A}^\star \mathbf{A})^{-1} \mathbf{A}^\star \mathbf{\Delta N} \tag{7.3}$$

The observation equations were formed for the differences between the geometric and gravimetric geoid heights at the GPS-levelling testing network and solved by applying the least-squares analysis. Since the realistic assessment of the accuracy of levelling, GPS and gravity data is problematic due to several reasons, no a priori information about the accuracy was used in the estimation model. The statistics of the least-squares residuals of the 3-parameter model for the results that incorporate the newly determined normal-orthometric heights are provided in Table 7.2. The same analysis was conducted for the results obtained after applying the LVD offsets relative to NZGeoid2009 and WHS. The statistics of the least-squares residuals when using the 3-parameter model are given in Table 7.2. The corresponding histograms of residuals are shown in Figures 7.1a, 7.1b, 7.1c and 7.1d.

The results obtained after applying the 3-parameter model (summarised in Table

7.2) revealed that the best RMS fit of the gravimetric solution with GPS-levelling data was attained for NZGM2010 and NZQM2010 when using the newly determined orthometric and normal heights. The RMS of differences between the geometric and gravimetric geoid/quasigeoid heights is 12 cm (for NZGM2010) and 15 cm (for NZQM2010). The application of the 3-parameter model thus improved the relative accuracy to about 70% for OTG12. Moreover, OTG12 also has the best RMS when using LVD offsets (relative to WHS). The RMS of differences between the geometric and gravimetric geoid/quasigeoid heights is 13 cm (for OTG12) and 14 cm (for NZGeoid2009).

Table 7.2: Statistics of the least-squares residuals after applying the 3-parameter model to fit the differences between the geometric and gravimetric geoid/quasigeoid heights at the GPS-levelling testing network calculated for NZGM2010, NZQM2010, NZGeoid2009 and OTG12 using LVD offsets relative to newly determined orthometric/normal heights, NZGeoid2009 and WHS. Unit: 1 m.

LVD offsets relative to Newly heights			
Model	**Differences**		
	Min	**Max**	**RMS**
NZGM2010	-0.46	1.06	0.12
NZQM2010	-0.46	1.05	0.15
NZGeoid2009	-0.46	1.02	0.12
OTG12	-0.43	0.95	0.12
LVD offsets relative to NZGeoid2009			
NZGM2010	-0.54	1.21	0.14
NZQM2010	-0.51	1.20	0.17
NZGeoid2009	-0.55	1.18	0.13
OTG12	-0.63	1.13	0.14
LVD offsets relative to WHS			
NZGM2010	-0.54	1.20	0.15
NZQM2010	-0.47	1.18	0.18
NZGeoid2009	-0.54	1.17	0.14
OTG12	-0.50	1.11	0.13

The application of the 3-parameter model improved the RMS fit of NZGeoid2009 with GPS-levelling data (for the newly determined normal and orthometric heights) from 15 to 12 cm. The application of the 3-parameter model has added much improvement to the RMS fit of all existing models with GPS-levelling data corrected for the LVD offset relative to NZGeoid2009, WHS and the newly determined heights; the ranges of RMS with and without applying the 3-parameter model are (82 to 42 cm) and (18 to 13 cm), respectively (cf. Figure 7.1a). Moreover, the RMS fits of NZGeoid2009, NZGM2010 and NZQM2010 are also very similar when using either

the LVD offsets (relative to NZGeoid2009 and WHS) or the newly determined normal heights.

The newly determined orthometric/normal heights improved the RMS fit (after applying the 3-parameter model) of OTG12 to about 30 cm compared to the corresponding results obtained when applying the LVD offsets. The results of the 3-parameter model applied for the newly determined orthometric/normal heights are the most consistent by means of the RMS fit and the range of differences (cf. Table 7.2). All three gravimetric solutions have the same range of the residuals of 1.60 m. NZGM2010 has the most regularly distributed residuals without the presence of significant systematic trends (cf. histograms in Figure 7.1c). This is regarded to using least-square-based modified Stokes formula where the least-square parameters refine the terrestrial gravity data and the contribution of the geopotential model. A similar, mainly regular, distribution of residuals is seen for NZGeoid2009 (cf. histograms in Figure 7.1a). On the other hand, large systematic discrepancies are found in the residuals for the NZQM2010 (cf. histograms in Figure 7.1b).

The quasigeoid model OTG12, NZGM2010 and NZGeoid2009 have the best RMS fit with GPS-levelling data of 12 cm (cf. Table 7.2). Nevertheless, this fit is only slightly better than the RMS fits of NZQM2010 (for the newly determined normal and orthometric heights). This model has RMS fit with GPS-levelling data of 15 cm. Compared with other models OTG12 has a considerably better agreement with GPS-levelling data by means of the range of least-squares residuals. This range is 1.38 m. The range of NZGM2010 (of 1.52 m) is similar to that found for NZQ2010 (of 1.51 m) and NZGeoid2009 (of 1.48 m). The official quasigeoid NZGeoid2009 has been computed to be the official model, therefore advanced computing facilities and the possibilities were utilised to obtain best results. Lack of computing facilities at the school has refrained us from trying several parameters as testing the SRBF approaches had occupied all available machines.

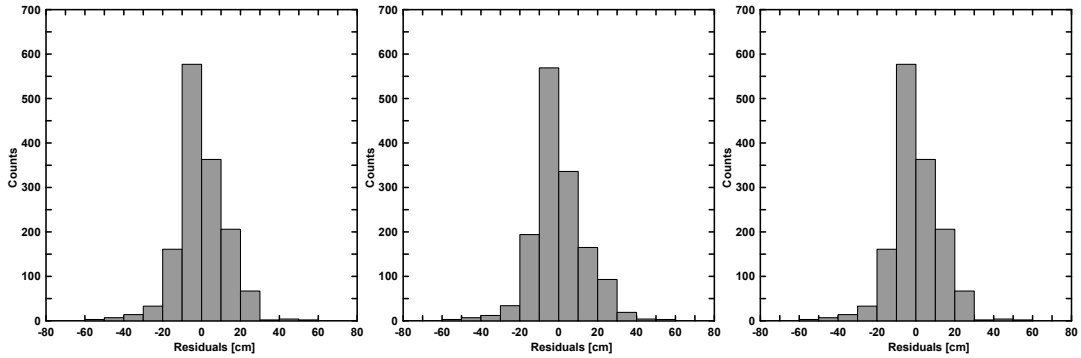

(a) NZGeoid2009

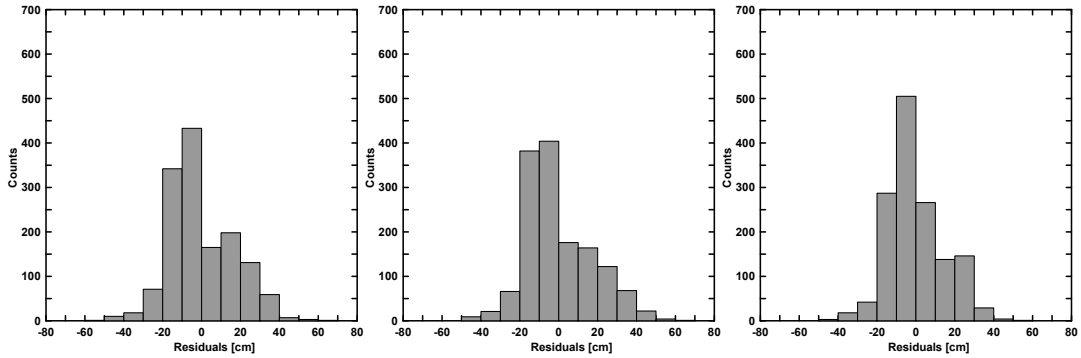

(b) NZQM2010

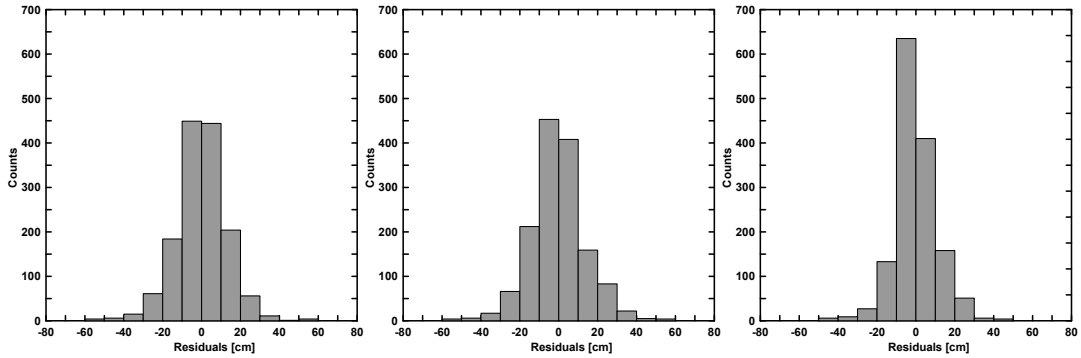

(c) NZGM2010

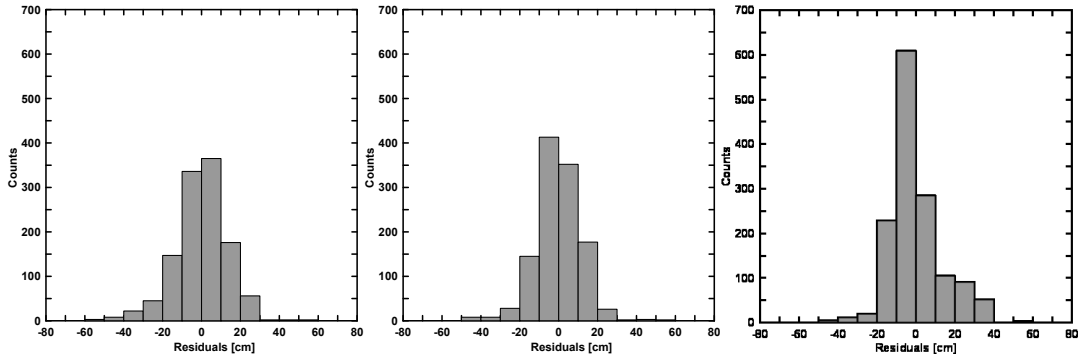

(d) OTG12

Figure 7.1: Histograms of the least-squares residuals (of the 3-parameter model) between the gravimetric solutions and GPS-levelling data at LVDs relative to NZGeoid2009, WHS and newly determined orthometric/normal heights (from left to right). Unit: 1 cm.

7.2 Testing of a relative offset between North Island and South Island

As seen from the histograms in Figures 7.1a, 7.1b, 7.1c and 7.1d, the least-squares residuals of all four regional geoid/quasigeoid models are irregularly distributed with a large number of the small negative residuals coupled by a much larger range of the positive residuals. This raises a question about the accuracy of the levelling networks in the North and South islands after the implementation of the geopotenial-value approach for unification of LVDs. It is important to investigate whether a relative offset between the levelling these networks is yet existing. Hence, the analysis of this offset using all gravimetric regional solution as well as GGMs and geodetic Mean Dynamic Topography (MDT) data is essential.

The aim of testing the newly adjusted levelling data is to study and identify the relation between the vertical realisations in each island. The central relation between the LVDs in the two islands is represented in the investigation of the relative offset between them. Several reasons can cause offsets between LVDs, for example, the systematic errors in GPS-levelling networks and gravity data sets, as well as in this study, the EGM2008 omission and commission errors can also have a contribution.

The investigation of the relative offsets between the levelling networks in the North and South islands in New Zealand has been conducted by testing the differences between the geometric (GPS-levelling) geoid/quasigeoid heights and the regional gravimetric solutions. Furthermore, the relative offset between vertical datums at gauges in Dunedin (North Island) and Wellington (South Island) have been also tested with respect to MSL applying analysis of oceanographic and MDT models.

7.3 MDT models

To study relative offset between the tide gauges in New Zealand, five different MDT models are employed to analyse differences between vertical datums in North and South islands with respect to MSL. The employed MDT models are as follows: CARS2009 (Ridgway *et al.*, 2002), ECCO2 (Menemenlis et al., 2008), the geodetic DTU10 model (Andersen, 2010), the geodetic MDT solutions derived from the data sets of sea surface topography DOT.DNSC08 (Tapley *et al.*, 2003) and CLS11 (Schaeffer *et al.*, 2011; Scharroo, 2011) after subtracting the EGM2008 marine geoid heights. The five MDT solutions are set within the New Zealand Study area and their statistics are summarised in Table 7.3.

Table 7.3: Statistics of the MDT models: CARS2009, ECCO2, DTU10, DNSC08-EGM2008 and CLS11-EGM2008 within the study area. Unit: 1 cm.

MDT	Min	Max	Mean	STD
CARS2009	164	245	216	17
ECCO2	-24	47	11	20
DTU10	-7	93	58	19
DNSC08-EGM2008	-49	61	27	19
CLS11-EGM2008	-31	69	29	18

The oceanographic MDT models CARS2009 and ECCO2 have a low resolution and spatial coverage. CARS2009 and ECCO2 have also a significantly smaller range of values within the study area than the geodetic MDT models; the range of CARS2009 is 81 cm, while only 71 cm for ECCO2. The MDT range of DTU10 and CLS11-EGM2008 is 100 cm. The DNSC08-EGM2008 has the largest MDT variations within the study area at the range of 110 cm. All investigated MDT solutions show a similar pattern with prevailing zonal trend of increasing MDT towards tropical seas due to latitudinal thermal gradient. Regional anomalous features associated with the configuration of ocean currents (dominated by the influence of Tasman and Sub-Antarctic Fronts) can also be recognised. For our analysis the most significant regional feature is a slightly higher MSL in Wellington compared with Dunedin's coastal sea (Tenzer *et al.*, 2012).

7.3.1 Numerical results on MDT models

The analysis of MSL in the vicinity of tide gauges in Wellington and Dunedin based on five MDT models show that the MSL offsets between these two tide gauges are between 18 and 25 cm when taking into consideration only the results of the geodetic models DTU10, DNSC08-EGM2008, and CLS11-EGM2008 (cf. Table 7.4). The MSL offset of 29 cm was found for the oceanographic model CARS2009, while only 1 cm for ECCO2. The representative MSL offset obtained by averaging these results is $\sim$ 19 cm. When disregarding ECCO2 model (which is more likely unrealistically small), the average MSL offset increases to $\sim$ 24cm.

The MSL offset between tide gauges in Wellington and Dunedin is estimated using the MDT models shown in Table 7.3. The MSL values were calculated by extrapolating the MDT grid values in the vicinity of these two tide gauges. The results are summarised in Table 7.4.

Table 7.4: Values of the MSL offset between the tide gauges in Wellington and Dunedin computed using the MDT solutions: CARS2009, ECCO2, DTU10, DNSC08-EGM2008, and CLS11 - EGM2008. Unit: 1 cm.

Model	TG. Wellington				TG. Dunedin				Relative
	Min	Max	Mean	STD	Min	Max	Mean	STD	offset
CARS2009	201	216	206	1	176	177	177	1	29
ECCO2	-3	-2.6	-2	0	-8	-2	-3	1	1
DTU10	50	63	55	3	29	42	31	2	24
DNSC08*	19	31	23	3	-5	6	-2	2	25
CLS11*	12	39	20	6	-5	13	2	3	18

7.4 Analysis of relative offset using regional gravimetric models

The geometric geoid/quasigeoid heights are compared with four regional gravimetric geoid/quasigeoid in the following two scenarios. In the first one, we consider the newly determined orthometric/normal heights at the newly adjusted levelling network (cf. Chapter 4) for the comparison versus the existing gravimetric models by deriving the geometrical geoid/quasigeoid heights, for example, the geometrical geoid heights were obtained by subtracting the normal heights from the GPS ellipsoidal heights while the quasigeoid heights were obtained by subtracting the normal heights from the GPS ellipsoidal heights, reminding that the geodetic ellipsoidal heights in New Zealand are based on NZGD2000 datum as mentioned in Section 1.4. For the comparison with the NZGM2010 geoid, the geometrical geoid heights are derived as for NZGeoid2009, NZQM2010 and OTG12. In the second one, we used the same analysis using the original levelling data set with respect to the old 13 LVDs. Comparisons between the geometric and gravimetric geoid/quasigeoid heights for the newly adjusted and original leveling data are plotted in Figures 7.2, 7.3, 7.4 and 7.5, respectively.

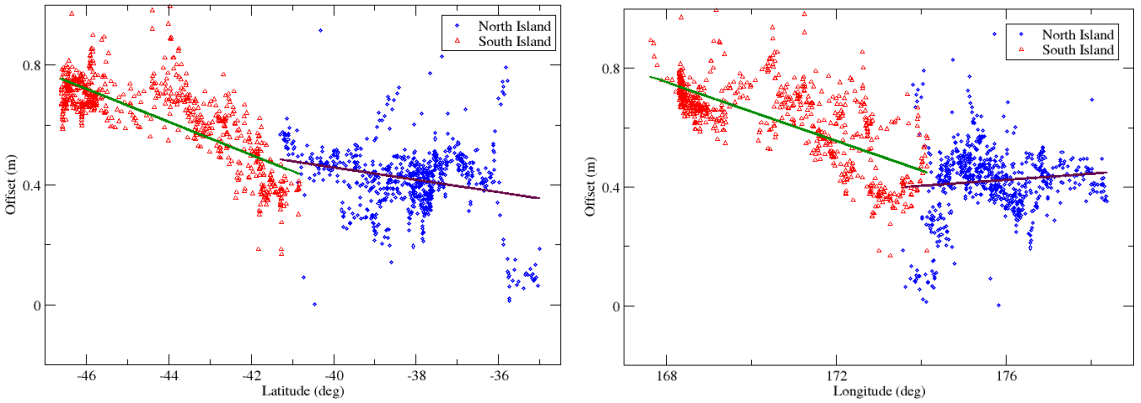

(a) NZGM2010.

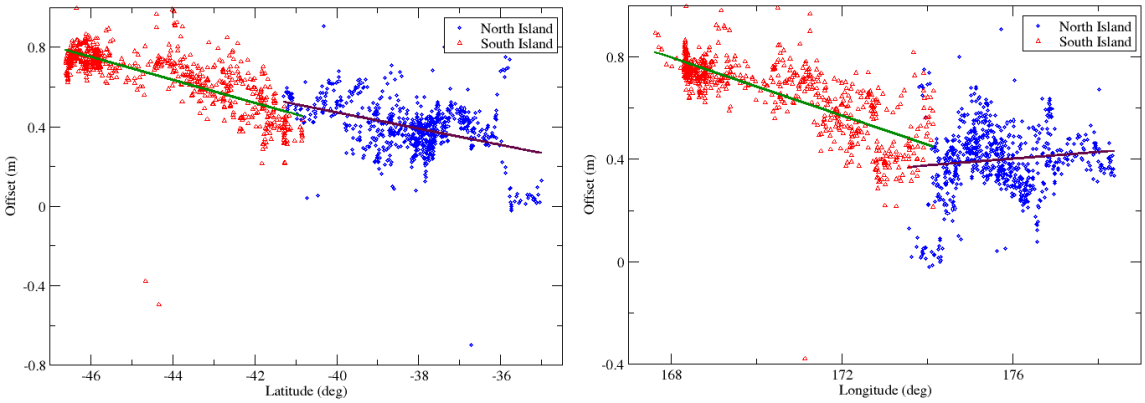

(b) NZGeoid2009.

Figure 7.2: Differences between the geometric and gravimetric geoid/quasigeoid heights along meridional (left panels) and parallel (right panels) profiles computed using: (a) NZGM2010, (b) NZGeoid2009. The geometric geoid/quasigeoid heights were computed based on the jointly adjusted leveling data at the South and North islands (and corrected for the average offsets relative to W_0).

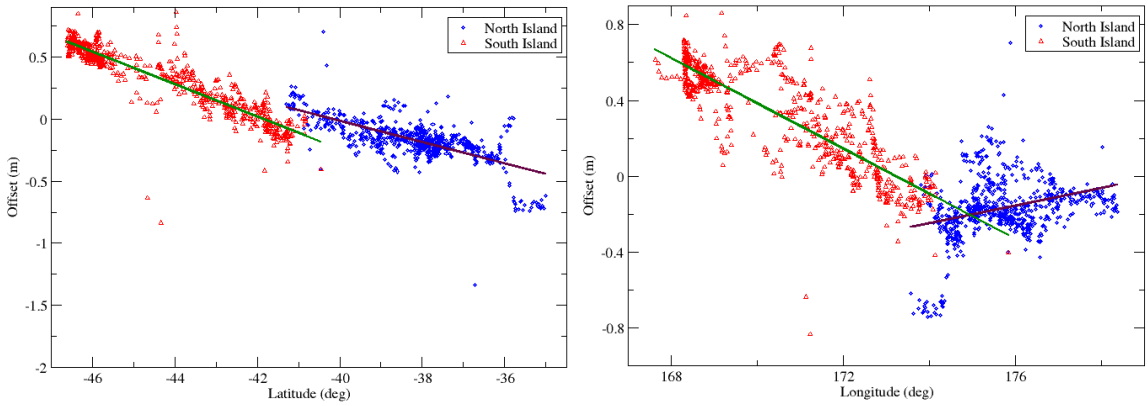

(a) NZQM2010.

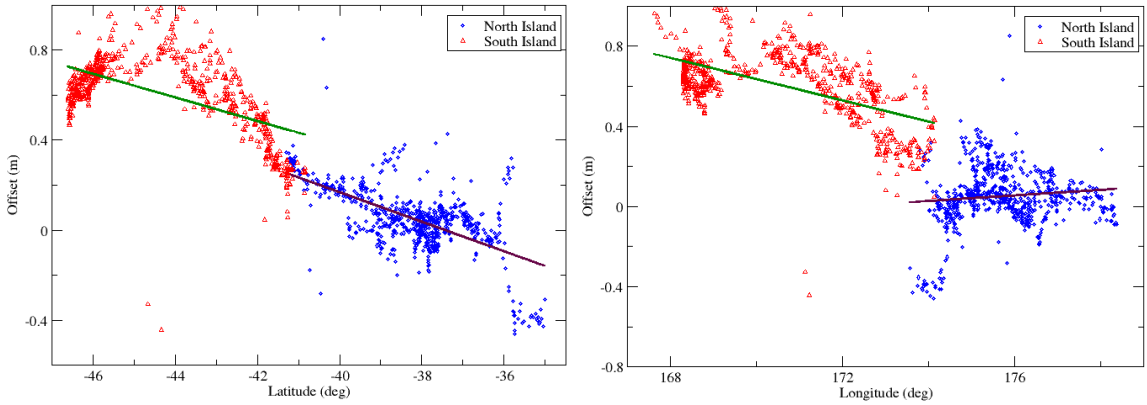

(b) OTG12.

Figure 7.3: Differences between the geometric and gravimetric geoid/quasigeoid heights along meridional (left panels) and parallel (right panels) profiles computed using: (a) NZGM2010, and (b) OTG12. The geometric geoid/quasigeoid heights were computed based on the jointly adjusted leveling data at the South and North islands (and corrected for the average offsets relative to W_0).

7.4.1 Numerical results on regional models

The geometric geoid/quasigeoid heights were computed based on the jointly adjusted leveling data at the South and North islands (and corrected for the average offsets relative to W_0). The linear regression analysis was applied to fit the differences by a linear trend function for each island.

Large discrepancies are seen when comparing the newly adjusted levelling data (corrected for the average offsets relative to W_0) with regard to the regional geoid/quasigeoid solutions. For NZGM2010 and NZGeoid2009 models, the differences between the geometric and the gravimetric geoid/quasigeoid heights are mostly positive with the largest values at the lower South Island, while the corresponding smallest difference is at the upper North Island. For NZQM2010 gravimetric quasigeoid model, there is no significant bias with the levelling data. The largest absolute differences ($\sim$ 50 cm) are seen at the lower South Island and the upper North Island. The differences between the GPS-levelling data and OTG12 reach maxima ($\sim$ 1 m) in central South Island while the largest negative differences ($\sim$ 40 cm) are detected at the upper North Island, and the rest of the North Island have differences within $\pm$20 cm.

As seen from these results, the NZGM2010 and NZGeoid2009 gravimetric solutions are biased with respect to the GPS-levelling results. In addition, the presence of a large systematic trend across New Zealand is seen in all four gravimetric solutions. The NZQM2010 and OTG12 gravimetric solutions have the largest systematic discrepancies (reaching up to $\sim$ 1 m). The misfit of the NZGM2010 and NZGeoid2009 gravimetric solutions with respect to GPS-levelling data is more similar; the range of geoid/quasigeoid heights differences is $\sim$ 40 cm (for NZGM2010) and $\sim$ 50 cm (for NZGeoid2009). These large discrepancies can be explained by systematic errors within either gravimetric solutions or levelling data. On the other hand, the presence of relative offset between the vertical datum realisations at two islands is less obvious. The character of the geoid/quasigeoid heights differences at GPS-levelling points at the upper South Island and the lower North Island (plotted in Figure 7.2) is relatively smooth without any significant (inter-islands) discontinuity. Similarly, the linear regression fit of the differences between the geometric and gravimetric geoid/quasigeoid heights computed separately for each island does not show any misfit. This is evident especially for the NZGM2010 and NZGeoid2009 solutions. The misfit of the linear regression trends between both islands is less than 10 cm, while the corresponding misfit for NZQM2010 and OTG12 is $\sim$ 20 cm.

The original levelling data were used to find more explanation regarding the large discrepancies involved with the newly adjusted levelling data. The NZGM2010 and

NZGeoid2009 geoid/quasigeoid models are systematically biased (∼50 cm) from GPS-levelling results. NZQM2010 model appears to have a better agreement with GPS-levelling data, the systematic discrepancies are detected at the South Island where differences are of (∼40cm). On the other hand, the OTG12 quasigeoid has a slightly different fit with GPS-levelling data in the South and North islands. The comparisons of all gravimetric solutions against the original GPS-levelling data defined in 13 LVDs are shown in Figure 7.4.

The averaged values of differences between the geometric and gravimetric geoid/quasigeoid heights at GPS-levelling points were used to estimate a relative offset between the vertical datum realisations at the North and South islands. This was done for the newly adjusted leveling data. The results are summarised in Table 7.5.

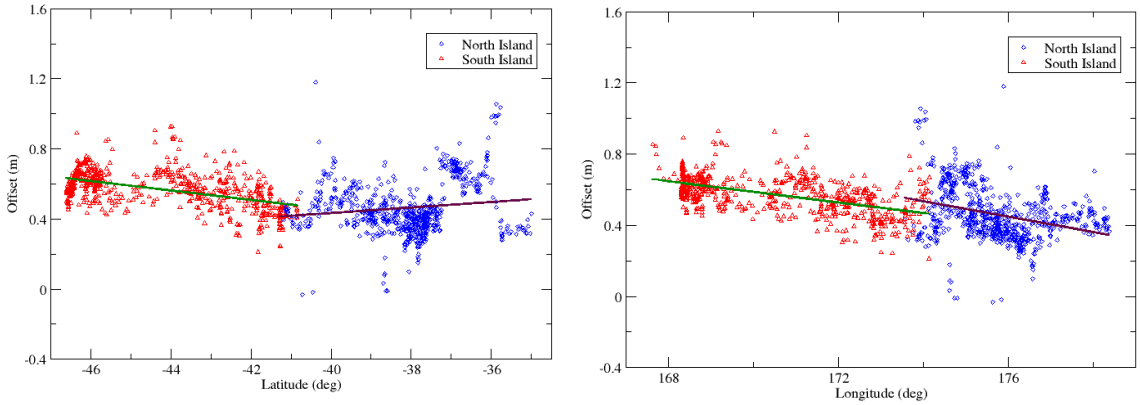

(a) NZGM2010.

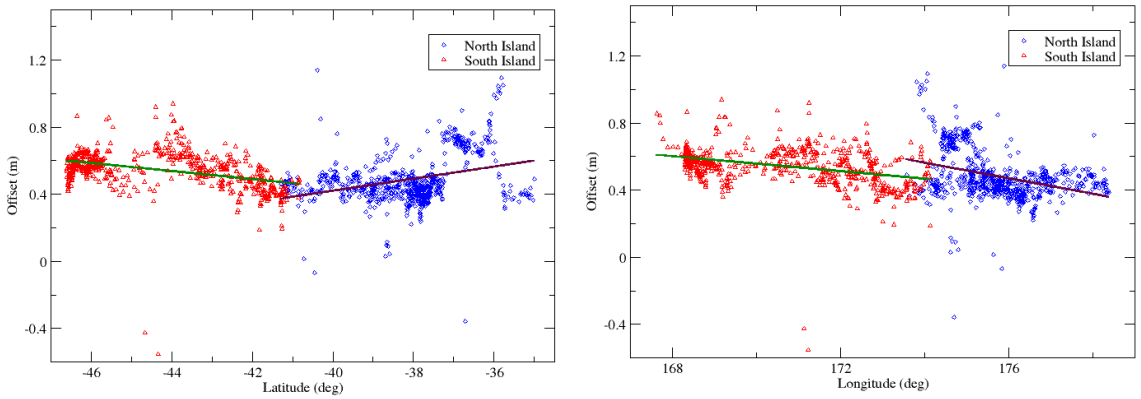

(b) NZGeoid2009.

Figure 7.4: Differences between the geometric and gravimetric geoid/quasigeoid heights along meridional (left panels) and parallel (right panels) profiles computed using: (a) NZGM2010, (b) NZGeoid2009. The geometric geoid/quasigeoid heights were computed using the original leveling data attributed to 13 LVDs.

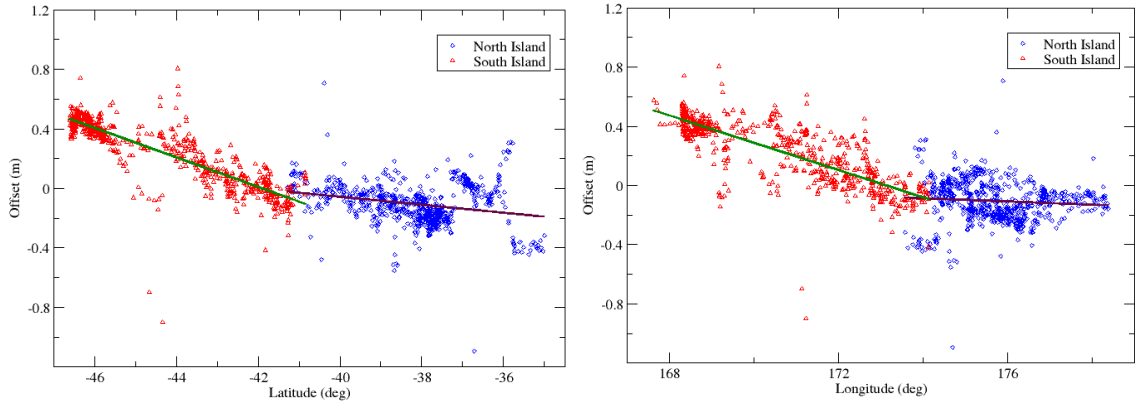

(a) NZQM2010.

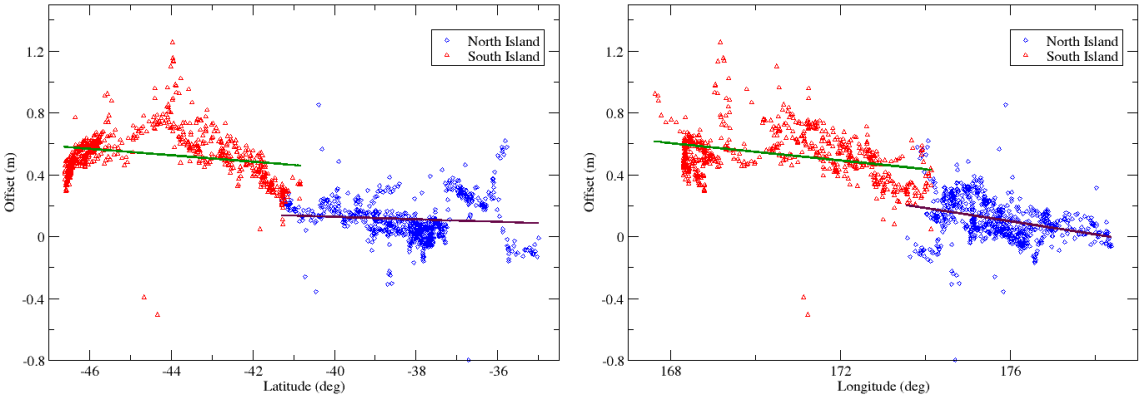

(b) OTG12.

Figure 7.5: Differences between the geometric and gravimetric geoid/quasigeoid heights along meridional (left panels) and parallel (right panels) profiles computed using: (a) NZQM2010, and (b) OTG12. The geometric geoid/quasigeoid heights were computed using the original leveling data attributed to 13 LVDs. The linear regression analysis was applied to fit the differences by a linear trend function for each island.

Table 7.5: Values of the relative offset between vertical datum realisations at the North and South islands computed for the newly adjusted levelling data for offsets relative to NZGeoid2009 (defined in 13 LVDs), using four regional gravimetric solutions (NZGM2010, NZGeoid2009, NZQM2010, and OTG12). Statistics of the differences between the geometric and gravimetric geoid/quasigeoid heights computed individually at the North and South islands. Unit: 1 cm.

Model	North Island				South Island				Relative
	Min	Max	Mean	STD	Min	Max	Mean	STD	offset
NZGM2010	-70	118	40	13	-49	100	14	65	-25
NZGeoid2009	0	91	42	12	17	99	63	13	-21
NZQM2010	-75	70	-17	16	-84	86	23	23	-40
OTG12	-46	85	5	14	-44	121	61	18	-56
LVD offsets relative to NZGeoid2009									
NZGM2010	-45	118	46	15	-56	93	57	12	-11
NZGeoid2009	-36	140	48	15	-55	94	55	11	-7
NZQM2010	-109	131	-11	15	-90	81	23	22	-34
OTG12	-80	85	11	14	-51	126	53	16	-42

The estimation of a relative offset between vertical datum realisations at the North and South islands could be biased by the presence of systematic trend, which is seen in plotted differences between the geometric and gravimetric geoid/quasigeoid heights (cf. Figure 7.2). Therefore, we estimated the relative offset between the North and South Island's newly established vertical datums from these differences but taken only at GPS-levelling points in the vicinity of tide gauges in Wellington and Dunedin. The results are summarised in Table 7.6.

Table 7.6: Values of the relative offset between vertical datum realisations at the North and South islands computed for the newly adjusted levelling data using four regional gravimetric solutions (NZGM2010, NZGeoid2009, NZQM2010, and OTG12). Unit: 1 cm.

Model	North Island		South Island		Relative
	Mean	STD	Mean	STD	offset
NZGM2010	56	2	73	6	-17
NZGeoid2009	54	3	80	5	-26
NZQM2010	10	2	62	6	-52
OTG12	31	3	75	4	-44

7.5 EGM2008 comparison

We further investigated the character of systematic distortions within the leveling networks and regional gravimetric solutions based on their comparison with the EGM2008 quasigeoid model (computed using the spherical harmonic coefficients complete to degree/order of 2160). The differences between the GPS-levelling and EGM2008 quasigeoid heights for the original and newly adjusted leveling data are plotted in Figure 7.6; statistics of these differences are given in Table 7.7. The differences between the regional gravimetric solutions and EGM2008 are plotted in Figure 7.7; statistics of these differences are given in Table 7.8. The geoid-to-quasigeoid correction was applied to the NZGM2010 geoid heights for the comparison with EGM2008.

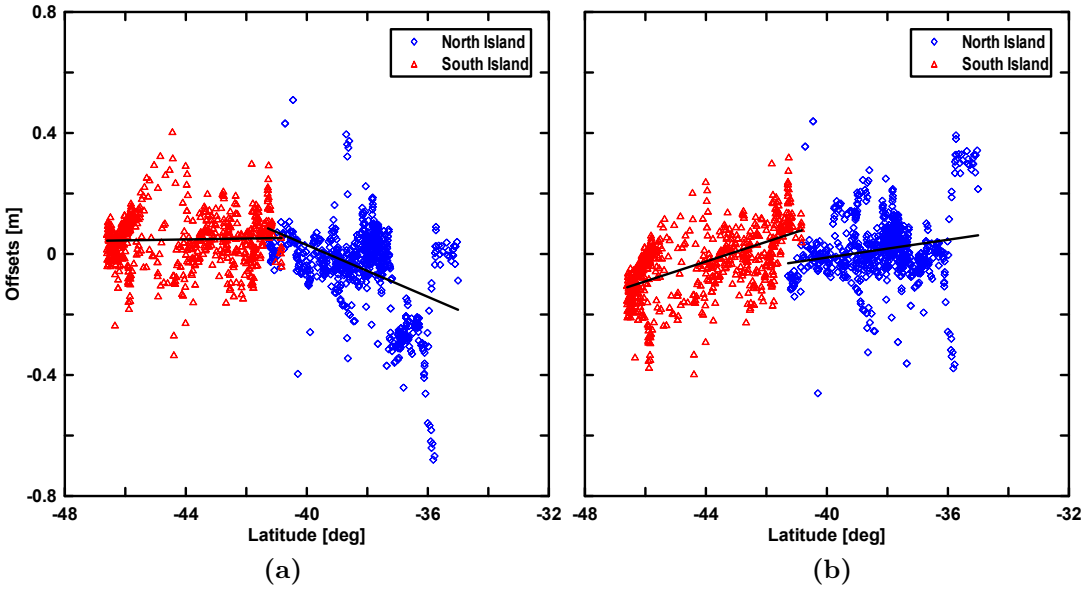

Figure 7.6: Differences between the geometric and EGM2008 (gravimetric) quasigeoid heights computed using: (a) the original leveling data attributed to 13 LVDs and (b) the newly adjusted leveling data (corrected for the average offsets relative to W_0).

The differences between EGM2008 and the newly adjusted GPS-levelling data has shown slight improvement (Table 7.7). For instance, the mean values of the differences in North and South islands are 1 and 3, respectively. The corresponding mean values of differences obtained when using the original levelling data are -5 and 5 cm for the North and South islands, respectively. The STD of differences computed using the newly adjusted leveling data is 11 cm for both islands. A better STD of differences of 8 cm was found for the original leveling data at the South Island, while the STD of differences at the North Island is 14 cm.

Table 7.7: Statistics of the differences between the GPS-levelling and EGM2008 quasigeoid heights computed using the original and newly adjusted leveling data shown in Figure 7.6. Unit: cm.

Model	North Island		South Island	
	Original	New	Original	New
Min	-68	-46	-33	-40
Max	51	44	40	32
Mean	-5	1	5	-3
STD	14	11	8	11

It is obvious from Figure 7.7 that all four regional gravimetric solutions are systematically shifted from EGM2008. The discrepancies between EGM2008 and the NZGM2010 and NZGeoid2009 regional gravimetric solutions are similar with the range of differences approximately within -30 to -80 cm. A much larger range of differences (within 40 to -80 cm) was found between the EGM2008 and NZQM2010 quasigeoid heights. The quasigeoid heights differences between EGM2008 and OTG12 are mainly within 20 and -80 cm.

Table 7.8: Statistics of the differences between the EGM2008 quasigeoid model and the regional gravimetric solutions (NZGM2010, NZGeoid2009, NZQM2010, and OTG12) shown in Figure 7.7. Unit: 1 cm.

Model	NZGM2010		NZGeoid2009		NZQM2010		OTG12	
	North	South	North	South	North	South	North	South
Min	-62	-114	-51	-108	-12	-94	-26	-141
Max	-27	-36	-25	-43	41	21	10	-17
Mean	-42	-65	-44	-59	16	-28	-6	-58
STD	6	11	3	9	10	20	7	17

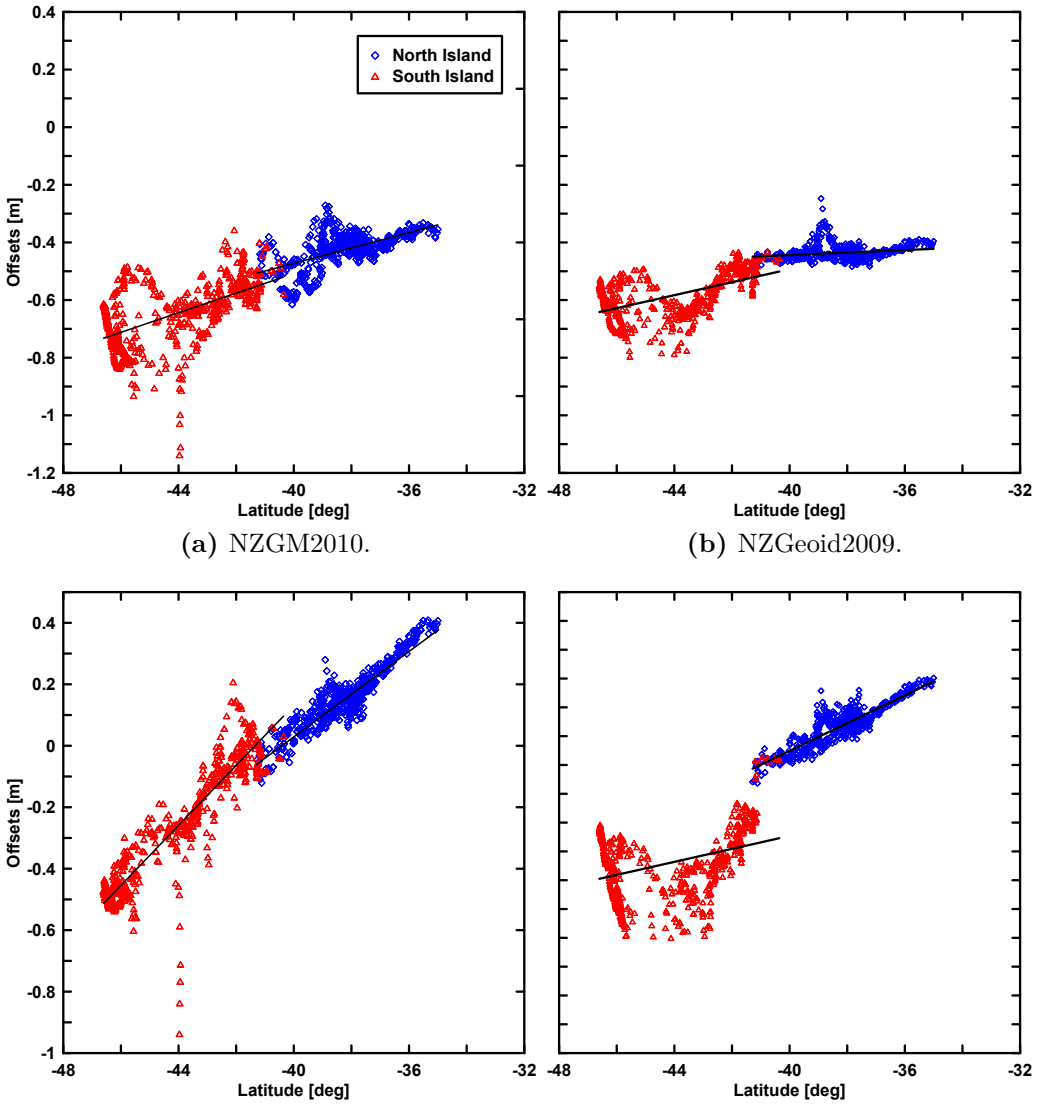

(a) NZGM2010. **(b)** NZGeoid2009.

(c) NZQM2010. **(d)** OTG12.

Figure 7.7: Differences between the EGM2008 and regional gravimetric geoid/quasigeoid models.

The results of numerical analysis further show that the relative offset between the vertical datum realisations at the North and South islands were to a large extent eliminated by correcting the heights of levelling benchmarks for the offset with respect to WHS (after applying the geopotential-value approach). This is evident from the plotted values of differences between GPS-levelling data and regional gravimetric solutions in Figure 7.2. As seen, these differences do not show any discontinuity between both islands. This is also confirmed from the comparison of the newly adjusted levelling data with EGM2008 (see. Figure 7.6a).

Chapter 8

Summary, results and future works

8.1 Summary and results

LVDs, levelling adjustment and GGM testing

In Chapter 4, the average offsets of the LVDs were estimated using the geopotential-value approach. The offsets were defined relative to WHS by adopting the geoidal geopotential value W_0. The largest offset value (37 cm) was found at One-Tree-Point 1964 LVD and the smallest value (1 cm) was estimated at Wellington 1963 LVD. The inconsistency between the permanent tide systems of the GPS and levelling points was overcome by converting the levelling heights from mean-tide to tide-free system, which is the same tide system of the GPS points (Section 4.3.1).

The joint adjustment approach (cf. Section 4.4) was combined with the geopotential-value approach (Section 4.3) for unification of LVDs at the North and South islands. The joint adjustment method was applied for the levelling networks in the both islands by fixing two tide gauge points at Wellington (North Island) and Dunedin (South Island). The normal-orthometric heights were computed using the commutative normal to normal-orthometric heights correction from the newly adjusted networks. The commutative normal to normal-orthometric height correction was used to convert the normal-orthometric heights to the normal heights in order to apply geopotential-value approach. The results of the joint adjustment showed a STD of least-squares residuals of normal-normal orthometric height difference is 2 mm. The residuals between levelling benchmarks vary from -2.5 cm and $+2.6$ cm at the North Island and they were found within ± 1.3 cm at the South Island. The

average offsets of the newly adjusted levelling networks were estimated at Dunedin (27.5 cm) and Wellington (10.6 cm).

The newly adjusted levelling networks are incorporated with the GPS data to validate the accuracy of the recently released satellite-only GGMs compiled using GRACE and GOCE data (cf. Table 5.1). The analysis of GGMs reveals that the GOCE satellite-only model GO-CONS-GCF-2 version TIM-R2 has the best agreement with GPS-levelling data; the RMS of differences is 57 cm and the mean of differences is 2 cm. However, GOCO-02S was found to be the best model to for quasigeoid computation based on minimum RMS of differences (56 cm).

Gravimetric solutions

Chapter 6, presented the regional gravimetric solutions undertaken in this study, NZGM2010 geoid was computed using a stochastic method utilises least-squares modification of Stokes formula which is known as the KTH method. (Section 6.4). In this method the approximate gravimetric heights were first computed using the modified Bruns-Stokes integral and thereafter the additive corrections account for topography (cf. Figure 6.2a), atmosphere (cf. Figure 6.2c) and the downward continuation of the gravity to MSL (cf. Figure 6.2b) were attached one by one to the approximate heights to introduce the final gravimetric solutions, the ellipsoidal correction was too small and therefore neglected. The second investigation was conducted to compute a new experimental quasigeoid NZQM2010 using the direct BEM approach (cf. Section 6.6).

Section 6.9 presents investigation of the accuracy of local gravity field modelling using four different types of the integral-equation-based approaches, namely the Poisson integral, Green integral, point-mass, and radial multipole approaches. We investigated the performance of these four discretised integral equations in three different scenarios, for instance, when the gravity data are corrected for the residual terrain model (RTM-correction) and for the reference gravity field (remove-restore scheme) and when there is no correction added to the gravity data. All integral equations are discretised below data points at the chosen constant depth relative to the Bjerhammar sphere. The choice of the optimal depth is done based on minimising the RMS fit between the observed and predicted gravity data. In all four approaches the number of unknown parameters is identical to the number of input gravity data and the systems of discretised integral equations are solved using Jacobi iteration. The results of numerical experiments are presented and discussed.

It was shown (in Section 6.11) that the application of the RTM-correction to gravity data slightly improves the accuracy of the gravity field approximation when using the Green integral approach. The application of the remove-restore technique did not reduce the systematic bias in local gravity solutions. However, the residual gravity anomalies (Figure 6.11a) show better accuracy against the GPS-levelling data than the RTM-corrected gravity anomalies (Figure 6.11b) in the computation of the gravimetric quasigeoid model over the selected area (cf. Table 6.3). The reason is due to the high frequency that propagated to the gravimetric solution in terms of the disturbing potential when applying RCR procedure. The numerical scheme described in Section 6.13 was applied to compile the OTG12 gravimetric quasigeoid model. The reference gravity field was evaluated from the satellite-only GGM model. The residual gravity field was treated individually for the near and far zones. The discretised integral-equation approach was applied to solve the near-zone contribution to the residual quasigeoid model while the far-zone contribution was evaluated by applying the far-zone modified spherical harmonics by means of Molodensky's truncation coefficients.

The accuracy of the regional geoid/quasigeoid models (OTG12, NZGeoid2009, NZQM2010 and NZGM2010) was analysed using the jointly adjusted levelling networks as well as using the individual levelling data defined in LVDs and corrected for the average offsets relative to NZGeoid2009 and WHS. The combination of the gravimetric solutions with GPS-levelling data was done by applying a 3-parameter model. The analysis revealed that the most consistent results were obtained after using the jointly adjusted levelling networks. The best RMS fit of the gravimetric solution with GPS-levelling data of 12 cm was attained for three of the gravimetric solutions, namely, OTG12, NZGM2010 and NZGeoid2009. OTG12 and NZGM2010 have shown similar accuracy to the official model (NZGeoid2009). The corresponding RMS fit of NZGQ2010 was found to be 15 cm.

The results obtained after using the jointly adjusted levelling networks thus confirmed a generally better agreement of the gravimetric solutions with GPS-levelling data than the results obtained after the jointly adjusted levelling networks. The best RMS fit of OTG12 with GPS-levelling data was obtained after the jointly adjusted levelling networks; the RMS of differences of 12 cm was achieved in this case. The RMS fit of OTG12 when applying LVDs corrected for WHS is 13 cm and it goes up to 14 cm when applying LVDs relative to NZGeoid2009. A difference of ± 1 cm in the RMS fit of the gravimetric solutions with GPS-levelling data is achieved when applying LVDs relative to WHS and NZGeoid2009. On the other hand, the difference was improved up to 3 cm (for NZGM2010 and NZQM2010) when using newly determined heights.

The comparison of the four regional geoid/quasigeoid models revealed that OTG12 has either comparable or better agreement with GPS-levelling data. Whereas the RMS fit of OTG12, NZGeoid2009, NZGM2010 and NZQM2010 is very similar (within 12-15 cm), the range of distortions computed for these models varies. The range of differences between OTG12 and GPS-levelling data is about 10% better when compared to NZGeoid2009 and NZGM2010 and NZQM2010, the range of differences between the regional solutions and the GPS-levelling data varies from about 10 cm to 15 cm, NZGeoid2009 is the closest model to OTG12 (cf. Section 7.1, Table 7.2). The largest systematic differences between NZGeoid2009, NZQM2010 and OTG12 up to several decimetres are along the Southern Alps. These large differences are most likely due to poor coverage and a low accuracy of gravity data.

Relative offset between North and South islands

In Chapter 7 The relative offset between the vertical datums at the North and South islands was investigated using three comparisons (regional, GGM and MTD models). The first comparison was to compare the newly adjusted GPS-levelling data with the regional gravimetric geoid/quasigeoid models. In addition, the regional gravimetric models were also compared with the global EGM2008. The results showed that NZGeoid2009 and NZGM2010 are biased with respect to the GPS-levelling data. The differences between the geometrical and gravimetric geoid/quasigeoid heights are mostly positive. NZQM2010 and OTG12 have the largest systematic discrepancies of $\sim$ 1 m. The misfit of the linear regression trend between the geometrical and gravimetric geoid/geoid heights for NZGeoid2009 is $\sim$ 50 cm, for NZGM2010 is $\sim$ 40 cm and $\sim$ 20 cm for NZQM2010 and OTG12. The corresponding differences when applying the original GPS-levelling revealed that the NZGeoid2009 and NZGM2010 are still biased to the GPS-levelling data, NZQM2010 model has systematic discrepancies of $\sim$ 40 cm at the South Island and OTG12 model has different agreement with the GPS-levelling data 11 and 53 cm at the North and South islands. In the same context, the comparison of the GPS-levelling with EGM2008 has shown better agreement in the differences, 1 and 3 cm at the North and South islands, respectively. The same comparison when considering the original GPS-levelling data (based on 13 LVDs) showed differences within $\pm$5 cm in both islands.

In the second comparison four MDT models were used, namely, CARS2009, DTU, DNSC08-EGM2008 and CLS11-EGM2008. The results showed that the average MSL offset between tide gauges in Wellington and Dunedin is $\sim$ 24 cm. This value is approximately $\sim$ 7 cm larger than the estimated relative offset (of 16.9 cm) between the jointly adjusted levelling networks at the North and South islands

obtained from their comparison with WHS (cf. Tenzer *et al.*, 2011). The relative offset between the vertical datums and the regional geoid/quasigeoid models are 25 cm for NZGM2010, 21 cm for NZGeoid2009 while for NZQM2010 and OTG12 are quite larger -40 and -56 cm, respectively (Table 7.1). The corresponding relative offsets of 17 cm (for NZGM2010) and 26 cm (for NZGeiod2009) were obtained when averaging the geoid/quasigeoid heights differences only at GPS-levelling points in close proximity of tide gauges.

8.2 Research outcome

- Three methods for computation gravimetric geoid/quasigeoid model were reviewed and applied. Analogously, three geoid/quasigeoid models, namely NZGM2010, NZQM2010 and OTG12, were computed and evaluated. Among all applied methods a new methodology for a quasigeoid modelling based on DIE approach was successfully investigated to computed OTG12.

- The final gravimetric solution OTG12 consisting of three components, namely, near-zone contribution, reference gravity field and far-zone contribution, was compiled on $1' \times 1'$ grid. The three components were combined using RCR scheme. The comparison of OTG with GPS-levelling data revealed that OTG12 has substantially better accuracy than the official quasigeoid model NZGeoid2009.

- The KTH method is more rigorous comparing with RCR and iterative method, thus we obtained a comparable result when using it. The KTH method has been used in the study for the sake of comparison. The primary aspect of this thesis was to investigate the SRBF methods and we did not have enough time to thoroughly investigate the KTH method and BEM method as we already suffered from the lack of computing capacity. This will be considered in the future works.

- The inconsistencies within several separate LVDs were removed and the number of LVDs was reduced into a couple of datums, one in the North Island (Wellington) and the second in the South Island (Dunedin), and levelling networks in each island were re-adjusted at the fixed points (Wellington and Dunedin) using the joint adjustment. The couple of datums were then unified using the geopotential-value approach by estimating their vertical offsets relative to WHS, and they were found to be 10.5 cm and 27.6 cm for Wellington and Dunedin, respectively.

- An extensive investigation of the relative offset between LVDs was conducted by comparing the newly determined GPS-levelling data and EGM2008 with regional gravimetric solutions. The analysis revealed large systematic errors within the regional gravimetric solutions (including the official quasigeoid model) those might happen due several reasons, which are discussed in Chapter 7. On the other hand, MDT models were used to test the relative offsets between LVDs in North and South islands relative to MSL.

8.3 Future works

The central direction of this research aimed to obtain an improved quasigeoid model over New Zealand. However, obtaining a precise quasigeoid model demands certain effortful investigations and deliberations with the acquired data sets before the quasigeoid computation.

- The GPS/levelling networks should be augmented and in both North and South islands by more reliable precision, especially over large parts of the South Island where levelling and gravity data are absent. Precise levelling data can be genuinely obtained by incorporating gravity measurements along the levelling network. That is important because any further improvement on the levelling data will analogously propagate into the accuracy of the regional gravimetric solution, especially over large parts of the South Island where levelling and gravity data are absent.

- The attributes of the terrestrial gravity data can be improved by filling data gaps in the existing terrestrial gravity data set. The existing terrestrial gravity data base consists of ~ 40 thousand points over the two islands as well as Gatham Island (Reilly, 1972). The average data distribution is one point per 7.5 squared metres (cf. Amos, 2007), considering that the gravity measurements are very dense around at the attainable areas where they were mainly established for geophysical purposes. Conversely, the gravity measurements are very poor in the remote and mountainous areas. Airborne gravimetry would be advantageous to improve the gravity coverage especially in the South Island gravity data gaps over the Southern Alps mountains where the gravity measurements are rare. Applying airborne gravimetry can guarantee more refined and reliable accuracy of quasigeoid in New Zealand.

- The unmodelled systematic errors within levelling networks and gravity solutions that exist due to a low and irregular spatial coverage of levelling and

gravity data do not represent the realistic accuracy of the gravimetric modelling in New Zealand. These unmodelled errors should be resolved in order to increase the level of the accuracy of the gravimetric solutions. We have scheduled this task in our forthcoming work. The novel innovation function based on the solution of a Cauchy boundary-value problem for the Laplace operator (Prutkin and Klees, 2007) would be worth using for this task. The innovation function also has a similar task as the corrector surface as it corrects the error of the unused gravity data outside the area of computation. The noise of the residual data can be reduced by adopting a proper depth of the downward continuation.

Bibliography

Abdalla, A. and Fairhead, D. (2011). A new gravimetric geoid model for Sudan using the KTH method. *Journal of African Earth Sciences*, *60*(4), 213–221.

Abdalla, A. and Tenzer, R. (2011). The evaluation of the New Zealand's geoid model using the KTH method. *Geodesy and Cartography*, *37*(1), 5–14.

Abdalla, A. and Tenzer, R. (2012a). Compilation of the regional quasigeoid model for New Zealand using the discretised integral-equation approach. *Journal of Geodetic Science*.

Abdalla, A. and Tenzer, R. (2012b). The global geopotential and regional gravimetric geoid/quasigeoid models testing using the newly adjusted levelling dataset for New Zealand. *Applied Geomatics*.

Abdalla, A. and Tenzer, R. (2012c). The integral-equation-based approaches for modelling the local gravity field in the remove-restore scheme. In *International Association of Geodesy Symposia*, Melbourne, Australia, 7. Springer. accepted.

Alberts, B. and Klees, R. (2004). A comparison of methods for the inversion of airborne gravity data. *Journal of Geodesy*, *78*(1-2), 55–65.

Allister, N. and Featherstone, W. (2001). Estimation of Helmert orthometric heights using digital barcode levelling, observed gravity and topographic mass-density data over part of the Darling Scarp. *Geomatics Research Australasia*, (75), 25–52.

Amos, M. J. (2007). *Quasigeoid modelling in New Zealand to unify multiple local vertical datums*. Doctoral dissertation, Curtin University of Technology, Perth, Australia.

Amos, M. J. and Featherstone, W. E. (2008). Unification of New Zealands local vertical datums: iterative gravimetric quasigeoid computations. *Journal of Geodesy*, *83*, 57–68.

Amos, M. J. and Featherstone, W. E. (2009). Unification of New Zealand's local vertical datums: iterative gravimetric quasigeoid computations. *Journal of Geodesy*, *83*(1), 57–68.

Andersen, O., Knudsen, P., Berry, P., Mathers, E., Trimmer, R., and Kenyon, S. (2005). Initial results from retracking and reprocessing the ERS-1 geodetic mission altimetry for gravity field purposes. In C. Jekeli, L. Bastos, and J. Fernandes (Eds.), *Gravity, Geoid and Space Missions*, Volume 129 of *International Association of Geodesy Symposia*, 1–5. Springer Berlin Heidelberg.

Andersen, O. B. (2010). The DTU10 Gravity field and Mean sea surface, Second international symposium of the gravity field of the Earth. Fairbanks, Alaska.

Andersen, O. B. and Knudsen, P. (2000). The role of satellite altimetry in gravity field modelling in coastal areas. *Physics and Chemistry of the Earth, Part A: Solid Earth and Geodesy*, *25*(1), 17–24.

Andersen, O. B., Knudsen, P., and Berry, P. A. M. (2009). The DNSC08GRA global marine gravity field from double retracked satellite altimetry. *Journal of Geodesy*, *84*, 191–199.

Ardalan, A. and Garafarend, E. (1999). A first test for W0 the time variation of W0 based on three GPS campaigns of the Baltic Sea level project. Technical Report 99(4), Finnish Geodetic Institute, Helsinki.

Balasubramania, N. (1994). *Definition and realization of a global vertical datum.* Doctoral dissertation, The Ohio State University, Columbus, USA.

Becker, J., Sandwell, D., Smith, W., Braud, J., Binder, B., Depner, J., Fabre, D., Factor, J., Ingalls, S., Kim, S., Ladner, R., Marks, K., Nelson, S., Pharaoh, A., Trimmer, R., Von Rosenberg, J., Wallace, G., and Weatherall, P. (2009). Global bathymetry and elevation data at 30 arc seconds resolution: SRTM30_PLUS. *Marine Geodesy*, *32*(4), 355–371.

Becker, M. (2012). Geodesy. In W. Kresse and D. M. Danko (Eds.), *Springer Handbook of Geographic Information*, 95–117. Institut für Geodäsie, Technische Universität Darmstadt, Petersenstrasse 13, 64287 Darmstadt, Germany: Springer Berlin Heidelberg.

Benning, W. (1987). Iterative ellipsoidische Lotfusspunktberechnung. *AVN,*, *7/1987*, 256–260.

Bjerhammar, A. (1962). A general method for an explicit determination of the shape of the earth from gravimetric data. *Bulletin Géodésique*, *65*, 215–220.

Bjerhammar, A. (1969). On the boundary value problem of physical geodesy. *Tellus*, *21*(4), 451–516.

Bjerhammar, A. and Svensson, L. (1983). On the geodetic boundary value problem for a fixed boundary surface - A satellite approach. *Bulletin Géodésique*, *57*(1-4), 382–393.

Blick, G. (2003). Implementation and development of NZGD2000. *New Zealand Surveyor*, (293), 15–19.

Bomford, G. (1971). *Geodesy* (3rd ed ed.). Oxford: Clarendon Press.

Borkowski, K. M. (1987). Transformation of Geocentric to Geodetic Coordinates Without Approximations. *Astrophysics and Space Science*, *139*, 1–4.

Borkowski, K. M. (1989). Accurate algorithms to transform geocentric to geodetic coordinates. *Bulletin Géodésique*, *63*(1), 50–56.

Bouwman, J. (1998). *Quality of regularization methods*. Number 2. Netherlands: TU Delft.

Bowin, C. (1983). Depth of principal mass anomalies contributing to the earth's geoidal undulations and gravity anomalies. *Marine Geodesy*, *7*(1-4), 61–100.

Bowring, B. R. (1976). Transformation from spatial to geographical coordinates. *Survey Review*, *181*(23), 323–327.

Bowring, B. R. (1985). The accuracy of geodetic latitude and height equations. *Survey Review*, *28*(218), 202–206.

Brebbia, C. A., Telles, J. C. F., and Wrobel, L. C. (1984). *Boundary element techniques : theory and applications in engineering*. Berlin, New York: Springer-Verlag.

Bruinsma, S., Marty, J., Balmino, G., Biancale, R., Foerste, C., Abrikosov, O., and Neumayer, H. (2010). GOCE Gravity Field Recovery by Means of the Direct Numerical Method. In *presented at the ESA Living Planet Symposium*.

Burke, K. F., True, S. A., Burša, M., and Radej, K. (1996). Accuracy estimates of geopotential models and global geoids. In *Global Gravity Field and its Temporal Variations*, Volume -1, 50–60.

Burša, M., Kenyon, S., Kouba, J., Raděj, K., Vatrt, V., Vojtíšková, M., and Šimek, j. (2002). World height system specified by geopotential at tide gauge stations. In *Vertical reference system*, Cartagena, Colombia, 291–296. Springer Verlag.

Burša, M. and Kostelecký, J. (1999). *Space Geodesy and Space Geodynamics*. Ministry of Defence, Topographic Dept. of the General Staff of the Army of the Czech Republic.

Burša, M., Kouba, J., Kumar, M., and et. al (1999a). Determination of the geopotential at the tide gauge defining the North American Vertical Datum 1988 (NAVD88). *Geomatica*, *53*, 459–466.

Burša, M., Kouba, J., Kumar, M., and et. al (1999b). Geoidal Geopotential and World Height System. *Studia Geophysica et Geodaetica*, *43*(4), 327–337. 10.1023/A:1023273416512.

Burša, M., Kouba, J., Müller, A., Raděj, K., True, S. A., Vatrt, V., and Vojtíšková, M. (2001). Determination of Geopotential Differences between Local Vertical Datums and Realization of a World Height System. *Studia Geophysica et Geodaetica*, *45*(2), 127–132. 10.1023/A:1021860126850.

Burša, M., Raděj, K., Šima, Z., True, S., and Vatrt, V. (1997). Determination of the Geopotential Scale Factor from TOPEX/POSEIDON Satellite Altimetry. *Studia Geophysica et Geodaetica*, *41*(3), 203–216.

Claessens, S., Hirt, C., Featherstone, W., and Kirby, J. F. (2009). Computation of a new gravimetric quasigeoid model for New Zealand. Technical report prepared for Land Information New Zealand by Western Australia Centre for Geodesy. Technical report, Curtin University of Technology, Perth, Australia.

Claessens, S. J., Hirt, C., Amos, M. J., Featherstone, W. E., and Kirby, J. F. (2011). The NZGeoid09 Model of New Zealand. *Survey Review*, *43*(319), 2–15.

Columbus, J., Sirguey, P., and Tenzer, R. (2011). A free, fully assessed 15-m DEM for New Zealand. *Survey Quaretly*, (66), 16–19.

Daras, I. (2008). Determination of a gravimetric geoid model of Greece using the method of KTH. Master's thesis, Royal Institute of Technology (KTH).

Dayoub, N., Moore, P., Edwards, S., and Penna, N. (2011). The geoid geopotential value for unification of vertical datums. Marrakech, Morocco.

De Witte, L. (1967). Truncation Errors in the Stokes and Vening Meinesz Formulae for Different Order Spherical Harmonic Gravity Terms. *Geophysical Journal of the Royal Astronomical Society*, *12*(5), 449–464.

Dentith, M. and Featherstone, W. (2003). Controls on intra-plate seismicity in southwestern Australia. *Tectonophysics*, *376*(3–4), 167–184.

DoSLI (1989). Geodetic Survey Branch Manual of Instruction. Technical report, Department of Survey and Land Information, Wellington.

Ellmann, A. (2001). *Least squares modification of Stokes formula with application to the Estonian geoid*. Licentiate thesis.

Ellmann, A. (2004). *The geoid for the Baltic countries determined by the least squares modification of Stokes formula*. dissertation.

Ellmann, A. (2005a). Computation of three stochastic modifications of Stokes's formula for regional geoid determination. *Computers & Geosciences*, *31*(6), 742–755.

Ellmann, A. (2005b). Computation of three stochastic modifications of Stokes's formula for regional geoid determination. *Computers & Geosciences*, *31*(6), 742–755.

Ellmann, A. (2005c). A numerical comparison of different ellipsoidal corrections to stokes' formula. *Window on the Future of Geodesy*, *128*, 409–414 619.

Ellmann, A. (2005d). Two deterministic and three stochastic modifications of Stokes's formula: a case study for the Baltic countries. *Journal of Geodesy*, *79*(1-3), 11–23.

Engels, J., Garafarend, E., Keller, W., Martinec, Z., Sansò, F., and Vaníček, P. (1993). The geoid as an inverse problem to be regularized. In G. Anger, R. Gorenflo, H. Jochmann, H. Moritz, and W. Webers (Eds.), *Inverse Problems: Principles and Applications in Geophysics, Technology, and Medicine* (1st ed.). John Wiley & Sons.

Fan, H. (1989). *Geoid determination by global geopotential models and integral formulas*. DissStockholm: KTH.

Faškovà, Z. (2008). *Numerical Methods for Solving Geodetic Boundary Value Problems*. Ph. D. thesis, Svf STU Bratislava, Slovakia.

Faškovà, Z., Čunderlìk, R., and Mikula, K. (2009). Finite element method for solving geodetic boundary value problems. *Journal of Geodesy*, *84*, 135–144.

Featherstone, W. and Kuhn, M. (2005). Height systems and vertical datums: a review in the Australian context. *Journal of Spatial Science*, *51*, 21–341.

Featherstone, W. E. (2003). Software for computing five existing types of deterministically modified integration kernel for gravimetric geoid determination. *Comput. Geosci.*, *29*(2), 183–193.

Featherstone, W. E., Evans, J. D., and Olliver, J. G. (1998). A Meissl-modified Vaníček and Kleusberg kernel to reduce the truncation error in gravimetric geoid computations. *Journal of Geodesy*, *72*(3), 154–160.

Featherstone, W. E. and Kuhn, M. (2006). Height systems and vertical datums: A review in the Australian context. *Journal of Spatial Science*, *51*(1), 21–41.

Filmer, M. (2011). *An examination of the Australian Height Datum.* Doctoral dissertation, Curtin University of Technology, Curtin, Australia.

Filmer, M., Featherstone, W., and Kuhn, M. (2010). The effect of EGM2008-based normal, normal-orthometric and Helmert orthometric height systems on the Australian levelling network. *Journal of Geodesy*, *84*(8), 501–513.

Forsberg, R., Solheim, D., and Kaminskis, K. (1997). Geoid of the Nordic and Baltic area from gravimetry and satellite altimetry. In *Gravity, Geoid and Marine Geodesy*, Volume 117, Tokyo, Japan, 540–547. Springer Verlag.

Forsberg, R. and Tscherning, C. (1997). Topographic effects in gravity field modelling for BVP. In F. Sansò and R. Rummel (Eds.), *Geodetic Boundary Value Problems in View of the One Centimeter Geoid*, Volume 65 of *Lecture Notes in Earth Sciences*, 239–272. Springer Berlin / Heidelberg.

Förste, C. (1979). Ein Verfahren zur Schätzung von Varianz- und Kovarianzkomponenten. *Allgemeine Vermessungsnachrichten*, *11*(12), 446–453.

Förste, C., Flechtner, F., Schmidt, R., König, R., Meyer, U., Stubenvoll, R., Rothacher, M., Barthelmes, F., Neumayer, H., Biancale, R., Bruinsma, S., Lemoine, J., and Loyer, S. (2006). A mean global gravity field model from the combination of satellite mission and altimetry/gravimetry surface data: EIGEN-GL04C. *Geophysical Research Abstracts*, *8*.

Fredholm, E. (1900). *On a new method for solving the Dirichlet problem. (Sur une nouvelle méthode pour la résolution du problème de Dirichlet.).* Stockh. Öfv. 57, 39-46 .

Gilliland, J. (1987). A review of the levelling networks of New Zealand. *New Zealand Surveyor*, *271*, 7–15.

Goiginger, H., Hoeck, E., Rieser, D., Mayer-Güuerr, T., Maier, A., Krauss, R., Pail, S., Fecher, T., Gruber, T., Brockmann, J., and Krasbutter, I. e. a. (2011). The combined satellite-only global gravity field model GOCO02S. In *System Earth via Geodetic-Geophysical Space Techniques*.

Grafarend, E. and Lohse, P. (1991). The minimal distance mapping of the topographic surface onto the (reference) ellipsoid of revolution. *Manuscripta Geodaetica*, (16), 92–110.

Grafarend, E. W. (1989). The geoid and the Gravimetric Boundary Value Problem. Technical Report 1018, Royal Institute of Technology, Stockholm.

Grafarend, E. W. and Ardalan, A. A. (1997a). W 0 : an estimate in the Finnish Height Datum N60, epoch 1993.4, from twenty-five GPS points of the Baltic Sea Level Project. *Journal of Geodesy*, *71*(11), 673–679.

Grafarend, E. W. and Ardalan, A. A. (1997b). W0: an estimate in the Finnish Height Datum N60, epoch 1993.4, from twenty-five GPS points of the Baltic Sea Level Project. *Journal of Geodesy*, *71*(11), 673–679.

Hagiwara, Y. (1976). A new formula for evaluating the truncation error coefficient. *Bulletin Géodésique*, *50*(2), 131–135.

Hansen, P. C. (1987). *Rank-Deficient and Discrete Ill-Posed Problems: Numerical Aspects of Linear Inversion*. SIAM.

Hansen, P. C. (2008). Regularization Tools: A Matlab Package for Analysis and Solution of Discrete Ill-Posed Problems. Technical report, Informatics and Mathematical Modelling Building 321, Technical University of Denmark, Denmark.

Heck, B. (1995). *Rechenverfahren und Auswertemodelle der Landesvermessung: Klassische und moderne Methoden*. Wichmann.

Heck, B. and Grüninger, W. (1987). Modification of Stokes integral formula by combining two classical approaches. In *Modification of Stokes integral formula by combining two classical approaches*, Volume 2, Vancouver, Canada, 309–337. XIX General Assembly of the International Union of Geodesy and Geophysics.

Heikkinen, M. (1978). *On the tide-generating forces* (85 ed.). Number 185. Publ Finn Geod Inst.

Heiskanen, W. and Moritz, H. (1967). *Physical Geodesy*. Series of books in geology. San Francisco: W. H. Freeman.

Helmert, F. R. (1884). *The mathematical and physical theories of higher geodesy (in German), Part2*. B. G. Teubner.

Helmert, F. R. (1890). Die schwerkraft im hochgebirge: insbesondere in den Tyroler Alpen.

Hinze, W. (2003). Bouguer reduction density, why 2.67? *Geophysics*, *68*(5), 1559.

Hirvonen, R. A. and Moritz, H. (1963). *Practical Computation of Gravity at High Altitudes*. Ohio State University Research Foundation.

Hobson, E. W. (1931). *The theory of spherical and ellipsoidal harmonics*. The University press.

Hofmann-Wellenhof, B., Lichtenegger, H., and Collins, J. (1997). *Global Positioning System: theory and practice*. Springer-Verlag.

Hunegnaw, A. (2001a). The effect of lateral density variation on local geoid determination. *Bollettino di geodesia e scienze affini*, *60*(2), 125–144.

Hunegnaw, A. (2001b). *Geoid determination over Ethiopia with emphasis on downward continuation of gravity anomailes*. Doctoral dissertation, Royal Institute of Technology (KTH), Stockholm, Sweden.

Hwang, C. and Hsiao, Y. (2003). Orthometric corrections from leveling, gravity, density and elevation data: a case study in Taiwan. *Journal of Geodesy*, *77*(5), 279–291.

IAG (1971). Geodetic Reference System 1967. Technical report, International Association of Geodesy.

Ilk, K. (1993). Regularization for high resolution gravity field recovery by future satellite techniques. In G. Anger, R. Gorenflo, H. Jochmann, H. Moritz, and W. Webers (Eds.), *Inverse Problems: Principles and Applications in Geophysics, Technology, and Medicine* (1st ed.). John Wiley & Sons.

J. Evans, W. F. (2000). Improved Convergence Rates for the Truncation Error in Gravimetric Geoid Determination. *Journal of Geodesy*, *74*(2), 239–248.

Janák, J. and Vaníček, P. (2005). Mean Free-Air Gravity Anomalies in the Mountains. *Studia Geophysica et Geodaetica*, *49*(1), 31–42.

Jeffreys, H. (1953). The use of Stokes's formula in the adjustment of surveys. *Bulletin Géodésique*, *30*(1), 331–338.

Jeffreys, H. (1962). *The Earth: Its Origin, History and Physical Constitution* (Reissue ed.). Cambridge University Press.

Jekeli, C. (1980). *Reducing the error of geoid undulation computations by modifying Stokes' function*. Dept. of Geodetic Science, The Ohio State University.

Jekeli, C. (1981). Modifying Stokes Function to Reduce the Error of Geoid Undulation Computations. *Journal of Geophysical Research*, *86*(Nb8), 6985–6990.

Jekeli, C. (2000). Heights, the Geopotential and Vertical Datums. Technical Report 459, The Ohio State University, Columbus, USA, Department of Civil and Environmental Engineering and Geodetic Science.

Jones, G. C. (2002). New solutions for the geodetic coordinate transformation. *Journal of Geodesy*, *76*(8), 437–446.

Kearsley, A. H. W. (1988). Tests on the recovery of precise geoid height differences from gravimetry. *Journal of Geophysical Research*, *93*(B6), 6559–6570.

Kellogg, O. D. (1929). *Foundations of Potential Theory*. Barman Press.

Kern, M. and Schwartz, K. (2002). A Comparison of Direct and Indirect Numerical Methods for the Downward Continuation of Airborne Gravity Data. In *General Assembly of IAG*, Budapest, Hungary.

Kiamehr, R. (2006). *Precise Gravimetric Geoid Model for Iran Based on GRACE and SRTM Data and the Least-Squares Modification of Stokes Formula : with Some Geodynamic Interpretations*. Doctoral dissertation, Royal Institute of Technology (KTH).

Kiamehr, R. and Sjöberg, L. E. (2006). Impact of a precise geoid model in studying tectonic structures - A case study in Iran. *Journal of Geodynamics*, *42*(1-3), 1–11.

Klees, R. (1996). Numerical calculation of weakly singular surface integrals. *Journal of Geodesy*, *70*(11), 781–797.

Klees, R. and Lehmann, R. (2001). Integration of a priori gravity field models in boundary element formulations to geodetic boundary value problems. *Iv Hotine-Marussi Symposium on Mathematical Geodesy*, (122), 103–109 183.

Klees, R. and Silverstein, J. (1992). Improved Biological Nitrification Using Recirculation in Rotating Biological Contactors. *Water Science and Technology*, *26*(3-4), 545–553.

Koch, K. and Kusche, J. (2002). Regularization of geopotential determination from satellite data by variance components. *Journal of Geodesy*, *76*(5), 259–268.

Koch, K. R. and Pope, A. J. (1972). Uniqueness and existence for the geodetic boundary value problem using the known surface of the earth. *Bulletin Géodésique*, *106*, 467–476.

Kotsakis, C. and Sideris, M. G. (1999). On the adjustment of combined GPS/levelling/geoid networks. *Journal of Geodesy*, *73*, 412–421.

Krakiwsky, E. (1965). *Heights*. MSc thesis submitted to the dept. of geodetic science and surveying, The Ohio State University, Columbus, USA.

Kusche, J. (2003). A Monte-Carlo technique for weight estimation in satellite geodesy. *Journal of Geodesy*, *76*(11-12), 641–652.

Lapaine, M. (1990). A new direct solution of the transformation problem of Cartesian into ellipsoidal coordinates. In R. H. Rapp and F. Sansó (Eds.), *Determination of the Geoid: Present and Future*, Symposium no. 106, Milano. Springer.

Lavrentev, M., Romanov, V. G., and Shishatskii, S. P. (1986). *Ill-Posed Problems of Mathematical Physics and Analysis*. American Mathematical Society.

Lehmann, R. (1997). *Studies on the Use of the Boundary Element Method in Physical Geodesy*. Verlag der Bayerischen Akademie der Wissenschaften.

Lehmann, R. and Klees, R. (1996). Parallel Setup of Galerkin Equation System for a Geodetic Boundary Value Problem. In *Hackbusch W., Wittum G. (Eds.): Boundary Elements: Implementation and Analysis of Advanced Algorithms: Proceedings of the Twelfth Gamm-Seminar Kiel, January 19 21, 1996*. Vieweg+Teubner Verlag.

Lemoine, F., Kenyon, S., Factor, J., Trimmer, R., Pavlis, N., Chinn, D., Cox, C., Klosko, S., Luthcke, S., Torrence, M., Wang, Y., Williamson, R., Pavlis, E., Rapp, R., and Olson, T. (1998). The development of the joint NASA GSFC and the National Imagery and Mapping Agency (NIMA) geopotential model EGM96. National Aeronautics and Space Administration NASA/TP-1998-206861, National Aeronautics and Space Administration, Maryland.

Li, X. and Götze, H. (2001). Ellipsoid, geoid, gravity, geodesy, and geophysics. *Geophysics*, *66*(6), 1660–1668.

Lin, K.-C. and Wang, J. (1995). Transformation from geocentric to geodetic coordinates using Newton's iteration. *Bulletin Géodésique*, *69*(4), 300–303.

MacMillan, W. D. (1930). *The theory of the potential*. McGraw-Hill Book Company, inc.

Mader, K. (1954). The orthometric weight correction of precision levelling in high terrain (in German). *Austrian Journal of Geodesy*, (Special issue 15).

Manoussakis, G., Delikaraoglou, D., and Ferentinos, G. (2008). An Alternative Approach for the Determination of Orthometric Heights Using a Circular-Arc Approximation for the Plumbline. In M. G. Sideris (Ed.), *Observing our Changing Earth*, Volume 133, 245–252. Berlin, Heidelberg: Springer Berlin Heidelberg.

Marchenko, A. N. (1998). *Parameterization of the Earth's Gravity Field: Point and Line Singularities*. Astronomical and Geodetic Society.

Martinec, Z. (1996). Stability investigations of a discrete downward continuation problem for geoid determination in the Canadian Rocky Mountains. *Journal of Geodesy*, *70*(11), 805–828.

Martinec, Z. (1998). *Boundary-Value Problems for Gravimetric Determination of a Precise Geoid*. Number 73 in Lecture notes in earth sciences. Berlin: Springer.

Martinec, Z. and Vaníček, P. (1996). Formulation of the boundary-value problem for geoid determination with a higher-degree reference field. *Geophysical Journal International*, *126*(1), 219–228.

Martinec, Z., Vaníček, P., Mainville, A., and Veronneau, M. (1995). The Effect of Lake Water on Geoidal Height. *Manuscripta Geodaetica*, *20*(3), 193–203.

Martinec, Z., Vaníček, P., Mainville, A., and Veronneau, M. (1996). Evaluation of topographical effects in precise geoid computation from densely sampled heights. *Journal of Geodesy*, *70*(11), 746–754.

Marych, M. I. and Gudz, I. N. (1982). Concerning the calculation of geodetic heights. *Geodeziia Kartografiia i Aerofotos*, *35*, 68–70.

Mayer-Gürr, T., Kurtenbach, E., and Eicker, A. (2010). ITG-Grace2010: the new GRACE gravity field release computed in Bonn. In *EGU General Assembly Conference Abstracts*, Volume 12, 2446.

Meissl, P. (1971). *Preparations for the Numerical Evaluation of Second Order Molodensky-type Formulas*. Ohio State University, Research Foundation.

Meissl, P. (1981). The use of finite elements in physical geodesy. *The use of finite elements in physical geodesy AFGL, -1.*

Meyer, T. H., Roman, D. R., and Zilkoski, D. B. (2007). What does height really mean? Paper 1, University of Connecticut, Department of Natural Resources and the Environmental Monographs, USA.

Migliaccio, F., Reguzzoni, M., Gatti, A., Sansò, F., and Herceg, M. (2011). A GOCE-only global gravity field model by the space-wise approach. In *The 4th International GOCE User Workshop 31 March - 1 April 2010*, Munich.

Migliaccio, F., Reguzzoni, M., Sansò, F., Tscherning, C., and Veicherts, M. (2010). GOCE data analysis: the space-wise approach and the first space-wise gravity field model. In H. Lacoste (Ed.), *Proceedings of the ESA Living Planet Symposium, 28 June - 2 July 2010, Bergen, Norway*. ESA.

Molodensky, M., Eremeev, V., and Yurkina, M. (1962). Methods for study of the external gravitational field and figure of the earth. *Jerusalem, Israel Program for Scientific Translations, 1962; [available from the Office of Technical Services, U.S. Dept. of Commerce, Washington]*, *-1.*

Moritz, H. (1980). Advanced physical geodesy. *Karlsruhe : Wichmann ; Tunbridge, Eng. : Abacus Press, 1980.*, *-1.*

Nahavandchi, H. (1998). *Precise gravimetric-GPS geoid determination with improved topographic corrections applied over Sweden*. Doctoral dissertation.

Nahavandchi, H. and Sjöberg, L. E. (2001). Precise geoid determination over Sweden using the Stokes-Helmert method and improved topographic corrections. *Journal of Geodesy*, *75*(2-3), 74–88.

Niemeier, W. (1987). Observation Techniques for Height Determination and their relation to usual height systems, determination of heights and height changes. In *Contributions to the Height Determination and Recent Vertical Crustal Movements in Western Europe*, Hannover, Germany, 85–108.

Niethammer, T. (1932). *Nivellement und Schwere als Mittel zur Berechnung wahrer Meereshöhen*. Kartenverl. d. schweiz.Schweizerische Geodätische Kommission, Berne.

Novák, P. (2003). Geoid determination using one-step integration. *Journal of Geodesy*, *77*(3), 193–206.

Novák, P. and Heck, B. (2002). Downward continuation and geoid determination based on band-limited airborne gravity data. *Journal of Geodesy*, *76*(5), 269–278.

Novotný, O. (1983). On the addition theorem for Legendre polynomials. *Ceskoslovenska Akademie Ved Geophys. Works*, *30*, 33–45.

Nsombo, P. (1996). *Geoid determination over Zambia*. Doctoral dissertation, Royal Institute of Technology (KTH), Stockholm, Sweden.

Olson, D. (1996). Converting Earth-centered, Earth-fixed coordinates to geodetic coordinates. *IEEE Transactions on Aerospace and Electronic Systems*, *32*(1), 473 –476.

Omang, O. C. D. and Forsberg, R. (2002). The northern European geoid: a case study on long-wavelength geoid errors. *Journal of Geodesy*, *76*(6-7), 369–380.

Pail, R., Goiginger, H., Mayrhofer, R., Schuh, W., Brockmann, J. M., Krasbutter, I., Hoeck, E., and Fecher, T. (2011). GOCE gravity field model derived from orbit and gradiometry data applying the time-wise method. In *The ESA Living Planet Symposium, 28 June - 2 July 2010*, Bergen, Norway. ESA.

Pail, R., Goiginger, H., Schuh, W., Höck, E., Brockmann, J. M., Fecher, T., Gruber, T., Mayer-Gürr, T., Kusche, J., Jäggi, A., and Rieser, D. (2010). Combined satellite gravity field model GOCO01S derived from GOCE and GRACE. *Geophysical Research Letters*, *37*, 5 PP.

Paul, M. K. (1973a). A method of evaluating the truncation error coefficients for geoidal height. *Bulletin Géodésique*, *110*(1), 413–425.

Paul, M. K. (1973b). A note on computation of Geodetic coordinates from geocentric (Cartesian) coordinate's. *Bulletin Géodésique*, *108*(1), 135–139.

Pavlis, N., Holmes, S., Kenyon, S., and Factor, J. (2008). An Earth Gravitational Model to degree 2160: EGM2008. In *Presented at the 2008 General Assembly of the European Geosciences Union*, Volume Vienna, Austria, April 13–18, 2008.

Pavlis, N. K., Holmes, S. A., Kenyon, S. C., and Factor, J. K. (2012). The development and evaluation of the Earth Gravitational Model 2008 (EGM2008). *Journal of Geophysical Research*, *117*(B4), B04406.

Penev, P. (1978). The transformation of rectangular coordinates into geographical by closed formulas. , (20), 175–177.

Pick, M., Pícha, J., and Vyskočil, V. (1973). *Theory of the Earth's Gravity Field. Elsevier, Amsterdam.* Amsterdam.

Pick, M. and Šimon, Z. (1985). Closed formulae for transformation of the cartesian coordinate system into a system of geodetic coordinates. *Studia Geophysica et Geodaetica*, *29*, 112–119.

Pollard, J. (2002). Iterative vector methods for computing geodetic latitude and height from rectangular coordinates. *Journal of Geodesy*, *76*(1), 36–40.

Pollard, J. (2005). A new approach to the iterative calculation of geodetic latitude and its application. *Survey Review*, *38*(296), 117–123.

Prutkin, I. and Klees, R. (2007). On the non-uniqueness of local quasi-geoids computed from terrestrial gravity anomalies. *Journal of Geodesy*, *82*(3), 147–156.

Ågren, J. (2004). *Regional Geoid Determination Methods for the Era of Satellite Gravimetry : Numerical Investigations Using Synthetic Earth Gravity Models.* dissertation.

Ågren, J., Sjöberg, L. E., and Kiamehr, R. (2009). The new gravimetric quasigeoid model KTH08 over Sweden. *Journal of Applied Geodesy*, *3*(3), 143–153.

Rapp, R. H. (1961). *The orthometric height.* Master's thesis, Ohio State University, Colombus, Ohio.

Rapp, R. H. (1989). The treatment of permanent tidal effects in the analysis of satellite altimeter data for sea surface topography. , *14*, 368–372.

Rapp, R. H. and Pavlis, N. K. (1991). The Development and Analysis of Geopotential Coefficient Models to Spherical Harmonic Degree 360. *Journal of Geophysical Research*, *95*(B13), PP. 21,885–21,911.

Rauhut, A. (1992). *Regularisation Methods for the Solution of the Inverse Stokes Problem.* Doctoral dissertation, Dept. of Geomatics Engineering, University of Calgary, Calgary, Canada.

Reilly, W. (1972). New Zealand gravity map series. *New Zealand Journal of Geology and Geophysics*, *15*(1), 13–15.

Reilly, W. (1990). The geoid and the needs of the GPS user,. *New Zealand Surveyor*, *33*(277), 35–41.

Report, I. (1995). Travaux de L´ Association Internationale Géodésie. Technical report, Tome 30, Paris.

Ridgway, K. R., Dunn, J. R., and Wilkin, J. L. (2002). Ocean Interpolation by Four-Dimensional Weighted Least Squares-Application to the Waters around Australasia. *Journal of Atmospheric and Oceanic Technology*, *19*(9), 1357–1375.

Ries, J. C., Eanes, R. J., Shum, C. K., and Watkins, M. M. (1992). Progress in the determination of the gravitational coefficient of the Earth. *Geophysical Research Letters*, *19*(6), 529–531.

Rizos, C. (1982). *The role of the geoid in high precision geodesy and oceanography.* Number Heft Nr. 96 in Reihe A–Theoretische Geodasie. Verlag der Bayerischen Akademie der Wissenschaften in Kommission bei C.H. Beckschen Verlagsbuchhandlung Munchen.

Rummel, R., Schwarz, K., and Gerstl, M. (1979). Least squares collocation and regularization. *Journal of Geodesy*, *53*(4), 343–361.

Sánchez, L. (2007). Definition and Realisation of the SIRGAS Vertical Reference System within a Globally Unified Height System. In P. Tregoning and C. Rizos (Eds.), *Dynamic Planet*, Volume 130 of *International Association of Geodesy Symposia*, 638–645. Springer Berlin Heidelberg.

Sansò, F. and Vaníček, P. (2006). The orthometric height and the holonomity problem. *Journal of Geodesy*, *80*(5), 225–232.

Santos, M., Vaníček, P., Featherstone, W., Kingdon, R., Ellmann, A., Martin, B., Kuhn, M., and Tenzer, R. (2006). The relation between rigorous and Helmert's definitions of orthometric heights. *Journal of Geodesy*, *80*(12), 691–704.

Schaeffer, P., Faugere, Y., and Legeais, F. (2011). The CNES CLS 2011 Global Mean Sea Surface. San-Diego, USA.

Schaffrin, B., Garafarend, E., and Schmitt, R. (1977). Kanonische Design gedatsicher Netze. *Manuscripta Geodaetica*, *1*(2), 263–306.

Scharroo, R. (2011). Evaluation of CNES-CLS11 mean sea surface. Technical Report 11-001.

Schatz, A. H., Thomée, V., and Wendland, W. L. (1990). *Mathematical theory of finite and boundary element methods*. Birkhäuser.

Shaofeng, B. and Dingbo, C. (1991). The finite element method for the geodetic boundary value problem. *Manuscripta Geodaetica*, (16), 353–359.

Shu, C. and Li, F. (2010). An iterative algorithm to compute geodetic coordinates. *Computers & Geosciences*, *36*(9), 1145–1149.

Sideris, M. G. (1987). *Spectral Methods for the Numerical Solution of Molodensky's Problem*. Doctoral dissertation, University of Calgary, Calgary, Canada.

Sideris, M. G. and Forsberg, R. (1991). Review of Geoid Prediction Methods in Mountainous Regions. In *Determination of the Geoid: Present and Future*, Volume -1, New York, USA, 51. Springer-Verlag.

Silver, P. G., Carlson, R. W., and Olson, P. (1988). Deep Slabs, Geochemical Heterogeneity, and the Large-Scale Structure of Mantle Convection: Investigation of an Enduring Paradox. *Annual Review of Earth and Planetary Sciences*, *16*(1), 477–541.

Sjöberg, L. E. (1979). Integral formulas for heterogeneous data in physical geodesy. *Bulletin Géodésique*, *53*, 297–315.

Sjöberg, L. E. (1980). Least squares combination of satellite harmonics and integral formulas in physical geodesy. *Gerlands Beitraege zur Geophysik*, *89*(5), 371–377.

Sjöberg, L. E. (1981). Least squares combination of satellite and terrestrial data in physical geodesy. *Annales de Geophysique*, *37*, 25–30.

Sjöberg, L. E. (1984). *Least squares modification of Stokes' and Vening Meinesz' formulas by accounting for errors of truncation, potential coefficients and gravity data*. University of Uppsala, Institute of Geophysics, Dept. of Geodesy.

Sjöberg, L. E. (1991a). Refined least-squares modification of Stokes formula. *Manuscripta Geodaetica*, *16*, 367–375.

Sjöberg, L. E. (1991b). Some Integral Formulas for a Non-Spherical Earth. In R. H. Rapp and F. Sansò (Eds.), *Determination of the Geoid: Present and Future.*, Symposium no. 106 held 11-13 June, 133. Milan, Italy: Springer-Verlag.

Sjöberg, L. E. (2001). Topographic and atmospheric corrections of gravimetric geoid determination with special emphasis on the effects of harmonics of degrees zero and one. *Journal of Geodesy*, *75*(5-6), 283–290.

Sjöberg, L. E. (2003a). A computational scheme to model the geoid by the modified Stokes formula without gravity reductions. *Journal of Geodesy*, *77*(7-8), 423–432.

Sjöberg, L. E. (2003b). A computational scheme to model the geoid by the modified Stokes formula without gravity reductions. *Journal of Geodesy*, *77*(7-8), 423–432.

Sjöberg, L. E. (2003c). A general model for modifying Stokes' formula and its least-squares solution. *Journal of Geodesy*, *77*(7-8), 459–464.

Sjöberg, L. E. (2003d). Improving modified Stokes formula by GOCE data. *Boll. Geod. Sci. Aff*, *61*(3), 215–225.

Sjöberg, L. E. (2003e). A solution to the downward continuation effect on the geoid determined by Stokes' formula. *Journal of Geodesy*, *77*(1-2), 94–100.

Sjöberg, L. E. (2004a). The effect on the geoid of lateral topographic density variations. *Journal of Geodesy*, *78*(1-2), 34–39.

Sjöberg, L. E. (2004b). A spherical harmonic representation of the ellipsoidal correction to the modified Stokes formula. *Journal of Geodesy*, *78*(3), 180–186.

Sjöberg, L. E. (2006). A new technique to determine geoid and orthometric heights from satellite positioning and geopotential numbers. *Journal of Geodesy*, *80*(6), 304–312.

Sjöberg, L. E. (2008). A strict transformation from Cartesian to geodetic coordinates. *Survey Review*, *40*(308), 156–163.

Sjöberg, L. E. and Fan, H. (1986). A Comparison of the Modified Stokes' Formula and Hotine's Formula in Physical Geodesy. Technical Report 4, Royal Institute of Technology (KTH), Department of Geodesy, Stockholm, Sweden.

Sjöberg, L. E. and Hunegnaw, A. (2000). Some modifications of Stokes' formula that account for truncation and potential coefficient errors. *Journal of Geodesy*, *74*(2), 232–238.

Sjöberg, L. E. and Nahavandchi, H. (2000). The atmospheric geoid effects in Stokes formula. *Geophysical Journal International*, *140*(1), 95–100.

Sneeuw, N. (2006). *Geodesy and Geodynamics* (2 ed.). Lecture notes. Stuttgart, Germany: University of Stuttgart.

Soler, T. and Hothem, L. (1989). Important Parameters Used in Geodetic Transformations. *Journal of Surveying Engineering*, *115*(4), 414–417.

Somigliana, C. (1929). Teoria generale del campo gravitazionale dell'ellissoide di rotazione. *Memorie della Societa Astronomica Italiana*, *4*, 425.

Stokes, G. (1849). On the variation of gravity and the surface of the earth. *Trans. Cambridge Phil. Soc.*, *8*, 672.

Strange, W. E. (1982). An evaluation of orthometric height accuracy using bore hole gravimetry. *Bulletin Géodésique*, *56*(4), 300–311.

Tapley, B. D., Chambers, D. P., Bettadpur, S., and Ries, J. C. (2003). Large scale ocean circulation from the GRACE GGM01 Geoid. *Geophysical Research Letters*, *30*(22), 2163.

Tarantola, A. (1987). *Inverse problem theory: methods for data fitting and model parameter estimation*. Elsevier.

Tenzer, R. (2008). On the accuracy assessment of input gravity data in local gravity field modeling. *Contributions to Geophysics and Geodesy*, *38*(2), 133–149.

Tenzer, R., Čunderlìk, R., Dayoub, N., and Abdalla, A. (2012). Application of the BEM approach for a determination of the regional marine geoid model and the mean dynamic topography in the Southwest PacificOcean and Tasman Sea. *Journal of Geodetic Science*, *2*(1), 8–14.

Tenzer, R., Dayoub, N., and Abdalla, A. (2013). Analysis of a relative offset between vertical datums at the North and South Islands of New Zealand. *Applied Geomatics*, 1–13.

Tenzer, R. and Klees, R. (2008). The choice of the spherical radial basis functions in local gravity field modeling. *Studia Geophysica Et Geodaetica*, *52*(3), 287–304.

Tenzer, R. and Novák, P. (2008). Conditionality of inverse solutions to discretised integral equations in geoid modelling from local gravity data. *Studia Geophysica Et Geodaetica*, *52*(1), 53–70.

Tenzer, R., Novak, P., Prutkin, I., Ellmann, A., and Vajda, P. (2009). Far-Zone Contributions to the Gravity Field Quantities by Means of Molodensky's Truncation Coefficients. *Studia Geophysica Et Geodaetica*, *53*(2), 157–167.

Tenzer, R., Novák, P., Vajda, P., Ellmann, A., and Abdalla, A. (2011). Far-zone gravity field contributions corrected for the effect of topography by means of Molodensky's truncation coefficients. *Studia Geophysica Et Geodaetica*, *55*(1), 55–71.

Tenzer, R., Prutkin, I., and Klees, R. (2012). A comparison of different integral-equation-based approaches for local gravity field modelling: Case study for the canadian Rocky Mountains. In S. Kenyon, M. C. Pacino, and U. Marti (Eds.), *Geodesy for Planet Earth*, Volume 136, 381–388. Berlin, Heidelberg: Springer Berlin Heidelberg.

Tenzer, R., Vaníček, P., Santos, M., Featherstone, W. E., and Kuhn, M. (2005). The rigorous determination of orthometric heights. *Journal of Geodesy*, *79*(1-3), 82–92.

Tenzer, R., Vatrt, V., Abdalla, A., and Dayoub, N. (2011). Assessment of the LVD offsets for the normal-orthometric heights and different permanent tide systems - a case study of New Zealand. *Applied Geomatics*, *3*(1), 1–8.

Tenzer, R., Vatrt, V., Gan, L., Abdalla, A., and Dayoub, N. (2011). Combined approach for the unification of levelling networks in New Zealand. *Journal of Geodetic Science*, *1*(4), 324–332.

Tikhonov, A. N. and Arsenin, V. (1977). *Solutions of ill-posed problems*. Winston.

Torge, W. (2001). *Geodesy* (3rd completely rev. and extended ed ed.). Berlin: W. de Gruyter.

Tscherning, C. C. and Rapp, R. H. (1974). Closed Covariance Expressions for Gravity Anomalies, Geoid Undulations, and Deflections of the Vertical Implied by Anomaly Degree Variance Models. Technical report.

Turner, J. (2009). A non-iterative and non-singular perturbation solution for transforming Cartesian to geodetic coordinates. *Journal of Geodesy*, *83*(2), 139–145.

Ulotu, P. E. (2009). *Geoid model of Tanzania from sparse and varying gravity data density by the KTH method*. Doctoral dissertation, Royal Institute of Technology (KTH), Stockholm, Sweden.

Vaníček, P., Castle, R. O., and Balazs, E. I. (1980). Geodetic leveling and its applications. *Reviews of Geophysics*, *18*(2), 505–524.

Vaníček, P. and Featherstone, W. E. (1998). Performance of three types of Stokes kernel in the combined solution for the geoid. *Journal of Geodesy*, *72*(12), 684–697.

Vaníček, P. and Kleusberg, A. (1987). The Canadian geoid-Stokesian approach. *Manuscripta Geodaetica*, *12*(2), 86–98.

Vaníček, P. and Krakiwsky, E. (1986). *Geodesy: The Concepts* (2nd ed.). Elsevier Science.

Vaníček, P. and Sjöberg, L. E. (1991). Reformulation of Stokes Theory for Higher Than 2nd-Degree Reference Field and Modification of Integration Kernels. *Journal of Geophysical Research-Solid Earth and Planets*, *96*(B4), 6529–6539.

Vaníček, P., Sun, W., Ong, P., Martinec, Z., Najafi, M., Vajda, P., and Ter Horst, B. (1996). Downward continuation of Helmert's gravity. *Journal of Geodesy*, *71*(1), 21–34.

Vatrt, V. (1999). Methodology of Testing Geopotential Models Specified in Different Tide Systems.

Čunderlík, R. and Mikula, K. (2010). Direct BEM for high-resolution global gravity field modelling. *Studia Geophysica et Geodaetica*, *54*(2), 219–238.

Čunderlík, R., Mikula, K., and Mojzeš, M. (2007). Numerical solution of the linearized fixed gravimetric boundary-value problem. *Journal of Geodesy*, *82*, 15–29.

Čunderlík, R., Tenzer, R., Abdalla, A., and Mikula, K. (2010). The quasigeoid modelling in New Zealand using the boundary element method. *Contributions to Geophysics and Geodesy*, *40*(4), 283–297.

Vincent, S. and Marsh, J. G. (1974). Global detailed gravimetric geoid. In *The Use of Artificial Satellites for Geodesy and Geodynamics*, Volume -1, 825–855.

Vincenty, T. (1980). Zur raeumlich-ellipsoidischen Koordinaten-Transformation. *ZfV*, *11/1980*, 519–521.

Wahr, J. M. (1996). *Geodesy and Gravity: Class Notes*. Samizdat Press.

Wenzel, H. (1981). Zur Geoidbestimmung durch Kombination von Schwereanomalien und einem Kugelfunktionsmodell mit Hilfe von Integralformeln. *ZfV*, *106*(3), 102–111.

Wenzel, H. (1982). Geoid computation by least-squares spectral combination using integral kernels. Tokyo, Japan, 438–453. Internation.

Wong, L. and Gore, R. (1969). Accuracy of Geoid Heights from Modified Stokes Kernels. *Geophysical Journal of the Royal Astronomical Society*, *18*(1), 81–91.

Wu, Y., Wang, P., and Hu, X. (2003). Algorithm of Earth-centered Earth-fixed coordinates to geodetic coordinates. *IEEE Transactions on Aerospace and Electronic Systems*, *39*(4), 1457 – 1461.

Xu, P. (1992). The value of minimum norm estimation of geopotential fields. *Geophysical Journal International*, *111*(1), 170–178.

Yang, Z. (1999). *Precise determination of local geoid and its geophysical interpretation*. Doctoral dissertation, The Hong Kong Polytechnic University.

You, R.-J. (2000). Transformation of Cartesian to Geodetic Coordinates without Iterations. *Journal of Surveying Engineering*, *126*(1), 1–7.

Young, D. M. (1971). *Iterative solution of large linear systems*. Academic Press.

Zadro, M. B. and Marussi, A. (1973). On the static effect of moon and sun on the shape of the earth. *Bollettino Geod. Scienzi Affini*, *32*, 253–260.

Zhang, C.-D., Hsu, H., Wu, X., Li, S., Wang, Q., Chai, H., and Du, L. (2005). An alternative algebraic algorithm to transform Cartesian to geodetic coordinates. *Journal of Geodesy*, *79*(8), 413–420.

Index

E

F

G

H

I

K

L

M

N

O

P

Q

R

S

T

U

V

W

Z

Publications

1. **Abdalla, A.**, Tenzer, R. (2011) The evaluation of the New Zealand's geoid model using the KTH method. *Journal of Geodesy and Cartography*. 37:1, 5-14. DOI:10:3846/13921341-2011-558326

2. **Abdalla, A.**, Tenzer, R. (2012a) Compilation of the regional quasigeoid model for New Zealand using the discretized integral-equation approach. *Journal of Geodetic Sciences*. 2(3), 206-215. DOI:10.2478/v10156-011-0041-8

3. **Abdalla, A.**, Tenzer, R. (2012b) The global geopotential and regional gravimetric geoid/quasigeoid models testing using the newly adjusted levelling dataset for New Zealand. *Journal of Applied Geomatics*. 4:187-195. DOI:10.1007/s12518-012-0089-x

4. **Abdalla, A.**, Tenzer, R. (2012c) The integral-equation-based approaches for modelling the local gravity field in the remove-restore scheme, International Association of Geodesy Symposia, 7pp. Springer. (**accepted**).

5. Čunderlík, R., Tenzer, R., **Abdalla, A.**, Mikula, K. (2010) The quasigeoid modelling in New Zealand using the boundary element method. *Contributions to Geophysics and Geodesy*. Vol. 40/4, 283–297. DOI: 10.2478/v10126-010-0011-7

6. Tenzer, R., Vatrt, V., **Abdalla, A.**, Dayoub, N. (2011) Assessment of the LVD offsets for the normal-orthometric heights and different permanent tide systems. *Journal of Applied Geomatics*. 3:1–8. DOI:10.1007/s12518-010-0038-5

7. Tenzer, R., Vatrt, V., Luzi G, **Abdalla, A.**, Dayoub, N. (2011) Combined approach for the unification of levelling networks in New Zealand. *Journal of Geodetic Sciences*.1(4), 324-332. DOI: 10.2478/v10156-011-0012-0

8. Tenzer, R., Dayoub, N. and **Abdalla, A.** (2013) Analysis of a relative offset between vertical datums at the North and South Islands of New Zealand. *Journal of Applied Geomatics*. DOI:10.1007/s12518-013-0106-8